

Electronic Thesis and Dissertation Repository

9-19-2011 12:00 AM

Addressing Computational Complexity of High Speed Distributed Circuits Using Model Order Reduction

Ehsan Rasekh, *The University of Western Ontario*

Supervisor: Dr A. Dounavis, *The University of Western Ontario*

A thesis submitted in partial fulfillment of the requirements for the Doctor of Philosophy degree in Electrical and Computer Engineering

© Ehsan Rasekh 2011

Follow this and additional works at: <https://ir.lib.uwo.ca/etd>



Part of the [Computational Engineering Commons](#), [Numerical Analysis and Scientific Computing Commons](#), and the [VLSI and Circuits, Embedded and Hardware Systems Commons](#)

Recommended Citation

Rasekh, Ehsan, "Addressing Computational Complexity of High Speed Distributed Circuits Using Model Order Reduction" (2011). *Electronic Thesis and Dissertation Repository*. 267.
<https://ir.lib.uwo.ca/etd/267>

This Dissertation/Thesis is brought to you for free and open access by Scholarship@Western. It has been accepted for inclusion in Electronic Thesis and Dissertation Repository by an authorized administrator of Scholarship@Western. For more information, please contact wlsadmin@uwo.ca.

ADDRESSING COMPUTATIONAL COMPLEXITY OF HIGH SPEED DISTRIBUTED
CIRCUITS USING MODEL ORDER REDUCTION

(Spine title: Numerical Reduction Techniques for Electronic Systems)

(Thesis format: Monograph)

by

Ehsan Rasekh

Graduate Program in Engineering Science
Department of Electrical and Computer Engineering

A thesis submitted in partial fulfillment
of the requirements for the degree of
DOCTOR OF PHILOSOPHY

The School of Graduate and Postdoctoral Studies
The University of Western Ontario
London, Ontario, Canada

© Ehsan Rasekh 2011

THE UNIVERSITY OF WESTERN ONTARIO
School of Graduate and Postdoctoral Studies

CERTIFICATE OF EXAMINATION

Supervisor

Examiners

Dr. A. Dounavis

Dr. K. Adamiak

Supervisory Committee

Dr. S. Asokanthan

Dr. R. Khazaka

Dr. J. Sabarinathan

The thesis by

Ehsan Rasekh

entitled:

**Addressing Computational Complexity of High Speed Distributed Circuits
Using Model Order Reduction**

is accepted in partial fulfillment of the
requirements for the degree of
Doctor of Philosophy

Date

Chair of the Thesis Examination Board

Abstract

Advanced in the fabrication technology of integrated circuits (ICs) over the last couple of years has resulted in an unparalleled expansion of the functionality of microelectronic systems. Today's ICs feature complex deep-submicron mixed-signal designs and have found numerous applications in industry due to their lower manufacturing costs and higher performance levels. The tendency towards smaller feature sizes and increasing clock rates is placing higher demands on signal integrity design by highlighting previously negligible interconnect effects such as distortion, reflection, ringing, delay, and crosstalk. These effects if not predicted in the early stages of the design cycle can severely degrade circuit performance and reliability.

The objective of this thesis is to develop new model order reduction (MOR) techniques to minimize the computational complexity of non-linear circuits and electronic systems that have delay elements. MOR techniques provide a mechanism to generate reduced order models from the detailed description of the original modified nodal analysis (MNA) formulation.

The following contributions are made in this thesis:

1. The first project presents a methodology for reduction of Partial Element Equivalent Circuit (PEEC) models. PEEC method is widely used in electromagnetic compatibility and signal integrity problems in both the time and frequency domains. The PEEC model with retardation has been applied to 3-D analysis but often result in large and dense matrices, which are computationally expensive to solve. In this thesis,

a new moment matching technique based on Multi-order Arnoldi is described to model PEEC networks with retardation.

2. The second project deals with developing an efficient model order reduction algorithm for simulating large interconnect networks with nonlinear elements. The proposed methodology is based on a multidimensional subspace method and uses constraint equations to link the nonlinear elements and biasing sources to the reduced order model. This approach significantly improves the simulation time of distributed nonlinear systems, since additional ports are not required to link the nonlinear elements to the reduced order model, yielding appreciable savings in the size of the reduced order model and computational time.
3. A parameterized reduction technique for nonlinear systems is presented. The proposed method uses multidimensional subspace and variational analysis to capture the variances of design parameters and approximates the weakly nonlinear functions as a Taylor series. An SVD approach is presented to address the efficiency of reduced order model. The proposed methodology significantly improves the simulation time of weakly nonlinear systems since the size of the reduced system is smaller than the original system and a new reduced model is not required each time a design parameter is changed.

Keywords

Reduced order systems, multi-order arnoldi, krylov-subspace, nonlinear systems, interconnections, transmission lines, analog circuits, partial element equivalent circuit (PEEC), time domain analysis, parameter extraction, numerical simulation.

Acknowledgments

This thesis could not be successful without the support of my supervisor Dr. Anestis Dounavis of the Department of Electrical and Computer Engineering, University of Western Ontario. His motivation and keen acumen in this field of research has always had a positive effect on my work.

I would also like to extend my thanks towards every faculty member, staff member and friend of the Department of Electrical and Computer Engineering, University of Western Ontario for their support and help at various stages of my thesis work. I would like to specially mention my colleagues Amir Beygi, Sourajeet Roy and Majid Ahmadloo for their invaluable advice.

Appreciation is also extended to the following IBM researchers who provided PowerPEEC software and valuable help used in my dissertation: Dr. Albert Ruehli and Samuel Connor.

I would also like to thank my family for the support they provided me through my entire life. My thanks go out to my late father Akbar, my mother Zahra, my sister Lila and my brothers Ali, Iman and Arman as being the source of inspiration in my studies. And most of all, I must acknowledge my lovely wife and best friend, Niloofar, without whose encouragement and endless support, I would not have had the opportunity to complete this study.

Table of Contents

CERTIFICATE OF EXAMINATION	ii
Abstract.....	iii
Acknowledgments.....	v
Table of Contents.....	vi
List of Tables	x
List of Figures.....	xi
Abbreviations.....	xiii
Chapter 1.....	1
1 Introduction.....	1
1.1 Background and Motivation	1
1.2 Scope And Goals.....	6
1.3 Organization of Thesis.....	8
Chapter 2.....	10
2 Interconnect Macromodeling and Simulation.....	10
2.1 Introduction.....	10
2.2 Interconnect Models.....	11
2.2.1 Quasi-Transverse Electromagnetic Models	11
2.2.2 Full Wave Models.....	13
2.3 Quasi TEM Macromodeling	14
2.3.1 Conventional Lumped Method	16

2.3.2	Method of Characteristics	17
2.4	Full-wave Macromodeling.....	21
2.4.1	The electric field integral equation (EFIE).....	21
2.4.2	The Partial Element Equivalent Circuit	23
Chapter 3	28
3	Simulation Techniques based on Model Order Reduction	28
3.1	Model Order Reduction of Linear Networks with Delay Elements	28
3.1.1	Description of Network Equations.....	28
3.1.2	MOR of Linear Delay Networks.....	29
3.2	Model Order Reduction of Nonlinear systems	34
3.2.1	Formulation of Non-linear Network Equations	34
3.2.2	MOR of Nonlinear Systems Based on Partitioning	36
3.2.3	Model Order Reduction of Weakly Nonlinear Systems	40
Chapter 4	45
4	A Multi-Order Arnoldi Approach for Model Order Reduction of PEEC Models with Retardation	45
4.1	Mutli-Order Arnoldi Algorithm For PEEC Networks With Retardation	46
4.1.1	Computation of the Reduced Order Model.....	46
4.1.2	Moment Relationship of Reduced Order Models	49
4.1.3	Orthonormal Subspace of Reduced Order Models	51
4.2	Numerical Examples.....	54
4.2.1	Example 4.1: Interconnect loop over a ground plane	54
4.2.2	Example 4.2: Three conductor wires with bend:	58

Chapter 5.....	63
5 A Multidimensional Krylov Reduction Technique with Constraint Variables to Model Nonlinear Distributed Networks	63
5.1 Formulation of Network Equations	64
5.2 Nonlinear Macromodeling Using Constraint Equations.....	66
5.2.1 Formulation of Nonlinear Network Equations	66
5.2.2 Construction of Reduced Order Model.....	69
5.3 Implementation of Proposed Model.....	74
5.3.1 Creating a Sparse Reduced Order Macromodel.....	74
5.3.2 Selecting the Order of the Reduced Order Model	78
5.4 Computational Results	81
5.4.1 Numerical Example 5.1	82
5.4.2 Numerical Example 5.2	85
Chapter 6.....	91
6 Compact Parameterized Model Order Reduction of Weakly Nonlinear System.....	91
6.1 Developing of the Parameterized Reduced Order Model	92
6.2 Improving the Efficiency of Reduced Order Model using SVD	97
6.2.1 Relationship of Moments in (6.4).....	97
6.2.2 Terminal Reduction Framework.....	100
6.3 Computational Results	103
6.3.1 Example 6.1: Diode Transmission Line.....	103
6.3.2 Example 6.2: Pulse Shaping Transmission Line.....	106
Chapter 7.....	110

7 Conclusion and Future Research.....	110
7.1 Conclusion	110
7.2 Suggestions for Future Research	112
Reference	114
Curriculum Vitae	128

List of Tables

Table 4.1 CPU Run Time and Macromodel Size Comparison-Example 4.1	57
Table 4.2 CPU Run Time and Macromodel Size Comparison-Example 4.2	60
Table 5.1 CPU Run Time and Macromodel Size Comparison -Example 5.1.	84
Table 5.2 CPU Run Time and Macromodel Size Comparison- Example 5.2.	89
Table 6.1 CPU Run Time and Macromodel Size Comparison of Nonlinear Diode Transmission Line-Example 6.1	105
Table 6.2 CPU Run Time and Macromodel Size Comparison of Pulse Shaping Transmission Line-Example 6.2.....	108

List of Figures

Figure 2.1 Top view and cross-sectional view of a micro-strip line network.....	11
Figure 2.2 Multi-conductor Transmission Line	14
Figure 2.3 Conventional Lumped Transmission line Model.	17
Figure 2.4 Circuit Representation of Method of Characteristic.....	20
Figure 2.5 Two-conductor cell (a) and their corresponding equivalent circuit (b).....	26
Figure 3.1 Arnoldi procedure.....	32
Figure 3.2 Model order reduction techniques based on partitioning the network into linear and nonlinear parts.....	37
Figure 4.1 Multi-order Arnoldi procedure.	48
Figure 4.2 An interconnect loop over a ground plane (Example 4.1).....	55
Figure 4.3 Frequency response comparison of the magnitude of the driving point impedance using one expansion point (Example 4.1).....	56
Figure 4.4 Frequency response comparison of the magnitude of the driving point impedance using two expansion point (Example 4.1).....	56
Figure 4.5 Three conductor wires with bend(a) layout and (b) cross-section (Example 4.2). 59	
Figure 4.6 Comparison of frequency response, (a) real and (b) imaginary part of self-impedance Z_{ab} (Example 4.2).	61
Figure 5.1 Example of a two-port network with a diode.	67

Figure 5.2 Nonlinear Distributed Interconnect Network (Example 5.1).	81
Figure 5.3 The transient response at node P2 for simulation of equation (5.32) (Example 5.1).	83
Figure 5.4 The transient response at node P2 for simulation of equation (5.33) (Example 5.1).	83
Figure 5.5 A coupled interconnect network with inverter terminations (Example 5.2).	86
Figure 5.6 Dynamic large-signal model of CMOS inverter (Example 5.2).	86
Figure 5.7 The transient response at nodes (a) P_{out} , and (b) V_{OUT} (Example 5.2).	88
Figure 6.1 A nonlinear transmission line (Example 6.1).	103
Figure 6.2 Small signal response of nonlinear network (Example 6.1).	104
Figure 6.3 Small signal response of nonlinear network parameterized in capacitance (Example 6.1).	105
Figure 6.4 A nonlinear pulse narrowing transmission line (Example 6.2).	106
Figure 6.5 Output of nonlinear network parameterized in inductance of pulse narrowing transmission line (Example 6.2).	107

Abbreviations

AWE	Asymptotic Waveform Evaluation.
CFH	Complex Frequency Hopping.
EFIE	Electrical Field Integration Equation.
EM	Electromagnetic.
IC	Integrated Circuit.
MNA	Modified Nodal Analysis.
MGS	Modified Gram Schmidt.
MOR	Model Order Reduction.
MRA	Matrix Rational Approximation.
ODE	Ordinary Differential Equation.
PDE	Partial Differential Equation.
PEEC	Partial Element Equivalent Circuit.
p.u.l.	Per-unit-length.
RF	Radio Frequency.
SVD	Singular Value Decomposition.
TEM	Transverse Electromagnetic.
VLSI	Very Large Scale Integration.

Chapter 1

1 Introduction

1.1 Background and Motivation

Advances in integrated circuit (IC) technology has increased operating speeds, packing density, system complexity of electronic devices and are placing significant demands on computer-aided design tools to provide the same efficiency and accuracy. The simulation and verification of mixed signal ICs pose a particular problem for time domain circuit simulators, which are based on implicit numerical integration methods that require solving a large set of nonlinear algebraic equations at each discrete time point. As a result, simulating the transient behaviour of ICs is arduous and computationally expensive task. This problem is further compounded when one considers the typical design process which includes optimization and design space exploration. Such design

processes require conducting a large number of repeated simulations of the same problem with different parameter values. At the same time shrinking process technologies generate a need to consider low-level physical effects such as parasitic effects, transistor-level effects, details of implementation, and signal integrity. Consequently, simple heuristic models may not be sufficient for computational prototyping of modern integrated circuits.

The rapid decrease in feature size and associated growth in circuit complexity, coupled with higher operating speeds, has made the analysis of interconnects a critical aspect of system reliability, speed of operation, and cost. As a result of these technological advancements, Electromagnetic (EM) analysis [1]- [2] has become essential in the design of high-speed integrated circuits. Among EM analysis techniques, the Partial Element Equivalent Circuit (PEEC) [3]- [4] method is often used to model complex three-dimensional interconnect and packaging structures since it can provide full wave and quasi-static circuit equivalent models which can be linked to traditional circuit simulators such as SPICE [5]. However, distributed interconnects and packaging problems modeled using PEEC result in large dense system matrices, simulation of which is computationally expensive.

Over the past years, model order reduction techniques have been proposed as an effective tool to combat computational complexity of large-scale distributed networks, as

they provide a mechanism to generate reduced order models from detailed descriptions [6]- [23]. MOR techniques such as asymptotic waveform evaluation (AWE) [9]- [12], complex frequency hopping (CFH) [13], Padé [14], Arnoldi [15]- [21], and truncated balance reduction [22]- [23] have proven to be efficient means to reduce large linear interconnect networks. Recently, model order reduction techniques have been extended to model PEEC networks [24]- [32].

Model order reduction techniques applied to PEEC models can be broadly classified into two main categories: approaches that use explicit moment matching based on direct Padé approximants [24]- [27] and approaches that use implicit moment matching based on projecting large matrices on its dominant eigenspace [28]- [32]. Explicit moment matching techniques such as Asymptotic Waveform Evaluation (AWE) have been proposed to solve both quasi-static PEEC models [24]- [25] and full-wave PEEC models that include retardation effects [26]. However, these techniques are inherently ill-conditioned in the moment generating process and hence the reduced order model obtained is limited to low order approximations [7]- [8]. To improve the accuracy of AWE, Complex Frequency Hopping (CFH) has been proposed which makes use of multiple expansion points to derive higher order transfer functions [27].

Alternatively, implicit moment matching techniques such as Krylov subspace methods take advantage of the Arnoldi process to achieve more accurate reduced order

models [28]- [32]. However, the traditional Arnoldi algorithm requires that the system equations have a linear dependency with respect to frequency. For PEEC models that include retardation effects, the transfer function contains elements with factors of $e^{-s\tau_i}$ where τ_i corresponds to a time delay (retardation) in the circuit. As a result, PEEC models with retardation are not directly compatible with the traditional Arnoldi algorithm since they contain many delay elements. To include retardation effects using Arnoldi, each exponential function of $e^{-s\tau_i}$ is expanded into a Taylor series and the polynomial equations are converted to have a linear dependency with respect to frequency by introducing extra state variables [31]- [32]. Conversely, this changes the structure of the reduced order system when compared to the original system and the extra state variables increases the computation and memory requirements to derive the reduced order model.

Furthermore, model order reduction approach has been extended for nonlinear circuit simulation problems [10], [19]- [20], [33]- [41]. A common strategy for simulating distributed interconnect networks is based on partitioning the network into linear and nonlinear parts [10], [19]- [20]. The linear network is then reduced using moment matching techniques to form a compact multi-port time-domain macromodel. This macromodel is then coupled with the nonlinear part of the network to obtain the overall network response. However, the efficiency of these techniques drops significantly as the number of ports of the linear sub-network increases due to having many nonlinear

terminations. This drop in efficiency is attributed to the fact that the size of the linear macromodel increases by q for each additional port, where q is the size of the reduced order macromodel with one port.

An alternative approach for model order reduction of nonlinear systems is to directly reduce the entire nonlinear distributed network (without partitioning the linear and nonlinear components) based on power series or piecewise polynomial approximations. Several model order reduction techniques have been proposed to reduce the computational complexity of nonlinear systems [34]- [41]. The reduction of weakly nonlinear systems has been demonstrated based on power series approximations [34]- [37]. For strongly nonlinear systems techniques based on trajectory piecewise polynomials have been reported [38]- [41]. While these algorithms provide significant CPU cost advantage when computing the transient response, a new reduced model is required each time a parameter is modified in the studied structure. Recently, parametric model order reduction techniques have been developed for linear systems, which produce reduced order models that are functions of frequency or time as well as other design parameters [42]- [47]. Nonetheless, these parametric models are not directly applicable to nonlinear systems. In [48], a parametric reduced order model for nonlinear systems is developed based on trajectory piecewise linear method.

1.2 Scope And Goals

The objective of this thesis is to develop efficient modeling techniques for high speed integrated circuit simulation. The focus of this research is based on model order reduction techniques to improve the computational complexity of PEEC structures with retardation and nonlinear distributed networks.

Distributed interconnects and packaging problems modeled using Partial Element Equivalent Circuit (PEEC) method results in large dense system matrices, simulation of which is computationally expensive. To include retardation effects using Arnoldi model order reduction methods, each exponential function of e^{-st_i} is expanded into a Taylor series and the polynomial equations are converted to a linear form by introducing extra state variables [31]- [32]. This changes the structure of the reduced order system when compared to the original system and the extra state variables increases the computation and memory requirements to derive the reduced order model. Techniques to improve the conditioning of the moment generating process of networks described by higher order polynomials have also been developed based on second order Arnoldi [49]- [51], multi-order Arnoldi [52]- [54] and well-conditioned AWE [55]. In this thesis, a multi-order Arnoldi algorithm will be developed to efficiently solve PEEC models with retardation. The advantages of the proposed approach when compared to other PEEC model order reduction techniques are that the moments of the original system

are calculated implicitly without having to introduce extra state variables and the structure of the reduced model is the same as the original system. Furthermore, it is shown that the orthonormal subspace of the system built by introducing extra state variables [31]- [32] is embedded in subspace built by the multi-order Arnoldi approach.

Partitioning the network into linear and nonlinear parts has been proposed for addressing complexity of nonlinear distributed interconnect networks [19]- [20]. However, the efficiency of these techniques drops significantly as the number of ports of the linear sub-network increases due to having many nonlinear terminations. In this thesis, a model order reduction algorithm will be developed to efficiently link nonlinear elements to the reduced order system without having to increase the number of ports. The proposed methodology uses a multidimensional Krylov subspace method and constraint variable equations to capture the variances of nonlinear functions and to link nonlinear functions to the reduced order macromodel. This approach significantly improves the simulation time of distributed nonlinear systems since additional ports are not required to link the nonlinear elements to the reduced order model. In addition, an approach is developed for generating sparse matrices and to select the order of the reduced order model.

The reduction of weakly nonlinear systems has been demonstrated based on power series approximations [34]- [37]. While these algorithms provide significant CPU

cost advantage when computing the transient response, a new reduced model is required each time a parameter is modified in the studied structure. Parameterized model order reduction techniques will be extended for weakly nonlinear systems in this research. The proposed algorithm uses a multidimensional subspace method along with variational analysis and Singular Value Decomposition (SVD) to capture the variances of design parameters and approximates the weakly nonlinear functions as a Taylor series. Such an approach is significantly more CPU efficient in optimization and design space exploration problems since a new reduced model is not required each time a design parameter is modified.

1.3 Organization of Thesis

The organization of the thesis is as follows. A brief review of high-speed interconnects, including quasi-TEM and full-wave formulations are provided in chapter 2. Full-wave analysis of complex three-dimensional interconnects using Partial Element Equivalent Circuit (PEEC) method is presented later in the same chapter. A review of various MOR techniques to model PEEC networks with retardation and nonlinear distributed networks are discussed in chapter 3. In addition model order reduction techniques of weakly nonlinear systems is also reviewed. Chapter 4 describes the details of a multi-order Arnoldi algorithm developed to efficiently solve PEEC models including delay elements.

Numerical examples of PEEC models with retardation are provided to illustrate the validity of the proposed technique. In chapter 5, a model order reduction algorithm using constraint variables is developed to efficiently link nonlinear elements to the reduced order system without having to increase the number of ports. In addition, an approach is developed for generating sparse matrices and to select the order of the reduced order model. Numerical examples are presented to demonstrate the efficiency of the proposed algorithm. Parameterized model order reduction techniques are extended for weakly nonlinear systems employing multidimensional subspace method, variational analysis and SVD in chapter 6. This chapter concludes presenting some numerical examples to show the efficiency of the algorithm. Chapter 7 presents a summary and suggestions for future works.

Chapter 2

2 Interconnect Macromodeling and Simulation

2.1 Introduction

Interconnects are conducting structures that are used to connect transistors and other devices on Integrated Circuits (IC). The physical structure of a micro-strip line interconnect network consisting of two conductors and ground plane is shown in Figure 2.1. As frequency increases, interconnects gradually display resistive, capacitive and inductive effects and cannot be considered as short circuit anymore. Improper consideration of these effects can harshly degrade the signal integrity analysis of the networks. As a result circuit designers must consider these effects to ensure the signal integrity and proper operation of devices. In this chapter, interconnect models are briefly reviewed.

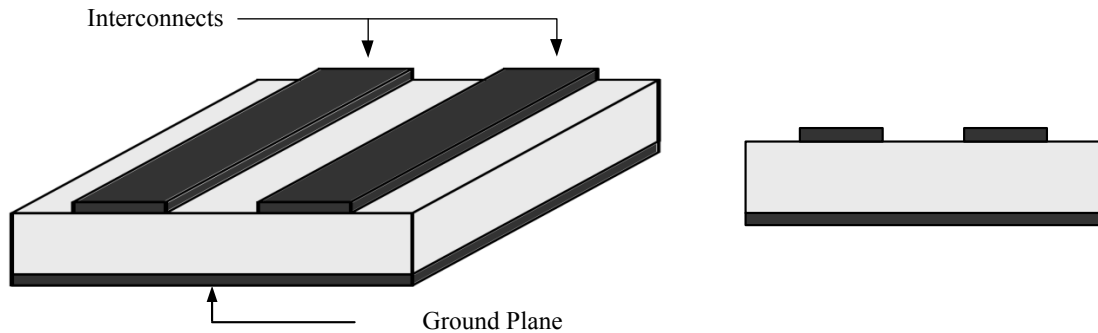


Figure 2.1 Top view and cross-sectional view of a micro-strip line network

2.2 Interconnect Models

Electrical models are employed to simulate interconnects along with other circuit elements in the network. The selection of the proper model depends on the physical interconnect structure as well as the operating frequency of the circuit [56], [57]. These two factors determine whether the modeling of interconnects is based on quasi-transverse electromagnetic (quasi-TEM) or full wave assumptions. These two methods are described in the following sections.

2.2.1 Quasi-Transverse Electromagnetic Models

Transverse electromagnetic (TEM) waves occur for interconnects with homogeneous mediums and perfect conductors. Under these conditions electric and magnetic fields are

perpendicular to each other and to the direction of propagation in TEM waves. Structures with imperfect conductor or inhomogeneous medium violate the TEM characteristics. Interconnects with inhomogeneous mediums produce electromagnetic waves with many velocities. Interconnects that have imperfect conductors also produce an electric field along the surface conductor. Such structures violate the TEM characteristics, since TEM waves propagate with only one velocity and have no electric field along the surface conductor. However, for many practical structures, the electromagnetic field structure can be approximated by TEM waves, which are referred to as quasi-TEM waves [56].

Quasi-TEM approximation remains the main trend for analyzing lossy MTLs, since the approximation is valid for most practical interconnect structures and offers relative low CPU cost compared to full wave approaches [56], [58]. Voltage and current equations derived from quasi-TEM models are described by partial differential equations (PDEs) widely known as Telegrapher's equations. As frequency increases proximity, edge, and skin effects become prominent and distributed models with frequency-dependent parameters are required. Quasi-TEM distributed models cannot be directly linked to circuit simulator such as SPICE [5], since SPICE solves nonlinear ordinary differential equations (ODEs). To overcome this difficulty, numerical techniques are used to convert distributed transmission line models into ODEs.

Conventional lumped segmentation model [56] is the simplest solution for

linking distributed transmission lines to circuit simulators. Electrical length of the transmission line determines the number of segments required for modeling. For transmission lines that the length of the line is much greater than the wavelength many segments are required for proper modeling. In addition to the lumped segmentation model, other more sophisticated algorithms exist such as the method of characteristics [59]- [63], Chebyshev polynomials [64]- [65], wavelets [66]- [67], Matrix Rational Approximation (MRA) [68] and congruent transformation [69].

2.2.2 Full Wave Models

If the cross-sectional dimensions of interconnects become a significant fraction of the circuit's operating wavelength, the field components in the direction of propagation can no longer be ignored [56] and quasi-TEM assumptions become inadequate in describing interconnects. Under these conditions, full wave models are required. These models are able to account for all possible field components and satisfy all boundary conditions required to accurately model the high-frequency effects of interconnect networks.

Full wave analysis of interconnect structures have been successfully implemented using partial element equivalent circuit (PEEC) models [3]- [4]. PEEC models including retardation effects provide a full wave solution. Regular PEEC models are lumped RLC elements that are extracted from the physical geometry using quasi-

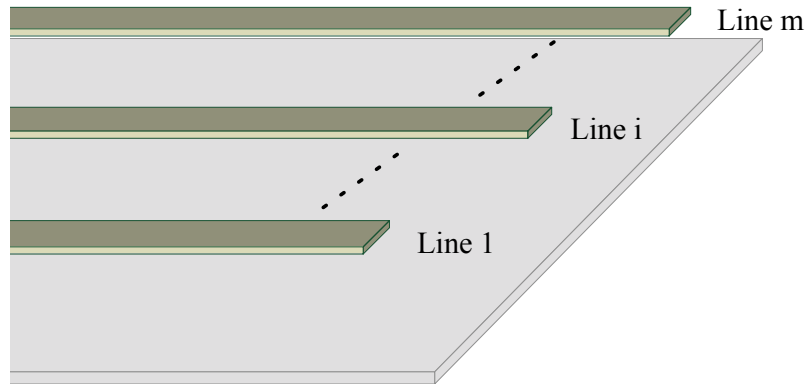


Figure 2.2 Multi-conductor Transmission Line

static solution of Maxwell's equations. These models usually produce large and dense circuit networks and are very CPU intensive to solve.

2.3 Quasi TEM Macromodeling

In this section, methods for quasi-TEM analysis of transmission lines are presented. Consider a lossy coupled interconnect network containing m signal conductors and one reference conductor as shown in Figure 2.2. The voltages and currents are functions of position x , and time t and can be defined as vectors $\mathbf{v}(x,t)$ and $\mathbf{i}(x,t) \in \mathfrak{R}^m$. Considering quasi-TEM distributed assumptions, voltages and currents are related by Telegrapher's equations [56] as

$$\begin{aligned}\frac{\partial}{\partial x} \mathbf{v}(x,t) &= -\mathbf{R}\mathbf{i}(x,t) - \mathbf{L} \frac{\partial}{\partial t} \mathbf{i}(x,t) \\ \frac{\partial}{\partial x} \mathbf{i}(x,t) &= -\mathbf{G}\mathbf{v}(x,t) - \mathbf{C} \frac{\partial}{\partial t} \mathbf{v}(x,t)\end{aligned}\tag{2.1}$$

where $\mathbf{R} \in \mathfrak{R}^{m \times m}$, $\mathbf{L} \in \mathfrak{R}^{m \times m}$, $\mathbf{G} \in \mathfrak{R}^{m \times m}$, $\mathbf{C} \in \mathfrak{R}^{m \times m}$ are per unit length (p.u.l.) resistance, inductance, conductance and capacitance of the multi-conductor transmission line, respectively.

To simulate interconnects with other linear and nonlinear elements, macromodels are required to convert Telegrapher's equations into ODEs which can be solved by commercial circuit simulators. Determining the frequency bandwidth of interest is an important issue in constructing macromodels. In digital applications, the frequency bandwidth of interest is governed by the rise/fall time of the signal. For instance, consider a trapezoidal pulse with an energy spectrum spread over an infinite frequency range, main part of the signal energy is concentrated in the low frequency region and eliminates rapidly with an increment in frequency [11]. Hence, disregarding the high-frequency component of the frequency spectrum above a maximum frequency of interest will not effect the overall signal shape. Relationship between the maximum frequency of interest f_{\max} and the rise/fall time of the trapezoidal pulse t_r is determined using

$$f_{\max} \approx k / t_r \quad (2.2)$$

where k typically ranges from 0.35 to 1 [11], [70]- [71].

The next sections review some of the simulation algorithms that are used for Quasi-TEM macromodeling of transmission lines.

2.3.1 Conventional Lumped Method

This method uses lumped equivalent circuits to approximate Telegrapher's Equation (2.1). Applying Euler's method [56] to discretize (2.1) yields

$$\begin{aligned} v(x + \Delta x, t) - v(x, t) &= -\Delta x \mathbf{R} \mathbf{i}(x, t) - \Delta x \mathbf{L} \frac{\partial}{\partial t} \mathbf{i}(x, t) \\ \mathbf{i}(x + \Delta x, t) - \mathbf{i}(x, t) &= -\Delta x \mathbf{G} v(x + \Delta x, t) - \Delta x \mathbf{C} \frac{\partial}{\partial t} v(x + \Delta x, t) \end{aligned} \quad (2.3)$$

where $\Delta x = d/M$ is the length of each section, d is the length of transmission line and M is the number of needed segments. A circuit representation of equation (2.3) is shown in Figure 2.3.

The conventional lumped model provides a direct discretization method for interconnects; however, the model is only valid if Δx is chosen to be a small fraction of the wavelength. If the circuit operates in high frequencies or if the interconnect is

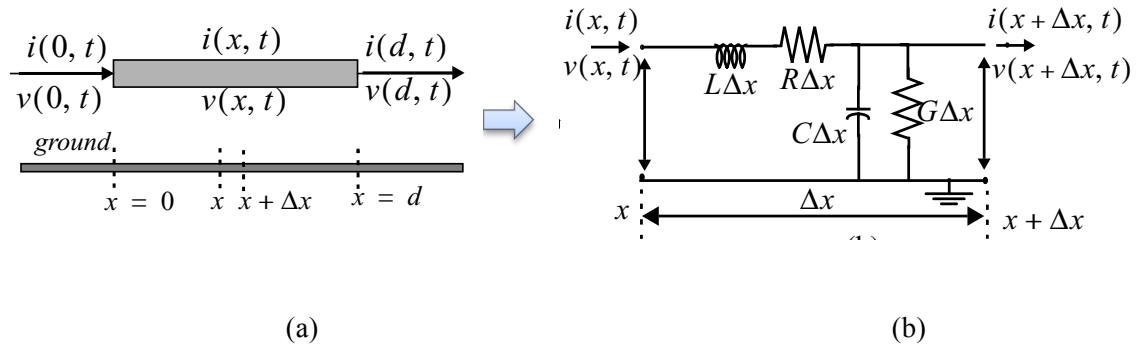


Figure 2.3 Conventional Lumped Transmission line Model.

electrically long many lumped elements are required. A rule of thumb for selecting the number of sections in Hspice [72] is

$$M = \frac{20\sqrt{LC} d}{t_r} \quad (2.4)$$

As the length of the line and as operating frequency increases many lumped sections are required to accurately capture the signal. This leads to large circuit matrices, making the method inefficient.

2.3.2 Method of Characteristics

The method of characteristics [59] represents lossless interconnects as ODEs containing

time delays. Method of characteristics was initially developed in the time-domain using what is referred as characteristic curves. A simpler alternative derivation in the frequency-domain is presented in this section. The Laplace domain solution of (2.1) for two-conductor transmission line [73] is

$$\begin{bmatrix} I_1 \\ I_2 \end{bmatrix} = \frac{1}{Z_0(1 - e^{-2\gamma d})} \begin{bmatrix} 1 + e^{-2\gamma d} & 2e^{-\gamma d} \\ -2e^{-\gamma d} & 1 + e^{-2\gamma d} \end{bmatrix} \begin{bmatrix} V_1 \\ V_2 \end{bmatrix} \quad (2.5)$$

where

$$\gamma = \sqrt{(R + sL)(G + sC)} \quad Z_0 = \sqrt{\frac{(R + sL)}{(G + sC)}} \quad (2.6)$$

γ is the propagation constant and Z_0 is the characteristic impedance. The terms in (2.5) can be re-formulated to

$$\begin{aligned} V_1 &= Z_0 I_1 + e^{-\gamma d} [2V_2 - e^{-\gamma d} (Z_0 I_1 + V_1)] \\ V_2 &= Z_0 I_2 + e^{-\gamma d} [2V_1 - e^{-\gamma d} (Z_0 I_2 + V_2)] \end{aligned} \quad (2.7)$$

Defining W_1 and W_2 as

$$\begin{aligned}
 W_1 &= e^{-\gamma d} [2V_2 - e^{-\gamma d} (Z_0 I_1 + V_1)] \\
 W_2 &= e^{-\gamma d} [2V_1 - e^{-\gamma d} (Z_0 I_2 + V_2)]
 \end{aligned}
 \tag{2.8}$$

and substituting (2.8) in (2.7) yields

$$\begin{aligned}
 V_1 &= Z_0 I_1 + W_1 \\
 V_2 &= Z_0 I_2 + W_2
 \end{aligned}
 \tag{2.9}$$

Eliminating the terms $Z_0 I_1$ and $Z_0 I_2$ in (2.8) using (2.9) results in

$$\begin{aligned}
 W_1 &= e^{-\gamma d} [2V_2 - e^{-\gamma d} (2V_1 - W_1)] \\
 W_2 &= e^{-\gamma d} [2V_1 - e^{-\gamma d} (2V_2 - W_2)]
 \end{aligned}
 \tag{2.10}$$

Considering the symmetry of (2.10) the following recursive relationship for W_1 and W_2 is obtained

$$\begin{aligned}
 W_1 &= e^{-\gamma d} [2V_2 - W_2] \\
 W_2 &= e^{-\gamma d} [2V_1 - W_1]
 \end{aligned}
 \tag{2.11}$$

For lossless transmission lines, γ and Z_0 are reduced to

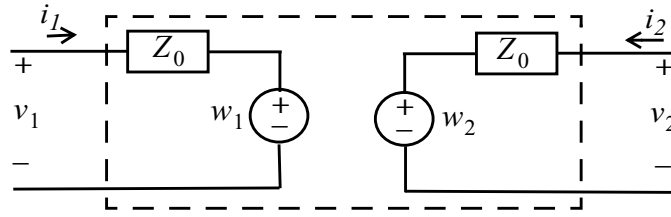


Figure 2.4 Circuit Representation of Method of Characteristic

$$\gamma = s\sqrt{LC} \quad Z_0 = \sqrt{\frac{L}{C}} \quad (2.12)$$

This restriction makes propagation constant γ purely imaginary and characteristic impedance Z_0 a real constant. The time-domain representation of (2.11) is obtained by taking the Laplace inverse, which replaces $e^{-\gamma d}$ by delays, expressed as

$$\begin{aligned} w_1(t + \tau) &= 2v_2(t) - w_2(t) \\ w_2(t + \tau) &= 2v_1(t) - w_1(t) \end{aligned} \quad (2.13)$$

A circuit representation of the transmission line modeled using method of characteristics is shown in Figure 2.4. For the case of lossy lines, propagation constant γ is not purely imaginary and characteristic impedance Z_0 is not a real constant, hence (2.10) cannot be directly expressed in time-domain. In order to model lossy transmission lines, the method of characteristics approximates the losses of propagation constant and characteristic

impedance as rational functions [60]- [61], [74]- [75]. In addition, the method of characteristics has been extended to multi-conductor transmission lines, by decoupling of the transmission line equations [62]- [63], [76].

2.4 Full-wave Macromodeling

In this section, the derivation of the electric field integral equation (EFIE) is described. From this discussion the Partial Element Equivalent Circuit (PEEC) macromodel is derived as a system of ordinary delay-differential equation.

2.4.1 The electric field integral equation (EFIE)

The total electric field inside a conductor is given by [77]

$$\mathbf{E}_p(\mathbf{r}, t) = \frac{\mathbf{J}(\mathbf{r}, t)}{\sigma} + \frac{\partial \mathbf{A}(\mathbf{r}, t)}{\partial t} + \nabla \varphi(\mathbf{r}, t) \quad (2.14)$$

where \mathbf{E}_p is a potential applied electric field, \mathbf{J} is a current density, \mathbf{A} is the magnetic vector potential, and φ is the scalar electric potential. The vector potential \mathbf{A} of a single conductor at any point $\mathbf{r} = (x, y, z)$ is given by

$$\mathbf{A}(\mathbf{r}, t) = \mu \int_{v'} G(\mathbf{r}, \mathbf{r}') \mathbf{J}(\mathbf{r}', t_d) dv' \quad (2.15)$$

where v' is the volume of material in which the current density is flowing and μ is the permeability of free space. The retarded time t_d is given by

$$t_d = t - \frac{|\mathbf{r} - \mathbf{r}'|}{c} \quad (2.16)$$

where c is the speed of light. The time delay equals the free space travel time between the points \mathbf{r} and \mathbf{r}' . The corresponding Green's function is given by

$$G(\mathbf{r}, \mathbf{r}') \equiv \frac{1}{4\pi} \frac{1}{|\mathbf{r} - \mathbf{r}'|} \quad (2.17)$$

Similarly, the scalar potential

$$\varphi(\mathbf{r}, t) = \frac{1}{\epsilon_0} \int_{v'} G(\mathbf{r}, \mathbf{r}') q(\mathbf{r}', t_d) dv' \quad (2.18)$$

where ϵ_0 is the dielectric constant in free space, and q is the charge density on the surface. Assuming external electric field is zero and substituting (2.15) and (2.18) into (2.14), The Electrical Field Integration Equation is obtained

$$\frac{\mathbf{J}(\mathbf{r}, t)}{\sigma} + \mu \int_{v'} G(\mathbf{r}, \mathbf{r}') \frac{\partial \mathbf{J}(\mathbf{r}', t_d)}{\partial t} dv' + \frac{\nabla}{\epsilon_0} \int_{v'} G(\mathbf{r}, \mathbf{r}') q(\mathbf{r}', t_d) dv' = 0 \quad (2.19)$$

2.4.2 The Partial Element Equivalent Circuit

Particular spatial discretization of the conductor geometry combined with the integral equation (2.19), lead to Partial Element Equivalent Circuit (PEEC) models with conventional circuit elements. By defining a suitable inner product, a weighted volume integral over the cells, the field equation (2.19) can be interpreted as Kirchhoff's voltage law over a PEEC cell. This is accomplished by the breakup of the geometry into 2-D or 3-D cells, the integration of (2.19) over each resulting conductor volume cell [3], and observing that the first term in (2.19) corresponds to a resistor, the second term can be transformed into partial inductances [78], and the last term corresponds to normalized coefficients of potential [79]. The partial inductances are defined as

$$L_{ij}(s) = \frac{\mu}{a_i a_j} \int_{v_j} \int_{v_i} G(\mathbf{r}_i, \mathbf{r}_j) e^{-st_d} dv_i dv_j \quad (2.20)$$

where a_i and a_j correspond to through the cell cross section of partial elements. The coefficients of potentials are computed as

$$P_{ij}(s) = \frac{1}{\epsilon_0 S_i S_j} \iint_{s_j} \iint_{s_i} G(\mathbf{r}_i, \mathbf{r}_j) e^{-st_d} ds_i ds_j \quad (2.21)$$

where S_i and S_j are cell areas. By using (2.20) and (2.21), the discretized EFIE (2.19) is reformulated in the form of [3]:

$$\begin{aligned} s\mathbf{L}(s)\mathbf{I} - \mathbf{B}\mathbf{P}(s)\mathbf{Q}(s) + \mathbf{R}\mathbf{I}(s) &= \mathbf{0} \\ \mathbf{B}^T\mathbf{I}(s) + s\mathbf{Q}(s) &= \mathbf{0} \end{aligned} \quad (2.22)$$

where \mathbf{B} contains the connectivity information of the discretization and

$$\begin{aligned} \mathbf{L}(s) &= \sum_{k=0}^{n_1} \mathbf{L}_k e^{-st_{dk}} \\ \mathbf{P}(s) &= \sum_{k=0}^{n_2} \mathbf{P}_k e^{-st_{dk}} \end{aligned} \quad (2.23)$$

n_1 and n_2 are number of delay terms of the coefficients of partial inductance and potential coefficients. $\mathbf{L}(s)$ and $\mathbf{P}(s)$ in (2.23) contain all partial inductance and potential coefficients respectively. Matrix elements in \mathbf{R} , \mathbf{Q} and \mathbf{I} are defined by the following equations

$$R_{ii} = \frac{l_i}{a_i \sigma}$$

$$Q_i(s) = \int_{v'} q_i(\mathbf{r}', s) dv' \quad (2.24)$$

$$I_i(s) = \int_a J_i(\mathbf{r}, s) ds$$

which are resistance, charge and current passing the i th cell, respectively

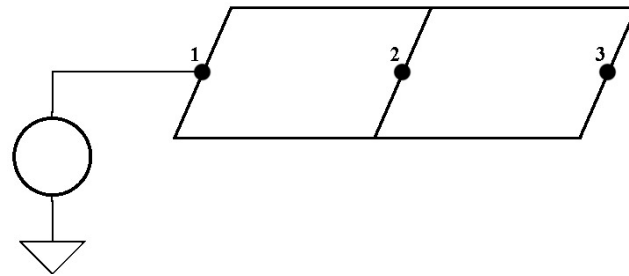
The system in (2.22) can be interpreted as an electronic circuit, where each circuit node represents a charge basis function and each current basis function is represented by circuit branch. The coefficients of potential are related to the electrostatic potential with $\mathbf{V}=\mathbf{PQ}$. The electrostatic potential at the charge segments will be the nodal voltages in the circuit. The charge accumulation on the charge segments is written as an extra set $\mathbf{I}=s\mathbf{Q}$. Substituting these two definitions in (2.22) yields [3]

$$s\mathbf{L}(s)\mathbf{I} - \mathbf{B}\mathbf{V} + \mathbf{R}\mathbf{I} = \mathbf{0} \quad (a)$$

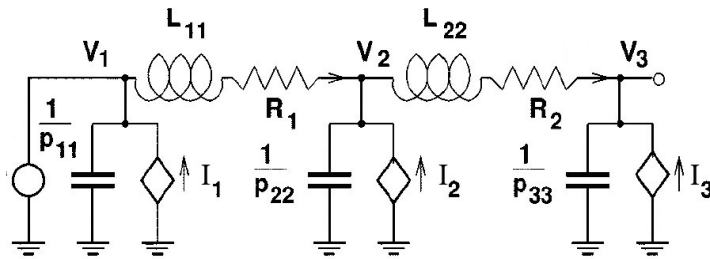
$$\mathbf{B}^T\mathbf{I} + \mathbf{I}_s = \mathbf{0} \quad (b) \quad (2.25)$$

$$\mathbf{P}(s)\mathbf{I}_s - s\mathbf{V} = \mathbf{0} \quad (c)$$

In this formulation, a set of branch constitutive relations for branches with a linear resistor, and an inductor that couples to all other inductors in (2.25.a), in series can be recognized. In (2.25.b) a set of Kirchhoff current laws, one for each charge basis function



(a)



(b)

Figure 2.5 Two-conductor cell (a) and their corresponding equivalent circuit (b).

is discerned. The third one, (2.25.c), can be interpreted as a set of branch constitutive relations for coupled capacitances. These capacitances store the charge that is accumulated on the charge segments. For PEEC models with retardation, the corresponding Modified Nodal Analysis (MNA) equations reduce to systems of linear, time-invariant, delay-differential-algebraic equations. After adding the relationship between the unknown variables and the output vectors of interest, the following complex

system is obtained

$$\left(s\mathbf{C}_0 + \mathbf{G}_0 + \sum_{k=0}^{n_T} (s\mathbf{C}_k + \mathbf{G}_k) e^{-st_{dk}} \right) \mathbf{X}(s) = \mathbf{B}\mathbf{u}(s) \quad (2.26)$$

$$\mathbf{i}(s) = \mathbf{L}^T \mathbf{X}(s)$$

where n_T is the total number of exponentials which corresponds to the number of time delays t_{dk} of the system. The matrices $\mathbf{G}_k, \mathbf{C}_k \in \mathfrak{R}^{N \times N}$ correspond respectively to the state and to the derivative of the state. $\mathbf{X}(s) \in \mathbb{C}^N$ is a vector of the unknown state variables. The matrices $\mathbf{B} \in \mathfrak{R}^{N \times k}$ and $\mathbf{L} \in \mathfrak{R}^{N \times k}$ are selector matrices which map the terminal port characteristics; k is the number of ports; $\mathbf{u}(s), \mathbf{i}(s) \in \mathbb{C}^k$ define the port voltages and currents of the network, respectively and N is the number of unknown variables in $\mathbf{X}(s)$. A schematic of a simple two-cell PEEC model is given in Figure 2.5. The discretization of two cells is shown in Figure 2.5(a) and Figure 2.5(b) shows corresponding equivalent circuit.

Chapter 3

3 Simulation Techniques based on Model Order Reduction

This chapter reviews Model Order Reduction (MOR) techniques used to model PEEC networks and nonlinear distributed interconnect networks.

3.1 Model Order Reduction of Linear Networks with Delay Elements

3.1.1 Description of Network Equations

As illustrated in section 2.4, a linear network characterized by PEEC models with retardation [3]- [4] can be expressed in the Laplace domain as

$$\left(s\mathbf{C}_0 + \mathbf{G}_0 + \sum_{k=0}^{n_T} (s\mathbf{C}_k + \mathbf{G}_k) e^{-s t_{dk}} \right) \mathbf{X}(s) = \mathbf{B}\mathbf{u}(s) \quad (3.1)$$

$$\mathbf{i}(s) = \mathbf{L}^T \mathbf{X}(s)$$

In general, distributed electrical networks characterized by PEEC models with retardation result in a very large system matrices which are dense and computationally expensive to solve. The next section briefly reviews model order reduction techniques which reduce the computational complexity of PEEC networks with retardation.

3.1.2 MOR of Linear Delay Networks

One approach to obtain a reduced order model for (3.1) is to explicitly calculate the moments and to use algorithms such as Modified Gram-Schmidt to construct the orthogonal subspace [80]. However as the number of moments increase, this leads to numerical difficulties since the higher order moments converge to the largest eigenvalue of the system and are almost identical or parallel to each other. To obtain numerically more accurate results, implicit moment matching techniques such as Arnoldi algorithm are usually preferred since they avoid explicit calculation of the moments [7], [81]. However, the original Arnoldi algorithm is only applicable for systems that have a linear dependency with respect to frequency (i.e. $(s\mathbf{C}_0 + \mathbf{G}_0)\mathbf{X}(s) = \mathbf{B}\mathbf{u}(s)$). Thus to calculate

the moments using Arnoldi, the exponential terms of (3.1) are expanded into a polynomial series as

$$e^{-t_d s} \approx e^{-t_d s_0} \left(\sum_{i=0}^M \frac{(-t_d)^i}{i!} (s - s_0)^i \right) \quad (3.2)$$

where s_0 is the expansion point and M is the order of the polynomial. Substituting (3.2) into (3.1), and matching coefficients of similar powers of $(s - s_0)$ yields

$$\left(\sum_{i=0}^M \Phi_i (s - s_0)^i \right) \mathbf{X}(s) = \mathbf{B} \mathbf{u}(s) \quad (3.3)$$

where

$$\Phi_i = \begin{cases} \mathbf{G}_0 + s_0 \mathbf{C}_0 + \sum_{k=1}^{n_r} (s_0 \mathbf{C}_k + \mathbf{G}_k) e^{-s_0 t_{dk}}, & i = 0 \\ \mathbf{C}_0 + \sum_{k=1}^{n_r} \mathbf{C}_k e^{-s_0 t_{dk}} + \sum_{k=1}^{n_r} (s_0 \mathbf{C}_k + \mathbf{G}_k) e^{-s_0 t_{dk}} (-t_{dk}), & i = 1 \\ \sum_{k=1}^{n_r} \mathbf{C}_k e^{-s_0 t_{dk}} \frac{(-t_{dk})^{i-1}}{(i-1)!} + \sum_{k=1}^{n_r} (s_0 \mathbf{C}_k + \mathbf{G}_k) e^{-s_0 t_{dk}} \frac{(-t_{dk})^i}{i!}, & i \geq 2 \end{cases} \quad (3.4)$$

Once the network is expressed as a polynomial series, the system of (3.3) is augmented to obtain a linear dependency with respect to frequency [31]- [32], [82] as

$$(\tilde{\mathbf{G}} + (s - s_0)\tilde{\mathbf{C}}) \tilde{\mathbf{X}} = \tilde{\mathbf{B}}\mathbf{u} \quad (3.5)$$

where

$$\tilde{\mathbf{C}} = \begin{bmatrix} \Phi_1 & \Phi_2 & \Phi_3 & \Phi_4 & \dots & \Phi_M \\ -\mathbf{I} & \mathbf{0} & \mathbf{0} & \mathbf{0} & \dots & \mathbf{0} \\ \mathbf{0} & -\mathbf{I} & \mathbf{0} & \mathbf{0} & \dots & \mathbf{0} \\ \vdots & & & & & \\ \mathbf{0} & \mathbf{0} & & & & \mathbf{0} \end{bmatrix}$$

$$\tilde{\mathbf{G}} = \begin{bmatrix} \Phi_0 & \mathbf{0} & \mathbf{0} & \mathbf{0} & \dots & \mathbf{0} \\ \mathbf{0} & \mathbf{I} & \mathbf{0} & \mathbf{0} & \dots & \mathbf{0} \\ \mathbf{0} & \mathbf{0} & \mathbf{I} & \mathbf{0} & \dots & \mathbf{0} \\ \vdots & & & & & \\ \mathbf{0} & \mathbf{0} & & & & \mathbf{I} \end{bmatrix}; \tilde{\mathbf{X}} = \begin{bmatrix} \mathbf{X} \\ \mathbf{z}_2 \\ \mathbf{z}_3 \\ \vdots \\ \mathbf{z}_M \end{bmatrix}; \tilde{\mathbf{B}} = \begin{bmatrix} \mathbf{B} \\ \mathbf{0} \\ \mathbf{0} \\ \vdots \\ \mathbf{0} \end{bmatrix} \quad (3.6)$$

and \mathbf{I} is identity matrix. The moments of (3.5) at the expansion point s_0 are calculated using the following recursive relationship

- Solve $\tilde{\mathbf{G}}\tilde{\mathbf{R}} = \tilde{\mathbf{B}}$ for $\tilde{\mathbf{R}}$
- $(\mathbf{q}_0, \mathbf{K}) = qr(\tilde{\mathbf{R}})$; *qr* factorization of $\tilde{\mathbf{R}}$
- Set $p =$ number of ports
- Set $n = \text{int}(q/p) + 1$
- For $k = 1, 2, \dots, n-1$
 - Solve $\tilde{\mathbf{G}}\tilde{\mathbf{A}} = -\tilde{\mathbf{C}}$ for $\tilde{\mathbf{A}}$
 - $\mathbf{q}_k^{(0)} = \tilde{\mathbf{A}}\mathbf{q}_{k-1}$
 - For $j = 1, \dots, k$
 - $\mathbf{H} = \mathbf{q}_{k-j}^T \mathbf{q}_k^{(j-1)}$
 - $\mathbf{q}_k^{(j)} = \mathbf{q}_k^{(j-1)} - \mathbf{q}_{k-j} \mathbf{H}$
 - $(\mathbf{q}_k, \mathbf{K}) = qr(\mathbf{q}_k^{(k)})$; *qr* factorization of $\mathbf{q}_k^{(k)}$
- Set $\mathbf{Q} = [\mathbf{q}_0 \mathbf{q}_1 \dots \mathbf{q}_{n-1}]$ and truncate \mathbf{Q} so that it has q columns only.

Figure 3.1 Arnoldi procedure.

$$\begin{aligned}\tilde{\mathbf{M}}_0 &= \tilde{\mathbf{R}} \\ \tilde{\mathbf{M}}_i &= \tilde{\mathbf{A}}\tilde{\mathbf{M}}_{i-1} = \tilde{\mathbf{A}}^i \tilde{\mathbf{R}}\end{aligned}\tag{3.7}$$

where $\tilde{\mathbf{R}} = \tilde{\mathbf{G}}^{-1}\tilde{\mathbf{B}}$ and $\tilde{\mathbf{A}} = -\tilde{\mathbf{G}}^{-1}\tilde{\mathbf{C}}$. The matrix generated using (3.7) forms a Krylov subspace.

$$\begin{aligned}\tilde{\mathbf{K}} &= [\tilde{\mathbf{M}}_0 \tilde{\mathbf{M}}_1 \tilde{\mathbf{M}}_2 \dots \tilde{\mathbf{M}}_n] \\ &= [\tilde{\mathbf{R}} \tilde{\mathbf{A}}\tilde{\mathbf{R}} \tilde{\mathbf{A}}^2\tilde{\mathbf{R}} \dots \tilde{\mathbf{A}}^n\tilde{\mathbf{R}}]\end{aligned}\tag{3.8}$$

Hence, the Arnoldi algorithm, as shown in Figure 3.1, can be used to convert (3.8) into an orthonormal matrix $\tilde{\mathbf{Q}}$ [7], [80]- [81], such that the column space of $\tilde{\mathbf{K}}$ matches the column space of $\tilde{\mathbf{Q}}$ as

$$\begin{aligned} \text{colsp}(\tilde{\mathbf{Q}}) &= \text{colsp}(\tilde{\mathbf{K}}) \\ \tilde{\mathbf{Q}}^T \tilde{\mathbf{Q}} &= \mathbf{I} \end{aligned} \quad (3.9)$$

Using (3.9), the augmented system of (3.5) is reduced by a congruent transformation,

$$(\hat{\mathbf{G}}_a + s\hat{\mathbf{C}}_a)\hat{\mathbf{X}}_a = \hat{\mathbf{B}}_a \mathbf{u} \quad (3.10)$$

where

$$\begin{aligned} \hat{\mathbf{G}}_a &= \tilde{\mathbf{Q}}^T \tilde{\mathbf{G}} \tilde{\mathbf{Q}}, \quad \hat{\mathbf{C}}_a = \tilde{\mathbf{Q}}^T \tilde{\mathbf{C}} \tilde{\mathbf{Q}} \\ \hat{\mathbf{B}}_a &= \tilde{\mathbf{Q}}^T \tilde{\mathbf{B}}, \quad \tilde{\mathbf{X}} = \tilde{\mathbf{Q}} \hat{\mathbf{X}}_a \end{aligned} \quad (3.11)$$

In [31]- [32], the system of (3.10) is used to efficiently express the transfer function of PEEC networks in terms of poles and residues. However, this approach requires introducing $M \cdot N$ state variables to convert the polynomial series of (3.3) into a first-order system. This changes the structure of the reduced order system when compared to the original system and the extra state variables increase the computation and memory

requirements to derive the reduced order model by $O(N^2M)$ [31]. In [82] a projection matrix is built using first M row of (3.8) to reduce the model in (3.1). This approach is able to preserve the structure of the reduced order system when compared to the original system. However, the block resulted by considering first M rows of (3.8) is not orthogonal and therefore another round of orthogonalization has to be carried out. Furthermore, the extra state variables increase the computation and memory requirements to derive the reduced order model.

To address the above concerns, a multi-order Arnoldi algorithm is developed for PEEC circuits with retardation in chapter 4. The advantages of this approach are that the moments of the original system are calculated implicitly without having to introduce extra state variables and the structure of the reduced model is the same as the original system.

3.2 Model Order Reduction of Nonlinear systems

3.2.1 Formulation of Non-linear Network Equations

Consider a general nonlinear network comprised of lumped and distributed interconnects. After discretizing the distributed components with lumped elements [56], the Modified Nodal Analysis (MNA) formulation [83] of such a network can be written as

$$\mathbf{C} \frac{d\mathbf{x}(t)}{dt} + \mathbf{G}\mathbf{x}(t) + \mathbf{f}(\mathbf{x}(t), t) = \mathbf{B}\mathbf{u}(t) \quad (3.12)$$

$$\mathbf{i}(t) = \mathbf{L}^T \mathbf{x}(t)$$

where

- $\mathbf{x}(t) \in \mathfrak{R}^N$ is a vector of node voltage waveforms appended by independent voltage source currents, linear inductor currents nonlinear capacitor charges, nonlinear inductor flux waveforms and currents and voltages due to nonlinear components.
- $\mathbf{G} \in \mathfrak{R}^{M \times M}$ and $\mathbf{C} \in \mathfrak{R}^{M \times M}$ are constant matrices describing the lumped memory and memoryless elements of the network, respectively;
- $\mathbf{f}(\mathbf{x}(t), t) \in \mathfrak{R}^M$ is a vector function describing the nonlinear elements in the network;
- $\mathbf{B} \in \mathfrak{R}^{M \times P}$ is a selector matrix that maps the port voltages into the node space of the network; $\mathbf{L} \in \mathfrak{R}^{M \times P}$ is a selector matrix that maps the port currents into the node space of the network;
- $\mathbf{i}(t) \in \mathfrak{R}^P$ is a vector comprised of the currents at the ports and $\mathbf{u}(t) \in \mathfrak{R}^P$ is a vector comprised of the voltages at the ports;

- M is the total number of variables in the MNA formulation and P is the number of ports

Generally, the network of (3.12) results in a large system of equations, due to discretization of high speed interconnects. In the following sections two approaches for model order reduction of nonlinear systems based on partitioning network in linear and nonlinear parts and weakly nonlinear macromodeling is presented.

3.2.2 MOR of Nonlinear Systems Based on Partitioning

To address the computational complexity of solving nonlinear distributed networks model order reduction techniques based on partitioning the network into linear and nonlinear parts have been proposed [19]- [20]. The partitioning algorithm begins with reformulating (3.12) by adding extra ports for connecting nonlinear elements. The linear network can be expressed as

$$\mathbf{C} \frac{d\mathbf{x}(t)}{dt} + \mathbf{G}\mathbf{x}(t) = \mathbf{B}_n \mathbf{u}_n(t) \quad (3.13)$$

$$\mathbf{i}(t) = \mathbf{L}_n^T \mathbf{x}(t)$$

where $\mathbf{B}_n \in \mathfrak{R}^{M \times (P+N_n)}$ and $\mathbf{L}_n \in \mathfrak{R}^{M \times (P+N_n)}$ are modified selector vectors that map the contributions of regular ports and nonlinear elements into the MNA equations; and N_p

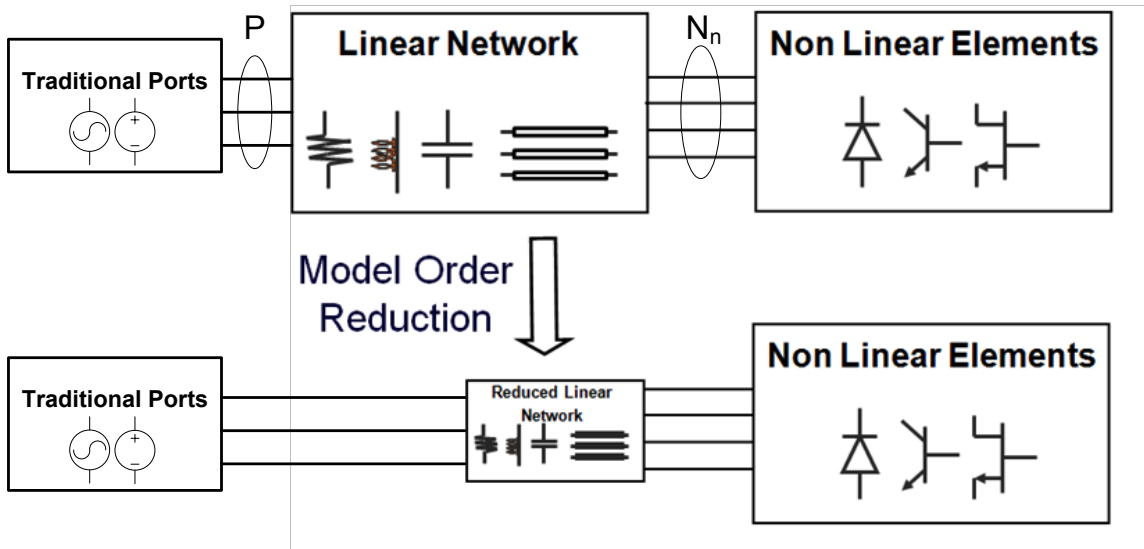


Figure 3.2 Model order reduction techniques based on partitioning the network into linear and nonlinear parts.

corresponds to the number of extra ports to link the nonlinear elements to the reduced order model as shown in Figure 3.2. Equation (3.13) can be written in the Laplace domain as

$$s\mathbf{C}\mathbf{X}(s) + \mathbf{G}\mathbf{X}(s) = \mathbf{B}_n \mathbf{u}_n(s) \quad (3.14)$$

$$\mathbf{i}(s) = \mathbf{L}_n^T \mathbf{X}(s)$$

The computation of the reduced order model expands $\mathbf{X}(s)$ of (3.14) into a Taylor series expansion with respect to frequency, expressed as

$$\mathbf{X}(s) = \sum_{i=0}^{\infty} \mathbf{M}_i s^i \quad (3.15)$$

The moments of the system are computed by substituting (3.15) into (3.14) and matching coefficients of corresponding powers of s , in a similar way as shown before in section 3.1.2. This gives following recursive relationship for the frequency moments

$$\begin{aligned} \mathbf{M}_0 &= \mathbf{R} \\ \mathbf{M}_1 &= \mathbf{A}\mathbf{M}_0 \\ &\dots \\ \mathbf{M}_N &= \mathbf{A}\mathbf{M}_{N-1} \end{aligned} \quad (3.16)$$

where $\mathbf{R} = \mathbf{G}^{-1}\mathbf{B}_n$ and $\mathbf{A} = -\mathbf{G}^{-1}\mathbf{C}$. Once all the moment coefficients are evaluated, the multidimensional subspace $\mathbf{K} \in \mathfrak{R}^{M \times N(P+Nn)}$ is constructed as

$$\begin{aligned} \mathbf{K} &= [\mathbf{M}_0 \mathbf{M}_1 \mathbf{M}_2 \dots \mathbf{M}_n] \\ &= [\mathbf{R} \ \mathbf{A}\mathbf{R} \ \mathbf{A}^2\mathbf{R} \dots \mathbf{A}^n\mathbf{R}] \end{aligned} \quad (3.17)$$

Since the matrix \mathbf{K} is generally ill-conditioned, it is converted into an orthonormal matrix \mathbf{Q} using Arnoldi procedure as shown in Figure 3.1 [7], [80].

$$\begin{aligned} \text{colspan}(\mathbf{Q}) &= \text{colspan}(\mathbf{K}) \\ \mathbf{Q}^T \mathbf{Q} &= \mathbf{I} \end{aligned} \quad (3.18)$$

where \mathbf{I} is the identity matrix. The reduced order model of (3.13) is obtained by a change of variables as illustrated in section 3.1.2

$$\mathbf{x}(t) = \mathbf{Q}\hat{\mathbf{x}}(t) \quad (3.19)$$

Substituting (3.19) into (3.13) and pre-multiplying by \mathbf{Q}^T yields

$$\begin{aligned} \hat{\mathbf{C}} \frac{d\hat{\mathbf{x}}(t)}{dt} + \hat{\mathbf{G}}\hat{\mathbf{x}}(t) &= \hat{\mathbf{B}}\mathbf{u}_n(t) \\ \mathbf{i}(t) &= \hat{\mathbf{L}}^T \hat{\mathbf{x}}(t) \end{aligned} \quad (3.20)$$

where

$$\hat{\mathbf{C}} = \mathbf{Q}^T \mathbf{C} \mathbf{Q}; \quad \hat{\mathbf{G}} = \mathbf{Q}^T \mathbf{G} \mathbf{Q}; \quad \hat{\mathbf{B}} = \mathbf{Q}^T \mathbf{B}_n; \quad \hat{\mathbf{L}} = \mathbf{Q}^T \mathbf{L}_n \quad (3.21)$$

The size of the reduced order model is very small compared to the size of the original system. Once the reduced order system of (3.20) is derived, it can be used to obtain the transient response of (3.12). However, the efficiency of these techniques drops significantly when the number of ports, $(P+N_n)$ in (3.13), increases as a result of having many nonlinear terminations. To address the above issue, chapter 5 describes a

methodology to efficiently link nonlinear elements with reduced order models without increasing the number of ports.

3.2.3 Model Order Reduction of Weakly Nonlinear Systems

For weakly nonlinear networks, the nonlinear functions of (3.12) are expanded in a series of polynomial functions as [34]- [37],

$$\mathbf{C} \frac{d\mathbf{x}(t)}{dt} + \mathbf{G}_1 \mathbf{x}(t) + \mathbf{G}_2 \mathbf{x}(t) \otimes \mathbf{x}(t) + \mathbf{G}_3 \mathbf{x}(t) \otimes \mathbf{x}(t) \otimes \mathbf{x}(t) + \dots = \mathbf{B}\mathbf{u}(t) \quad (3.22)$$

$$\mathbf{i}(t) = \mathbf{L}^T \mathbf{x}(t).$$

where \otimes represents a Kronecker tensor product [84] and

$$\mathbf{G}_i = \begin{cases} \mathbf{G} + \left. \frac{\partial \mathbf{f}(\mathbf{x}(t))}{\partial \mathbf{x}} \right|_{\mathbf{x}=\mathbf{x}_0} & i = 1 \\ \frac{1}{i!} \left. \frac{\partial^i \mathbf{f}(\mathbf{x}(t))}{\partial \mathbf{x}^i} \right|_{\mathbf{x}=\mathbf{x}_0} & i > 1 \end{cases} \in \mathfrak{R}^{N \times N} \quad (3.23)$$

is the i th-order conductance matrix.

To reduce the computational complexity of weakly nonlinear networks, the order of (3.22) is reduced using moment matching techniques. For this purpose, $\mathbf{x}(t)$ is

expressed as a power series with respect to a variational parameter a , as

$$\mathbf{x}(t) = a\mathbf{x}_1(t) + a^2\mathbf{x}_2(t) + a^3\mathbf{x}_3(t) + \dots \quad (3.24)$$

Substituting (3.24) into (3.22) and equating terms with similar power of a results in the following expressions

$$\mathbf{C} \frac{d\mathbf{x}_1(t)}{dt} + \mathbf{G}_1\mathbf{x}_1(t) = \mathbf{B}\mathbf{u}(t), \quad (a)$$

$$\mathbf{C} \frac{d\mathbf{x}_2(t)}{dt} + \mathbf{G}_1\mathbf{x}_2(t) = -\mathbf{G}_2\mathbf{x}_1(t) \otimes \mathbf{x}_1(t), \quad (b)$$

$$\mathbf{C} \frac{d\mathbf{x}_3(t)}{dt} + \mathbf{G}_1\mathbf{x}_3(t) = -\mathbf{G}_2(\mathbf{x}_1(t) \otimes \mathbf{x}_2(t) \quad (c) \quad (3.25)$$

$$+ \mathbf{x}_2(t) \otimes \mathbf{x}_1(t)) - \mathbf{G}_3(\mathbf{x}_1(t) \otimes \mathbf{x}_1(t) \otimes \mathbf{x}_1(t)),$$

...

Note that each system in (3.25) can be treated as a linear state-space system with the same matrices \mathbf{C} and \mathbf{G}_1 and that only the inputs of each system vary. For (3.25.a), the moments of the system are calculated using linear moment matching techniques to obtain an orthonormal projection matrix \mathbf{Q}_1 . The reduced order model of (3.25.a) is obtained by following the procedure of section 3.2.2. A change of variables $\mathbf{x}_1(t) = \mathbf{Q}_1\hat{\mathbf{x}}_1(t)$ result in the following reduced order system [34],

$$\hat{\mathbf{C}} \frac{d\hat{\mathbf{x}}_1(t)}{dt} + \hat{\mathbf{G}}_1 \hat{\mathbf{x}}_1(t) = \hat{\mathbf{B}} \mathbf{u}(t), \quad (3.26)$$

where $\hat{\mathbf{C}} = \mathbf{Q}_1^T \mathbf{C} \mathbf{Q}_1$, $\hat{\mathbf{G}}_1 = \mathbf{Q}_1^T \mathbf{G}_1 \mathbf{Q}_1$, and $\hat{\mathbf{B}} = \mathbf{Q}_1^T \mathbf{B}$.

To minimize the number of input variables $\mathbf{x}_1(t) = \mathbf{Q}_1 \hat{\mathbf{x}}_1(t)$ is substituted in (3.25.b). Using the identity $\mathbf{Q}_1 \hat{\mathbf{x}}_1(t) \otimes (\mathbf{Q}_1 \hat{\mathbf{x}}_1(t)) = (\mathbf{Q}_1 \otimes \mathbf{Q}_1) (\hat{\mathbf{x}}_1(t) \otimes \hat{\mathbf{x}}_1(t))$ yields

$$\begin{aligned} \mathbf{C} \frac{d\mathbf{x}_2(t)}{dt} + \mathbf{G}_1 \mathbf{x}_2(t) = & -\mathbf{G}_2 (\mathbf{Q}_1 \hat{\mathbf{x}}_1(t)) \otimes (\mathbf{Q}_1 \hat{\mathbf{x}}_1(t)) = \\ & -\mathbf{G}_2 (\mathbf{Q}_1 \otimes \mathbf{Q}_1) (\hat{\mathbf{x}}_1(t) \otimes \hat{\mathbf{x}}_1(t)) \end{aligned} \quad (3.27)$$

Defining $\mathbf{B}_2 = -\mathbf{G}_2 (\mathbf{Q}_1 \otimes \mathbf{Q}_1)$ and $\mathbf{u}_2(t) = \hat{\mathbf{x}}_1(t) \otimes \hat{\mathbf{x}}_1(t)$ and replacing these expressions in (3.27) yields

$$\mathbf{C} \frac{d\mathbf{x}_2(t)}{dt} + \mathbf{G}_1 \mathbf{x}_2(t) = \mathbf{B}_2 \mathbf{u}_2(t). \quad (3.28)$$

The system of (3.28) is similar in form to (3.25.a) and hence an orthonormal projection matrix \mathbf{Q}_2 can be calculated using moment matching techniques. This procedure can be repeated to calculate higher orders of the nonlinear expansion. Once the orthonormal projection matrices are calculated for the systems in (3.25), the subspace \mathbf{Q} is constructed as

$$\text{colspan}(\mathbf{Q}) = \text{colspan}\left(\begin{bmatrix} \mathbf{Q}_1 & \mathbf{Q}_2 & \cdots \end{bmatrix}\right) \quad (3.29)$$

The reduced order model for the weakly nonlinear system is obtained by substituting a change of variables $\mathbf{x}(t) = \mathbf{Q}\hat{\mathbf{x}}(t)$ and performing a congruent transformation on (3.22) to obtain the following reduced order system [34],

$$\begin{aligned} \hat{\mathbf{C}} \frac{d\hat{\mathbf{x}}(t)}{dt} + \hat{\mathbf{G}}_1 \hat{\mathbf{x}}(t) + \hat{\mathbf{G}}_2 \hat{\mathbf{x}}(t) \otimes \hat{\mathbf{x}}(t) + \hat{\mathbf{G}}_3 \hat{\mathbf{x}}(t) \otimes \hat{\mathbf{x}}(t) \otimes \hat{\mathbf{x}}(t) + \cdots &= \hat{\mathbf{B}}\mathbf{u}(t), \\ \mathbf{i}(t) &= \hat{\mathbf{L}}^T \hat{\mathbf{x}}(t), \end{aligned} \quad (3.30)$$

where

$$\begin{aligned} \hat{\mathbf{C}} &= \mathbf{Q}^T \mathbf{C} \mathbf{Q}, \quad \hat{\mathbf{G}}_1 = \mathbf{Q}^T \mathbf{G}_1 \mathbf{Q}, \\ \hat{\mathbf{G}}_2 &= \mathbf{Q}^T \mathbf{G}_2 \mathbf{Q} \otimes \mathbf{Q}, \dots, \quad \hat{\mathbf{B}} = \mathbf{Q}^T \mathbf{B}, \quad \hat{\mathbf{L}} = \mathbf{Q}^T \mathbf{L} \end{aligned} \quad (3.31)$$

Once the reduced system of (3.30) is obtained, it can be used to efficiently calculate the time domain response of weakly nonlinear systems. However, each time a design parameter is changed, (3.30) is no longer valid and the reduction procedure must be repeated to obtain a new reduced order model. Note that the increase in memory and computational requirements of tensor multiplication as the order of nonlinearity increases makes this method practical for only weakly nonlinear systems.

It is also important to note that the number of required moments grows exponentially with order of the polynomial expansion [85]. Also, the reduced second order and third order matrices is usually dense and has $O(n^3)$ and $O(n^4)$ entries, respectively, where n is the number of unknowns of the reduced model [37]. Therefore, size of reduced order model has to be addressed properly for an efficient weakly nonlinear model order reduction technique.

In order to address these issues, a parameterized model order reduction of weakly nonlinear systems based on a multidimensional subspace and Singular Value Decomposition (SVD) is proposed in chapter 6 to minimize the size of reduced order model.

Chapter 4

4 A Multi-Order Arnoldi Approach for Model Order Reduction of PEEC Models with Retardation

In this chapter, a multi-order Arnoldi algorithm is developed to efficiently solve PEEC models with retardation. The advantages of the proposed approach when compared to other PEEC model order reduction techniques are that the moments of the original system are calculated implicitly without having to introduce extra state variables and the structure of the reduced model is the same as the original system. Furthermore, it is shown that the orthonormal subspace of the system built by introducing extra state variables [31]- [32] is embedded in subspace built by the multi-order Arnoldi approach.

The organization of this chapter is as follows: The development of the proposed model order reduction algorithm is described in section 4.1. Numerical examples of PEEC models with retardation are provided to illustrate the validity of the proposed technique in section 4.2.

4.1 Mutli-Order Arnoldi Algorithm For PEEC Networks With Retardation

4.1.1 Computation of the Reduced Order Model

As shown in section 2.4.2, a linear network characterized by PEEC models with retardation [3]- [4] can be expressed in the Laplace domain as

$$\left(s\mathbf{C}_0 + \mathbf{G}_0 + \sum_{k=0}^{n_r} (s\mathbf{C}_k + \mathbf{G}_k) e^{-s t_{dk}} \right) \mathbf{X}(s) = \mathbf{B}\mathbf{u}(s) \quad (4.1)$$

$$\mathbf{i}(s) = \mathbf{L}^T \mathbf{X}(s)$$

The exponential terms of (4.1) are expanded into a polynomial series as illustrated in section 3.1.2.

$$\left(\sum_{i=0}^M \Phi_i (s - s_0)^i \right) \mathbf{X}(s) = \mathbf{B}\mathbf{u}(s) \quad (4.2)$$

where Φ_i is defined in (3.4). To calculate the moments of the original network, $\mathbf{X}(s)$ is expanded as a power series

$$\mathbf{X}(s) = \sum_{i=0}^n \mathbf{M}_i (s - s_0)^i \quad (4.3)$$

Substituting (4.3) into (4.2) and matching coefficients of similar powers of $(s - s_0)$ results in the following recursive relationship

$$\begin{aligned} \mathbf{M}_0 &= \mathbf{R} \\ \mathbf{M}_1 &= \mathbf{A}_1 \mathbf{M}_0 \\ \mathbf{M}_2 &= \mathbf{A}_1 \mathbf{M}_1 + \mathbf{A}_2 \mathbf{M}_0 \\ &\dots \\ \mathbf{M}_n &= \left(\sum_{i=1}^n \mathbf{A}_i \mathbf{M}_{n-i} \right) \end{aligned} \quad (4.4)$$

where $\mathbf{R} = \Phi_0^{-1} \mathbf{B}$ and $\mathbf{A}_i = -\Phi_0^{-1} \Phi_i$ for $i = \{1, 2, \dots, n\}$. Note that (4.4) is not compatible with the traditional Arnoldi algorithm, since the moments of $\mathbf{K} = [\mathbf{M}_0 \mathbf{M}_1 \dots \mathbf{M}_n]$ are generated by a different recursive relationship than in (3.7). In [49], a second order Arnoldi algorithm is derived to calculate the orthonormal matrix for second order systems. These concepts were later extended for higher order polynomial systems [52]-[53]. In this chapter, the multi-order Arnoldi algorithm is extended to efficiently model

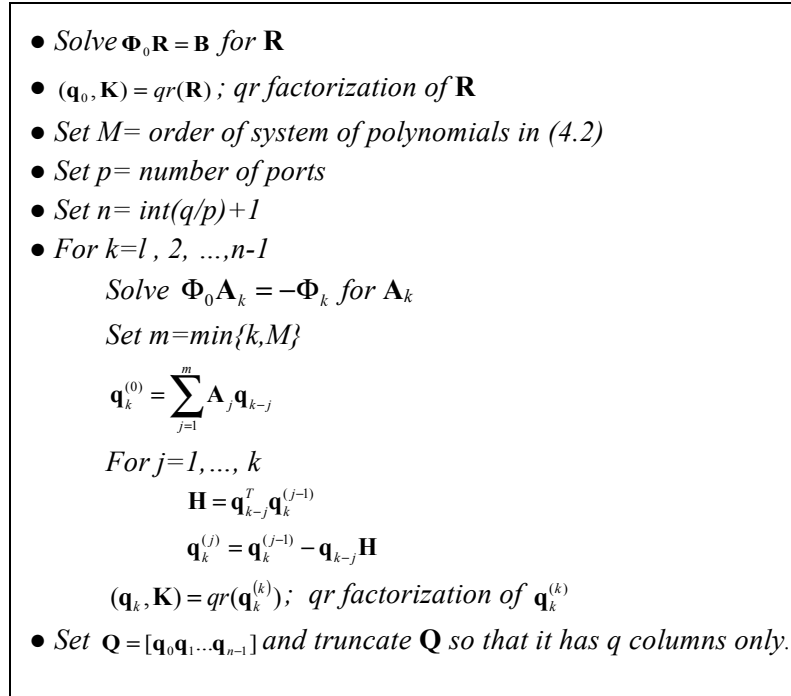


Figure 4.1 Multi-order Arnoldi procedure.

PEEC networks with retardation. The description of the proposed algorithm is provided in Figure 4.1.

Note that for the case when the order of the polynomial is one, the procedure reduces to the standard Arnoldi algorithm. Using the orthonormal matrix \mathbf{Q} derived from Figure 4.1, the reduced order model is obtained by a congruent transformation of the system of (4.1), as

$$\left(s\hat{\mathbf{C}}_0 + \hat{\mathbf{G}}_0 + \sum_{k=1}^{n_T} (s\hat{\mathbf{C}}_k + \hat{\mathbf{G}}_k) e^{-st_{dk}} \right) \hat{\mathbf{X}}(s) = \hat{\mathbf{B}}\mathbf{u}(s) \quad (4.5)$$

where

$$\begin{aligned} \hat{\mathbf{C}}_k &= \mathbf{Q}^T \mathbf{C}_k \mathbf{Q} \in \mathfrak{R}^{q \times q}, \quad \hat{\mathbf{G}}_k = \mathbf{Q}^T \mathbf{G}_k \mathbf{Q} \in \mathfrak{R}^{q \times q}, \\ \mathbf{X}(s) &= \mathbf{Q} \hat{\mathbf{X}}(s) \in \mathbb{C}^q, \quad \hat{\mathbf{B}} = \mathbf{Q}^T \mathbf{B} \in \mathfrak{R}^{q \times k} \end{aligned} \quad (4.6)$$

and q corresponds to number of columns in the matrix \mathbf{Q} . Once the reduced order system of (4.5) is derived, it can be used to evaluate the response of the original system within a certain frequency range of interest.

The next two sections illustrate the validity of the proposed algorithm by establishing the relationship of the moments and the orthonormal subspace between the reduced order systems of (3.10) and (4.5).

4.1.2 Moment Relationship of Reduced Order Models

This section shows the moment relationships between the reduced order systems of (3.10) and (4.5). The augmented system of (3.5) has a linear dependency with respect to frequency and the moments generated create a Krylov subspace. Substituting the matrices of (3.6) into (3.7), the following relationships are established

$$\tilde{\mathbf{M}}_0 = \tilde{\mathbf{R}} = \begin{bmatrix} \mathbf{R} \\ \mathbf{0} \\ \mathbf{0} \\ \vdots \\ \mathbf{0} \end{bmatrix} = \begin{bmatrix} \mathbf{M}_0 \\ \mathbf{0} \\ \mathbf{0} \\ \vdots \\ \mathbf{0} \end{bmatrix} \quad (4.7)$$

$$\tilde{\mathbf{M}}_1 = \tilde{\mathbf{A}}\tilde{\mathbf{M}}_0 = \begin{bmatrix} \mathbf{A}_1\mathbf{R} \\ \mathbf{R} \\ \mathbf{0} \\ \vdots \\ \mathbf{0} \end{bmatrix} = \begin{bmatrix} \mathbf{M}_1 \\ \mathbf{M}_0 \\ \mathbf{0} \\ \vdots \\ \mathbf{0} \end{bmatrix} \quad (4.8)$$

$$\tilde{\mathbf{M}}_2 = \tilde{\mathbf{A}}\tilde{\mathbf{M}}_1 = \begin{bmatrix} \mathbf{A}_1\mathbf{M}_1 + \mathbf{A}_2\mathbf{M}_0 \\ \mathbf{A}_1\mathbf{R} \\ \mathbf{R} \\ \mathbf{0} \\ \vdots \\ \mathbf{0} \end{bmatrix} = \begin{bmatrix} \mathbf{M}_2 \\ \mathbf{M}_1 \\ \mathbf{M}_0 \\ \mathbf{0} \\ \vdots \\ \mathbf{0} \end{bmatrix} \quad (4.9)$$

⋮

$$\tilde{\mathbf{M}}_n = \tilde{\mathbf{A}}\tilde{\mathbf{M}}_{n-1} = \begin{bmatrix} \mathbf{M}_n \\ \mathbf{M}_{n-1} \\ \mathbf{M}_{n-2} \\ \vdots \end{bmatrix} \quad (4.10)$$

Note that the vector sequence of the first row of (4.7)-(4.10) provides the same recursive relationship given by (4.4). Thus (4.4) provides a procedure to capture the Krylov sequence of the augmented system without having to introduce extra state variables. It also suggests that the orthonormal subspace of the augmented system can be embedded in the same subspace as the one obtained using the multi-order Arnoldi algorithm. This will be illustrated in the next section.

4.1.3 Orthonormal Subspace of Reduced Order Models

This section shows the relationship of the orthonormal subspace between the reduced order systems of (3.10) and (4.5). The orthonormal basis generated using the procedure of Figure 4.1, can be expressed as

$$\begin{aligned}
 \mathbf{K} &= [\mathbf{M}_0 \mathbf{M}_1 \mathbf{M}_2 \dots \mathbf{M}_n] \\
 &= [\mathbf{q}_0 \mathbf{q}_1 \mathbf{q}_2 \dots \mathbf{q}_n] \mathbf{R}_n \\
 &= \mathbf{Q} \mathbf{R}_n
 \end{aligned}
 \tag{4.11}$$

where the orthonormal matrix \mathbf{Q} has the same column space as the matrix \mathbf{K} as

$$\begin{aligned}
 \text{colsp}(\mathbf{Q}) &= \text{colsp}(\mathbf{K}) \\
 \mathbf{Q}^T \mathbf{Q} &= \mathbf{I}
 \end{aligned}
 \tag{4.12}$$

and $\mathbf{R}_n \in \mathfrak{R}^{q \times q}$ is a non-singular upper-triangular matrix obtained using n moments.

Using (4.7)-(4.10), the Krylov subspace of (3.8) can be expressed as

$$\tilde{\mathbf{K}} = \begin{bmatrix} \mathbf{M}_0 & \mathbf{M}_1 & \mathbf{M}_2 & \dots & \mathbf{M}_n \\ \mathbf{0} & \mathbf{M}_0 & \mathbf{M}_1 & \dots & \mathbf{M}_{n-1} \\ \mathbf{0} & \mathbf{0} & \mathbf{M}_0 & \dots & \mathbf{M}_{n-2} \\ \vdots & \vdots & \vdots & & \vdots \\ \mathbf{0} & \mathbf{0} & \mathbf{0} & \dots & \mathbf{M}_{n-M} \end{bmatrix} \quad (4.13)$$

Note that (4.13) describes the Krylov subspace of (3.8) in terms of the moments generated by (4.4). Next, the subspace of augmented system given by (4.13) is expressed in terms of the subspace obtained using the multi-order Arnoldi algorithm as

$$\tilde{\mathbf{K}} = \begin{bmatrix} \mathbf{Q} & \mathbf{0} & \mathbf{0} & \dots & \mathbf{0} \\ \mathbf{0} & \mathbf{Q} & \mathbf{0} & \dots & \mathbf{0} \\ \mathbf{0} & \mathbf{0} & \mathbf{Q} & \dots & \mathbf{0} \\ \vdots & & & & \vdots \\ \mathbf{0} & \mathbf{0} & \mathbf{0} & \dots & \mathbf{Q} \end{bmatrix} \begin{bmatrix} \mathbf{R}'_n \\ \mathbf{R}'_{n-1} \\ \mathbf{R}'_{n-2} \\ \vdots \\ \mathbf{R}'_{n-M} \end{bmatrix} \quad (4.14)$$

where

$$\begin{aligned}
 \mathbf{R}'_n &= \mathbf{R}_n \\
 \mathbf{R}'_{n-1} &= \begin{bmatrix} \mathbf{0} & \mathbf{R}_{n-1} \\ \mathbf{0} & \mathbf{0} \end{bmatrix} \\
 \mathbf{R}'_{n-2} &= \begin{bmatrix} \mathbf{0} & \mathbf{0} & \mathbf{R}_{n-2} \\ \mathbf{0} & \mathbf{0} & \mathbf{0} \\ \mathbf{0} & \mathbf{0} & \mathbf{0} \end{bmatrix} \\
 &\dots
 \end{aligned} \tag{4.15}$$

and \mathbf{R}_{n-i} corresponds to the upper-triangular matrix obtained using the first $n-i$ moments and $\mathbf{R}'_{n-i} \in \mathfrak{R}^{q \times q}$. The expression of (4.14) shows that the orthonormal subspace of the augmented system is embedded in subspace built by the multi-order Arnoldi approach as

$$\text{colsp}(\tilde{\mathbf{Q}}) \subseteq \text{colsp} \left(\begin{bmatrix} \mathbf{Q} & \mathbf{0} & .. & \mathbf{0} \\ \mathbf{0} & \mathbf{Q} & & \mathbf{0} \\ \vdots & \vdots & & \vdots \\ \mathbf{0} & \mathbf{0} & .. & \mathbf{Q} \end{bmatrix} \right) \tag{4.16}$$

This illustrates that (4.11) can be used to construct orthonormal subspace of the augmented system.

In this section, a reduced order model is presented to efficiently solve large PEEC networks that include retardation effects. The proposed algorithm is based on a

multi-order Arnoldi algorithm used to implicitly calculate the moments with respect to frequency. This procedure generates reduced order models that preserve the structure of the original system. The proposed approach eliminates the need to build an augmented linear system to extract projection subspace and saves on the computation and memory requirements to derive the reduced order model. Furthermore, it is shown that the orthonormal subspace of the proposed multi-order Arnoldi algorithm can be used to construct the same orthonormal subspace obtained using the traditional Arnoldi algorithm. Following section presents two numerical examples to illustrate the validity of proposed algorithm.

4.2 Numerical Examples

In this section, two numerical examples are presented. The PEEC models include retardation effects and were generated using PowerPEEC [86]. The proposed algorithm was implemented in MATLAB [87]. All computations were performed on a Pentium 4 (2.80 GHz) PC with 64 GB memory.

4.2.1 Example 4.1: Interconnect loop over a ground plane

An interconnect loop over a ground plane, is shown in Figure 4.2. The interconnect structure is discretized using PEEC method and the total number of unknown variables

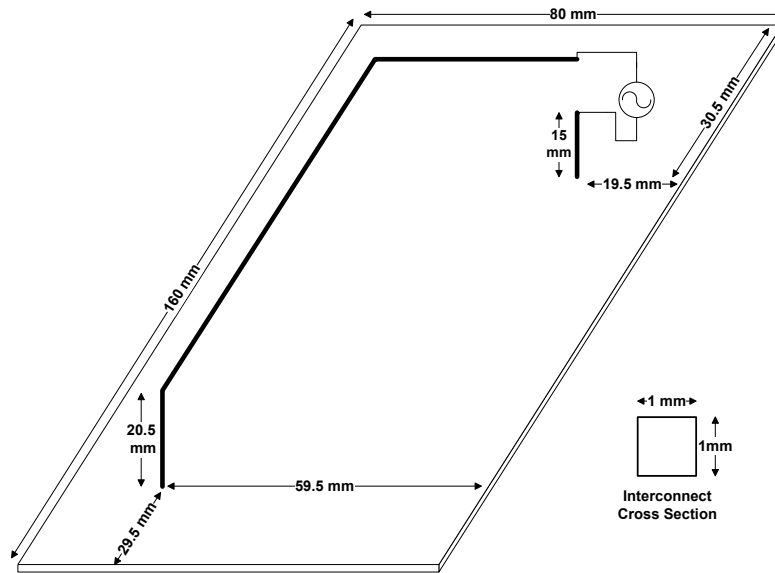


Figure 4.2 An interconnect loop over a ground plane (Example 4.1).

are 4850. The time delays for this example are significant and range up to 0.5967 ns. The frequency bandwidth of interest for this problem is from 0 to 5 GHz.

To illustrate the numerical accuracy of multi-order Arnoldi, the proposed algorithm is compared with modified Gram Schmidt (MGS) approach [80]. Within the context of this section, MGS refers to explicitly calculating the moments using (4.4) and applying MGS to construct the orthonormal matrix Q . To derive equivalent size reduced order models using the proposed approach and MGS, 35 frequency moments are selected

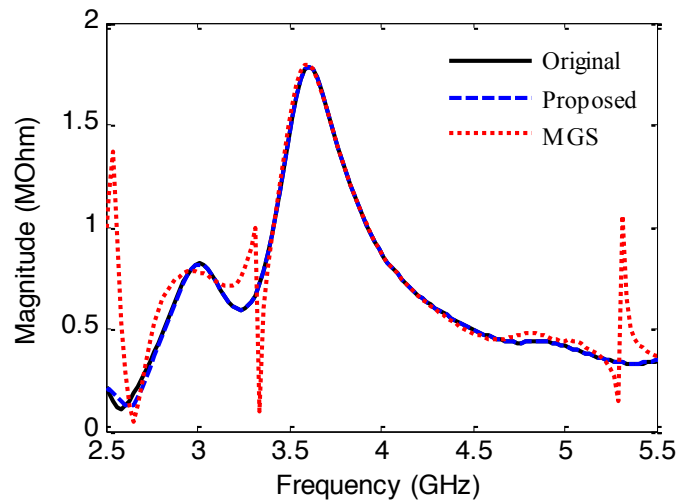


Figure 4.3 Frequency response comparison of the magnitude of the driving point impedance using one expansion point (Example 4.1).

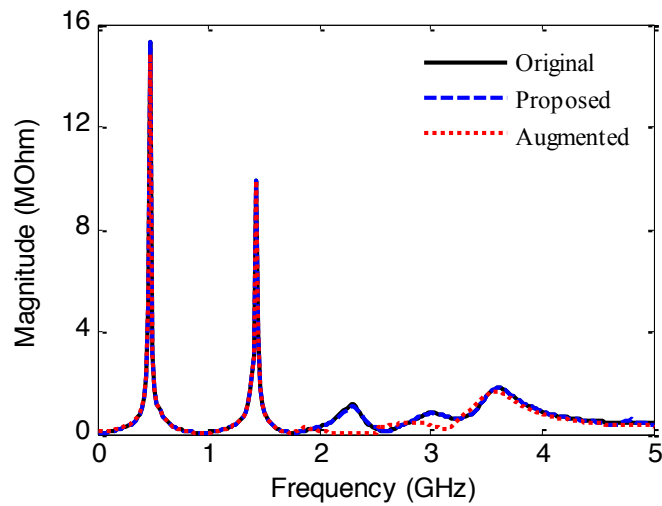


Figure 4.4 Frequency response comparison of the magnitude of the driving point impedance using two expansion points (Example 4.1).

Table 4.1 CPU Run Time and Macromodel Size Comparison-Example 4.1

	Original	Reduced	Savings in Size	Speed-Up Factor
Size of Macromodel	4850	140	96.27%	-
CPU Run Time(s)	5245	3.6	-	1447

at expansion point 4 GHz. Figure 4.3 shows the magnitude of the driving point impedance for both approaches. Both the proposed and MGS are accurate near the expansion point of 4 GHz. However, the proposed algorithm is able to achieve better accuracy since it implicitly calculates the moments using the multi-order Arnoldi algorithm.

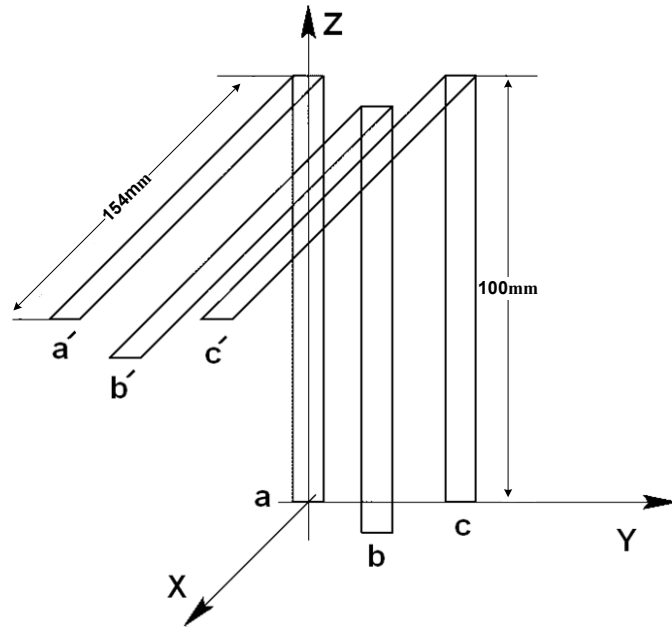
To select appropriate size of the reduced order model, the frequency response is evaluated at the ports by computing the differences between two successive orders of approximations as described in [88]- [89]. If the error difference between the two models is below a given tolerance for the frequency range of interest, then the reduced model is assumed to be accurate. Otherwise additional frequency moments using (4.4) or multiple

expansion points [13] can be used to improve the accuracy of the frequency response. To match the frequency response of this example up to 5 GHz using the proposed approach two expansion points are selected at 1 GHz and 4 GHz, where each expansion point uses 35 frequency moments. A reduced order model is also derived using the augmented system approach of (3.5)-(3.11) using the same number of frequency moments and expansion points. The total size of both reduced order models contained 140 unknown variables. Figure 4.4 shows the magnitude of the driving point impedance for the original system and the reduced order models. For this example, both reduced order models are accurate at the expansion points of 1 GHz and 4 GHz, however, the proposed algorithm is able to achieve better accuracy since it preserves the structure of the original system and has more degrees of freedom to capture the entire frequency response.

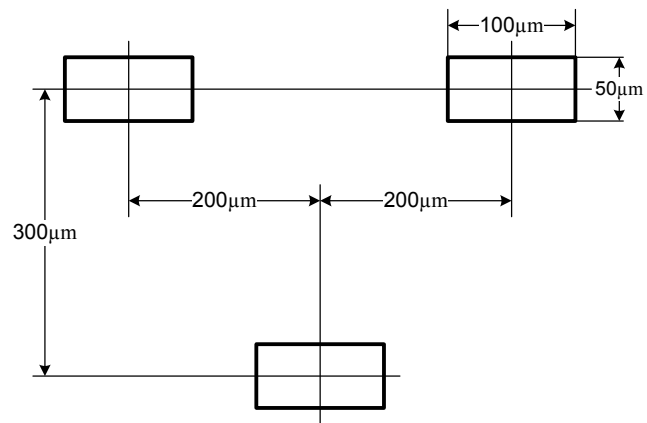
Table 4.1 compares the total size and simulation times of the original and proposed algorithm using MATLAB. For this example, a speed up of 1447 was achieved using the proposed approach when compared to solving the original system.

4.2.2 Example 4.2: Three conductor wires with bend:

Figure 4.5 shows three parallel bent wires that terminate on the same vertical plane. The interconnect network is discretized using PEEC with retardation and the total number of



(a)



(b)

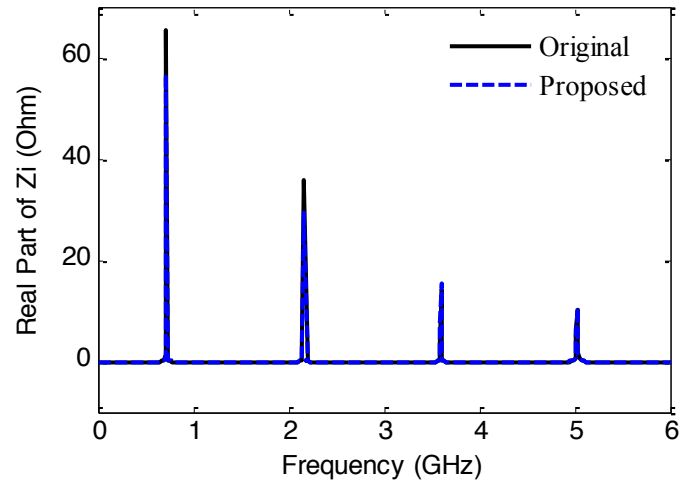
Figure 4.5 Three conductor wires with bend(a) layout and (b) cross-section (Example 4.2).

Table 4.2 CPU Run Time and Macromodel Size Comparison-Example 4.2

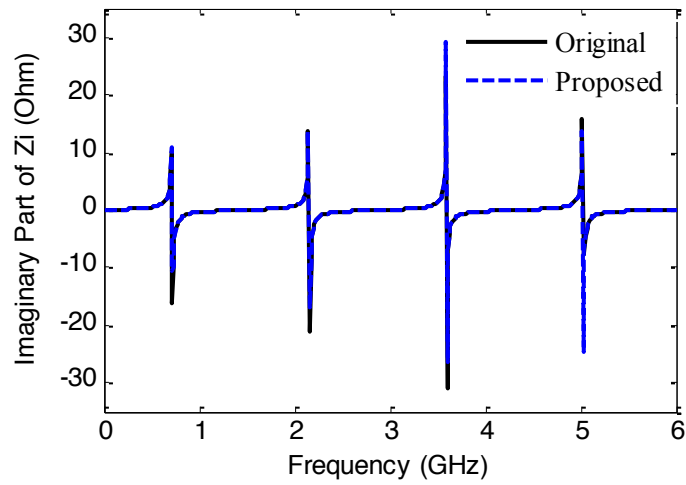
	Original	Reduced	Savings in Size	Speed-Up Factor
Size of Macromodel	4464	220	95.07%	-
CPU Run Time(s)	11508	37.3	-	308

unknown variables are 4464. The maximum time delay in this example equals 0.6131 ns and the bandwidth of interest ranges from 0–6 GHz.

A 1 mA current source across terminals a and b is applied to the network. To derive a compact reduced order model, two expansion points are selected at 1.5 GHz and 4.5 GHz. The expansion point at 1.5 GHz uses 45 moments, while the expansion point at 4.5 GHz requires 65 moments. Figure 4.6 shows the real and imaginary parts of the self-impedance Z_{ab} . The reduced order model obtained using the proposed approach shows good agreement with the results of the original PEEC model.



(a)



(b)

Figure 4.6 Comparison of frequency response, (a) real and (b) imaginary part of self-impedance Z_{ab} (Example 4.2).

Table 4.2 compares the total size and simulation times of the original and proposed reduced order model using MATLAB. For this example, the simulation time of the reduced order model is about 308 times faster when compared to the original system.

Chapter 5

5 A Multidimensional Krylov Reduction Technique with Constraint Variables to Model Nonlinear Distributed Networks

In this chapter a model order reduction algorithm is developed to efficiently link nonlinear elements to the reduced order system without having to increase the number of ports. The proposed methodology is based on the concepts reported in [90], and uses a multidimensional Krylov subspace method and constraint variable equations to capture the variances of nonlinear functions and to link nonlinear functions to the reduced order macromodel. This approach significantly improves the simulation time of distributed nonlinear systems since additional ports are not required to link the nonlinear elements to the reduced order model. In addition, an approach is developed for generating sparse matrices and to select the order of the reduced order model.

The organization of this chapter is as follows: A brief review of the formulation of the nonlinear network equations is presented in section 5.1, and the development of the proposed model order reduction algorithm is described in section 5.2. Section 5.3 describes the creation of a sparse macromodel and the order selection of the reduced order system. Numerical examples are provided in section 5.4.

5.1 Formulation of Network Equations

Consider a general nonlinear network comprised of lumped and distributed interconnects. After discretizing the distributed components with lumped elements [56], the Modified Nodal Analysis (MNA) formulation [83] of such a network can be written as

$$\begin{aligned} \mathbf{C} \frac{d\mathbf{x}(t)}{dt} + \mathbf{G}\mathbf{x}(t) + \mathbf{f}(\mathbf{x}_n(t), t) &= \mathbf{B}\mathbf{u}(t) + \mathbf{b}(t) \\ \mathbf{i}(t) &= \mathbf{L}^T \mathbf{x}(t) \end{aligned} \quad (5.1)$$

where

- $\mathbf{x}(t) = [\mathbf{x}_l \ \mathbf{x}_n]^T \in \mathfrak{R}^N$ is a vector of node voltage waveforms appended by independent voltage source currents, linear inductor currents, nonlinear capacitor charges, nonlinear inductor flux waveforms and currents and voltages due to nonlinear components. The vector \mathbf{x}_n is comprised of variables that are governed

by the nonlinearities in the network whereas the vector \mathbf{x}_l contains the variables governed by the linear components in the network;

- $\mathbf{G} \in \mathfrak{R}^{M \times M}$ and $\mathbf{C} \in \mathfrak{R}^{M \times M}$ are constant matrices describing the lumped memory and memoryless elements of the network, respectively;
- $\mathbf{f}(\mathbf{x}(t), t) \in \mathfrak{R}^M$ is a vector function describing the nonlinear elements in the network;
- $\mathbf{b}(t) \in \mathfrak{R}^M$ is a vector with entries that are determined by the independent biasing sources in the network, e.g. the dc-biasing voltage source of transistors.
- $\mathbf{B} \in \mathfrak{R}^{M \times P}$ is a selector matrix that maps the port voltages into the node space of the network; $\mathbf{L} \in \mathfrak{R}^{M \times P}$ is a selector matrix that maps the port currents into the node space of the network;
- $\mathbf{i}(t) \in \mathfrak{R}^P$ is a vector comprised of the currents at the ports and $\mathbf{u}(t) \in \mathfrak{R}^P$ is a vector comprised of the voltages at the ports;
- M is the total number of variables in the MNA formulation and P is the number of ports

5.2 Nonlinear Macromodeling Using Constraint Equations

This section describes a multidimensional Krylov subspace method to capture the variances of constraint variables used to connect nonlinear elements and biasing sources to the reduced order model.

5.2.1 Formulation of Nonlinear Network Equations

The proposed algorithm begins with reformulating (5.1) such that the vectors describing the nonlinear elements are decomposed into a summation of the scalar functions and vector contributions to the MNA equations as

$$\mathbf{C} \frac{d\mathbf{x}(\bar{\alpha}, t)}{dt} + \mathbf{G}\mathbf{x}(\bar{\alpha}, t) + \sum_{k=1}^F \alpha_{nk} \mathbf{h}_{nk} = \mathbf{B}\mathbf{u}(t) + \alpha_s \mathbf{h}_s \quad (5.2)$$

$$\mathbf{i}(t) = \mathbf{L}^T \mathbf{x}(t)$$

$$\alpha_{nk} = f_k(\mathbf{x}_n(\bar{\alpha}, t), t) \quad (5.3)$$

$$\alpha_s = b_k(t)$$

where $\bar{\alpha} = [\alpha_s, \alpha_{n1}, \alpha_{n2}, \dots]$, $\mathbf{h}_{nk} \in \mathfrak{R}^M$ are selector vectors that map the contributions of each nonlinear element into the MNA equations; $\mathbf{h}_s \in \mathfrak{R}^M$ is a selector vector that maps the DC biasing sources into the MNA equations; $\mathbf{x}(\bar{\alpha}, t)$ is the transient response of the

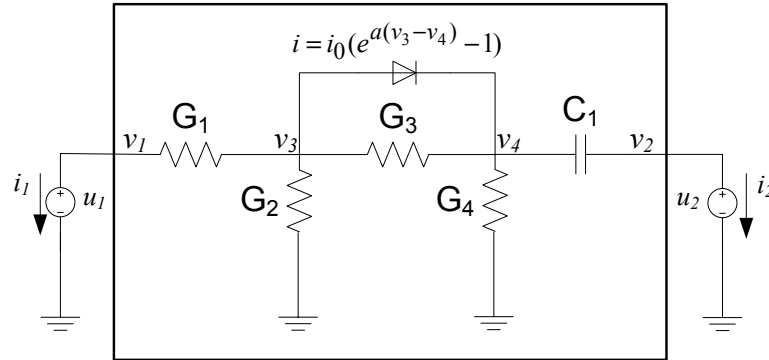


Figure 5.1 Example of a two-port network with a diode.

nonlinear network and now depends on the time variable t and the $\bar{\alpha}$ variables; $f_k(\mathbf{x}(\bar{\alpha}, t), t)$ is the k^{th} nonlinear scalar function in the nonlinear network; $b_k(t)$ is a DC biasing source function and F corresponds to the number of nonlinear elements.

To illustrate the formulation of (5.2) and (5.3), consider the two-port network of Figure 5.1, which includes a nonlinear diode. The values G_1 , G_2 , G_3 and G_4 correspond to the conductance of resistors, while C_1 corresponds to a capacitance value. The matrices of (5.2) and (5.3) are expressed as

$$\mathbf{G} = \begin{bmatrix} G_1 & 0 & -G_1 & 0 & 1 & 0 \\ 0 & 0 & 0 & 0 & 0 & 1 \\ -G_1 & 0 & G_1 + G_2 + G_3 & -G_3 & 0 & 0 \\ 0 & 0 & -G_3 & G_3 + G_4 & 0 & 0 \\ -1 & 0 & 0 & 0 & 0 & 0 \\ 0 & -1 & 0 & 0 & 0 & 0 \end{bmatrix} \quad (5.4)$$

$$\mathbf{C} = \begin{bmatrix} 0 & 0 & 0 & 0 & 0 & 0 \\ 0 & C_1 & 0 & -C_1 & 0 & 0 \\ 0 & 0 & 0 & 0 & 0 & 0 \\ 0 & -C_1 & 0 & C_1 & 0 & 0 \\ 0 & 0 & 0 & 0 & 0 & 0 \\ 0 & 0 & 0 & 0 & 0 & 0 \end{bmatrix}; \mathbf{h}_{n1} = \begin{bmatrix} 0 \\ 0 \\ 1 \\ -1 \\ 0 \\ 0 \end{bmatrix}; \mathbf{h}_s = \mathbf{0} \quad (5.5)$$

$$\mathbf{x}(\alpha_{n1}, t) = \begin{bmatrix} V_1 \\ V_2 \\ V_3 \\ V_4 \\ i_{p1} \\ i_{p2} \end{bmatrix}; \mathbf{B} = \mathbf{L} = \begin{bmatrix} 0 & 0 \\ 0 & 0 \\ 0 & 0 \\ 0 & 0 \\ -1 & 0 \\ 0 & -1 \end{bmatrix}; \alpha_{n1} = i_0(e^{a(v_3-v_4)} - 1) \quad (5.6)$$

The introduction of the constraint variables decomposes the nonlinear network of (5.1) into equation (5.2) and the constraint equations of (5.3). For the purposes of obtaining a reduced order macromodel, the constraint variables are regarded as independent variables and hence, equation (5.2) is treated as a linear system with respect to time t and the

constraint variables $\bar{\alpha}$. This equation can therefore be written in the Laplace domain as

$$s\mathbf{C}\mathbf{X}(\bar{\alpha}, s) + \mathbf{G}\mathbf{X}(\bar{\alpha}, s) + \sum_{k=1}^F \alpha_{nk} \mathbf{h}_{nk} = \mathbf{B}\mathbf{u}(s) + \alpha_s \mathbf{h}_s \quad (5.7)$$

$$\mathbf{i}(s) = \mathbf{L}^T \mathbf{X}(s)$$

The formulation of (5.7) treats $\alpha_{nk} \mathbf{h}_{nk}$ and $\alpha_s \mathbf{h}_s$ as independent variables in the network. A reduced order macromodel is obtained by using a multi-dimensional Krylov subspace method to capture the variance with respect to frequency and the $\bar{\alpha}$ variables.

5.2.2 Construction of Reduced Order Model

The computation of the reduced order model expands $\mathbf{X}(\bar{\alpha}, s)$ of (5.7) into a multidimensional Taylor series expansion with respect to frequency and the $\bar{\alpha}$ variables. For ease of presentation and without loss of generality, a one port macromodel is derived for the case when there is only one constraint variable $\bar{\alpha} = [\alpha_{n1}]$. The vector $\mathbf{X}(\alpha_{n1}, s)$ is expanded into a two-dimensional Taylor series at $s_o = 0$ and $\alpha_{n1o} = 0$, expressed as

$$\mathbf{X}(\alpha_{n1}, s) = \sum_{i=0} \mathbf{M}_{i0} s^i + \sum_{j=1} \mathbf{M}_{0j} (\alpha_{n1})^j + \sum_{i=1} \sum_{j=1} \mathbf{M}_{ij} s^i (\alpha_{n1})^j \quad (5.8)$$

where the first and second summation terms of (5.8) correspond to the self-terms with respect to s and α_{n1} , respectively, and the double summation terms of (5.8) correspond to

the cross terms. The moments of the system are computed by substituting (5.8) into (5.7) and matching coefficients of corresponding powers of s and α_{n1} . This gives following recursive relationship for the frequency moments

$$\begin{aligned}
 \mathbf{M}_{00} &= \mathbf{R} \\
 \mathbf{M}_{10} &= \mathbf{A}\mathbf{M}_{00} \\
 &\dots\dots \\
 \mathbf{M}_{N0} &= \mathbf{A}\mathbf{M}_{(N-1)0}
 \end{aligned} \tag{5.9}$$

where $\mathbf{R} = \mathbf{G}^{-1}\mathbf{B}$ and $\mathbf{A} = -\mathbf{G}^{-1}\mathbf{C}$. Matching the coefficients of corresponding powers of α_{n1} yields

$$\begin{aligned}
 \mathbf{M}_{01} &= -\mathbf{G}^{-1}\mathbf{h}_1 \\
 \mathbf{M}_{0j} &= \mathbf{0}, \text{ for } j = \{2,3,\dots\}
 \end{aligned} \tag{5.10}$$

Only one self moment with respect to α_{n1} is required since the matrices \mathbf{G} and \mathbf{C} are not a function of α_{n1} . Similarly, the nonzero cross moments are

$$\mathbf{M}_{i1} = \mathbf{A}\mathbf{M}_{(i-1)1} \text{ for } i = \{1,2,\dots\} \tag{5.11}$$

Once all the moment coefficients with respect to frequency and α_{n1} are evaluated, the

multidimensional subspace \mathbf{K} is constructed as

$$\mathbf{K} = [\mathbf{M}^s \quad \mathbf{M}^{a_{n1}} \quad \mathbf{M}^X] \quad (5.12)$$

where $\mathbf{M}^s = [\mathbf{M}_{00}, \mathbf{M}_{10}, \mathbf{M}_{20}, \dots, \mathbf{M}_{N0}] \in \mathfrak{R}^{M \times N \cdot P}$ contains the self moments with respect to frequency; $\mathbf{M}^{a_{n1}} = [\mathbf{M}_{01}] \in \mathfrak{R}^M$ contains the self moment with respect to α_{n1} ; $\mathbf{M}^X = [\mathbf{M}_{11}, \mathbf{M}_{21}, \dots, \mathbf{M}_{J1}] \in \mathfrak{R}^{M \times J}$ contains the cross moments; N and J are the number of frequency and cross moments respectively. To derive a P -port macromodel with F constraint variables due to the nonlinear elements and one DC biasing source, the multidimensional subspace \mathbf{K} becomes

$$\mathbf{K} = [\mathbf{M}^s \quad \mathbf{M}^{a_s} \quad \mathbf{M}^{a_{n1}} \quad \mathbf{M}^{a_{n2}} \quad \dots \quad \mathbf{M}^{a_{nF}} \quad \mathbf{M}^X] \quad (5.13)$$

where the size of the moment matrices due to the additional ports and constraint variables are $\mathbf{M}^s \in \mathfrak{R}^{M \times N \cdot P}$; $\mathbf{M}^{a_{nk}} \in \mathfrak{R}^M$; $\mathbf{M}^{a_s} \in \mathfrak{R}^M$; $\mathbf{M}^X \in \mathfrak{R}^{M \times J_T}$. The matrices $\mathbf{M}^{a_{nk}}$ contain the self moment with respect to the α_{nk} variables; \mathbf{M}^{a_s} contains the self moment with respect to α_s variable, and J_T corresponds to the number of cross moments in \mathbf{M}^X . Since the matrix \mathbf{K} is generally ill-conditioned, it is converted into an orthonormal matrix \mathbf{Q} using Arnoldi procedure as [7], [66].

$$\begin{aligned} \text{colspan}(\mathbf{Q}) &= \text{colspan}(\mathbf{K}) \\ \mathbf{Q}^T \mathbf{Q} &= \mathbf{I} \end{aligned} \tag{5.14}$$

where \mathbf{I} is the identity matrix. The reduced order model of (5.1) is obtained by a change of variables

$$\mathbf{x}(\bar{\alpha}, t) = \begin{bmatrix} \mathbf{x}_l(\bar{\alpha}, t) \\ \mathbf{x}_n(\bar{\alpha}, t) \end{bmatrix} = \mathbf{Q} \hat{\mathbf{x}}(\bar{\alpha}, t) = \begin{bmatrix} \mathbf{Q}_l \\ \mathbf{Q}_n \end{bmatrix} \hat{\mathbf{x}}(\bar{\alpha}, t) \tag{5.15}$$

where \mathbf{Q}_l maps the reduced order variables of $\hat{\mathbf{x}}(\bar{\alpha}, t)$ to $\mathbf{x}_l(\bar{\alpha}, t)$ and \mathbf{Q}_n maps $\hat{\mathbf{x}}(\bar{\alpha}, t)$ to $\mathbf{x}_n(\bar{\alpha}, t)$; $\hat{\mathbf{x}}(\bar{\alpha}, t) \in \mathfrak{R}^q$ and $q = N \cdot P + J_T + F + 1$ corresponds to the number of columns in (5.13). Substituting (5.15) into (5.2) and pre-multiplying by \mathbf{Q}^T yields

$$\begin{aligned} \hat{\mathbf{C}} \frac{d\hat{\mathbf{x}}(\bar{\alpha}, t)}{dt} + \hat{\mathbf{G}} \hat{\mathbf{x}}(\bar{\alpha}, t) + \sum_{k=1}^F \alpha_{nk} \hat{\mathbf{h}}_{nk} &= \hat{\mathbf{B}} \mathbf{u}(t) + \alpha_s \hat{\mathbf{h}}_s \\ \mathbf{i}(t) &= \hat{\mathbf{L}}^T \hat{\mathbf{x}}(\bar{\alpha}, t) \end{aligned} \tag{5.16}$$

$$\begin{aligned} \alpha_{nk} &= f_k(\mathbf{Q}_n \hat{\mathbf{x}}(\bar{\alpha}, t), t) \\ \alpha_s &= b_k(t) \end{aligned} \tag{5.17}$$

where

$$\begin{aligned} \hat{\mathbf{C}} &= \mathbf{Q}^T \mathbf{C} \mathbf{Q}; \quad \hat{\mathbf{G}} = \mathbf{Q}^T \mathbf{G} \mathbf{Q}; \quad \hat{\mathbf{h}}_{nk} = \mathbf{Q}^T \mathbf{h}_{nk}; \quad \hat{\mathbf{h}}_s = \mathbf{Q}^T \mathbf{h}_s \\ \hat{\mathbf{B}} &= \mathbf{Q}^T \mathbf{B}; \quad \hat{\mathbf{L}} = \mathbf{Q}^T \mathbf{L}; \quad \mathbf{Q} = \begin{bmatrix} \mathbf{Q}_l \\ \mathbf{Q}_n \end{bmatrix} \end{aligned} \quad (5.18)$$

The size of the reduced order model depends on the order q which is very small compared to the size of the original system. Once the reduced order system of (5.16) and (5.17) is derived, it can be used to obtain the transient response of (5.1).

It is to be noted that with traditional ports any load terminations can be applied to the ports of the reduced order model which is not possible with the proposed constraint variable approach. For example, the α_{n1} variable in Figure 5.1 represents a current variable of a diode, and only functions modeling current can be assigned while using the same reduced order model. If a nonlinear voltage or charge source is assigned to α_{n1} using (5.17), then the reduced order model will give wrong simulation results, since it will treat α_{n1} as a current variable instead of a voltage or charge variable. To model nonlinear elements with different units requires modifying the MNA equations of the original system and recalculating the moments of the reduced order system. Nonetheless, the constraint variable approach provides a mechanism to connect nonlinear elements to reduced order models without significantly increasing the size of the reduced order model. This will be illustrated in the numerical example section.

5.3 Implementation of Proposed Model

This section describes how to create a sparse macromodel and to select the size of the reduced order system.

5.3.1 Creating a Sparse Reduced Order Macromodel

The transient response of (5.16) and (5.17) is obtained using conventional integration techniques such as trapezoid method and Newton-Raphson iterations [91]. This requires inverting the Jacobian matrix which is a function of $\hat{\mathbf{C}}$, $\hat{\mathbf{G}}$ and $(d\alpha_{nk} / d\hat{\mathbf{x}})\hat{\mathbf{h}}_{nk} = (df_k(\mathbf{Q}_n\hat{\mathbf{x}}) / d\hat{\mathbf{x}})\hat{\mathbf{h}}_{nk}$. As a consequence, the Jacobian matrix is dense which can significantly affect the efficiency of the simulation. To improve the simulation time of reduced order models, eigen-transformation techniques [92] have been used to construct sparse reduced order macromodels. However, these methods cannot be directly applied to (5.16) and (5.17) since the model includes constraint variables with nonlinear functions. To obtain a sparse Jacobian matrix, the system of (5.16) and (5.17) is reformulated as

$$\begin{bmatrix} 0 & 0 & 0 \\ 0 & 0 & 0 \\ 0 & 0 & \hat{\mathbf{G}}^{-1}\hat{\mathbf{C}} \end{bmatrix} \begin{bmatrix} d\mathbf{x}_n / dt \\ d\mathbf{x}_\alpha / dt \\ d\hat{\mathbf{x}} / dt \end{bmatrix} + \begin{bmatrix} \mathbf{I} & 0 & -\mathbf{Q}_n \\ 0 & \mathbf{I} & 0 \\ 0 & \mathbf{H} & \mathbf{I} \end{bmatrix} \begin{bmatrix} \mathbf{x}_n \\ \mathbf{x}_\alpha \\ \hat{\mathbf{x}} \end{bmatrix} + \begin{bmatrix} 0 \\ -\mathbf{I} \\ 0 \end{bmatrix} \bar{\alpha} = \begin{bmatrix} 0 \\ 0 \\ \hat{\mathbf{G}}^{-1}\hat{\mathbf{B}} \end{bmatrix} u(t) \quad (5.19)$$

$$\mathbf{i}(t) = \hat{\mathbf{L}}^T \hat{\mathbf{x}}(\bar{\alpha}, t)$$

$$\mathbf{H} = \hat{\mathbf{G}}^{-1} [-\hat{\mathbf{h}}_s \hat{\mathbf{h}}_{n1} \hat{\mathbf{h}}_{n2} \dots \hat{\mathbf{h}}_{nF}] \quad (5.20)$$

$$\mathbf{x}_\alpha = \bar{\alpha} \quad (5.21)$$

$$\alpha_{nk} = f_k(\mathbf{x}_n(\bar{\alpha}, t), t) \quad (5.22)$$

Note that the nonlinear functions of (5.22) depend on \mathbf{x}_n by substituting (5.15) (i.e. $\mathbf{x}_n(\bar{\alpha}, t) = \mathbf{Q}_n \hat{\mathbf{x}}(\bar{\alpha}, t)$) into (5.17). As a result, extra equations have been introduced in (5.19) which define the relationship of the \mathbf{x}_n variables to the $\hat{\mathbf{x}}$ variables, and \mathbf{x}_α to the nonlinear functions. Next, to create a sparse system of equations for (5.19), $\hat{\mathbf{G}}^{-1}\hat{\mathbf{C}}$ is converted to a diagonal matrix following the procedure of [92], as

$$\hat{\mathbf{G}}^{-1}\hat{\mathbf{C}} = \mathbf{VDV}^{-1} \quad (5.23)$$

where \mathbf{D} is a diagonal matrix containing the eigenvalues, and \mathbf{V} contains the corresponding eigenvectors. Since $\hat{\mathbf{G}}^{-1}\hat{\mathbf{C}}$ is a real matrix, any complex eigenvalue or eigenvector will have a conjugate and hence, real matrices can be obtained using the following similarity transform

$$\mathbf{V}_r = \mathbf{VP}^{-1} \quad \text{and} \quad \mathbf{D}_r = \mathbf{PDP}^{-1} \quad (5.24)$$

where the entries in the transformation matrix \mathbf{P} are defined in the following manner

- If $\mathbf{D}_{i,j}$ is real, $\mathbf{P}_{i,i} = 1$

- If $\mathbf{D}_{i,j} = \bar{\mathbf{D}}_{i+1,j+1}$, $\mathbf{P}_{i:i+1, i:i+1} = \begin{bmatrix} 1 & 1 \\ j & -j \end{bmatrix}$

The eigen-decomposition of the real matrix $\hat{\mathbf{G}}^{-1}\hat{\mathbf{C}}$ can then be expressed as

$$\hat{\mathbf{G}}^{-1}\hat{\mathbf{C}} = \mathbf{V}_r\mathbf{D}_r\mathbf{V}_r^{-1} \quad (5.25)$$

Using (5.25), the system of (5.19) is expressed as

$$\begin{bmatrix} 0 & 0 & 0 \\ 0 & 0 & 0 \\ 0 & 0 & \mathbf{D}_r \end{bmatrix} \begin{bmatrix} d\mathbf{x}_n / dt \\ d\mathbf{x}_\alpha / dt \\ d\tilde{\mathbf{x}} / dt \end{bmatrix} + \begin{bmatrix} \mathbf{I} & 0 & -\tilde{\mathbf{Q}}_n \\ 0 & \mathbf{I} & 0 \\ 0 & \tilde{\mathbf{H}} & \mathbf{I} \end{bmatrix} \begin{bmatrix} \mathbf{x}_n \\ \mathbf{x}_\alpha \\ \tilde{\mathbf{x}} \end{bmatrix} + \begin{bmatrix} 0 \\ -\mathbf{I} \\ 0 \end{bmatrix} \bar{\alpha} = \begin{bmatrix} 0 \\ 0 \\ \tilde{\mathbf{B}} \end{bmatrix} u(t) \quad (5.26)$$

$$\mathbf{i}(t) = \tilde{\mathbf{L}}^T \tilde{\mathbf{x}}(\bar{\alpha}, t)$$

where

$$\begin{aligned} \tilde{\mathbf{x}} &= \mathbf{V}_r^{-1} \mathbf{Q}^T \mathbf{x}; & \tilde{\mathbf{Q}}_n &= \mathbf{Q}_n \mathbf{V}_r; & \tilde{\mathbf{H}} &= \mathbf{V}_r^{-1} \mathbf{H}; \\ \tilde{\mathbf{B}} &= \mathbf{V}_r^{-1} \hat{\mathbf{G}}^{-1} \mathbf{Q}^T \mathbf{B}; & \tilde{\mathbf{L}} &= \mathbf{V}_r^T \mathbf{Q}^T \mathbf{L} \end{aligned} \quad (5.27)$$

Using the formulation of (5.26), (5.20)-(5.22) the matrices \mathbf{D}_r and \mathbf{I} are sparse, while the matrices $\tilde{\mathbf{Q}}_n$, $\tilde{\mathbf{H}}$, $\tilde{\mathbf{B}}$ and $\tilde{\mathbf{L}}$ are dense. In addition the contribution of the nonlinear elements to the Jacobian matrix (i.e. $d\bar{\alpha} / d \mathbf{x}_n$) is also a dense matrix. The size of the sparse matrix \mathbf{D}_r depends only on the number of $\tilde{\mathbf{x}}$ variables, while the sizes of the dense matrices depend on the number of \mathbf{x}_n or \mathbf{x}_α variables or the number of ports. Typically, nonlinear distributed networks comprised of high frequency components such as interconnects have relatively fewer variables that are governed by nonlinearities when compared to the size of the reduced system (i.e. $\tilde{\mathbf{x}} \gg \mathbf{x}_n + \mathbf{x}_\alpha$). As a result, the formulation of (5.26), (5.20)-(5.22) is relatively sparse and the extra variables \mathbf{x}_n and \mathbf{x}_α allow for fewer nonzero entries to the Jacobian matrix from the nonlinear functions.

5.3.2 Selecting the Order of the Reduced Order Model

The accuracy of (5.26), (5.20)-(5.22) depends on the rate of change of the applied signals at the ports and well as the variance of the α_{nk} variables due to the nonlinear elements. In most cases, it may not be possible to a priori determine the variance of the nonlinear function without solving the original problem. Furthermore, the proposed algorithm provides a mechanism to replace the nonlinear functions of (5.22) with other functions of similar units. For example, the nonlinear diode of Figure 5.1 can be replaced with another nonlinear current function. As a result, to test the accuracy for different modeling scenarios, the reduced order model is verified at two levels: the first level determines the initial size of the reduced order model and the second level verifies the accuracy of the transient response. If the transient response of the reduced order model does not satisfy the error tolerances of the simulation, a procedure is described to increase the order of the reduced order system.

At the first level, the frequency response of the reduced model is evaluated when the α_{nk} and α_s variables are treated as independent sources in the network. For this purpose, the reduced order model is considered to be a linear network similar to (5.7) and is expressed as

$$(s\hat{\mathbf{C}} + \hat{\mathbf{G}})\hat{\mathbf{x}}(\bar{\alpha}, s) + \sum_{k=1}^F \alpha_{nk} \hat{\mathbf{h}}_{nk} = \hat{\mathbf{B}}\mathbf{u}(s) + \alpha_s \hat{\mathbf{h}}_s \quad (5.28)$$

$$\mathbf{i}(t) = \hat{\mathbf{L}}^T \hat{\mathbf{x}}(\bar{\alpha}, t)$$

To capture the variance of frequency, α_{nk} and α_s are set to zero and the frequency response is evaluated at the ports by computing the differences between two successive orders of approximations as described in [88]- [89]. If the error difference between the two models is below a given tolerance for the frequency range of interest, then the reduced model is assumed to be accurate. Otherwise additional frequency moments using (5.9) or multiple expansion points [13] can be used to improve the accuracy of the frequency response. To capture the variance of α_{nk} and α_s only one moment is required for each constraint variable as illustrated in section 5.2.2. Following the above steps provides an efficient means to estimate the initial size of the reduced order model.

However, the accuracy of (5.26), (5.20)-(5.22) is not assured without a second level of verification which checks the variances of α_{nk} and α_s due to the nonlinear functions and biasing conditions. For this purpose, the residual error of (5.1) is verified in the time domain as

$$\varepsilon = \frac{\left\| \mathbf{C} \frac{d\mathbf{x}(t)}{dt} + \mathbf{G}\mathbf{x}(t) + \mathbf{f}(\mathbf{x}_n(t), t) - \mathbf{B}\mathbf{u}(t) - \mathbf{b}(t) \right\|}{\|\mathbf{x}(t)\|} \quad (5.29)$$

where $\mathbf{x}(t)$ is the approximate solution of (5.26), (5.20)-(5.22) given by (5.15) and $\| \cdot \|$ denotes the magnitude of function. Furthermore, the residual error of each nonlinear equation of (5.1) is also examined as

$$\varepsilon_{nk} = \frac{\left\| \mathbf{C}_k \frac{d\mathbf{x}(t)}{dt} + \mathbf{G}_k \mathbf{x}(t) + f_k(\mathbf{x}_n(t), t) - \mathbf{B}_k \mathbf{u}(t) - b_k(t) \right\|}{\|f_k(\mathbf{x}_N(t), t)\|} \quad (5.30)$$

where \mathbf{C}_k , \mathbf{G}_k , $f_k(\mathbf{x}_n(t), t)$, \mathbf{B}_k and b_k are the row entries of \mathbf{C} , \mathbf{G} , $\mathbf{f}(\mathbf{x}_n(t), t)$, \mathbf{B} and \mathbf{b} , respectively, when $f_k(\mathbf{x}_n(t), t)$ is nonzero. For the example presented in Figure 5.1, the residual errors due to the nonlinear functions are

$$\begin{aligned} \varepsilon_{n3} &= \frac{\left\| -G_1 V_1 + (G_1 + G_2 + G_3) V_3 - G_3 V_4 + i_0 (e^{a(v_3 - v_4)} - 1) \right\|}{\|i_0 (e^{a(v_3 - v_4)} - 1)\|} \\ \varepsilon_{n4} &= \frac{\left\| -G_3 V_3 + (G_3 + G_4) V_4 - C_1 d(V_2 - V_4)/dt - i_0 (e^{a(v_3 - v_4)} - 1) \right\|}{\|i_0 (e^{a(v_3 - v_4)} - 1)\|} \end{aligned} \quad (5.31)$$

If the residual errors ε and ε_{nk} are below the specified tolerances, then the reduced order model of (5.26), (5.20)-(5.22) is assumed to be accurate. Otherwise additional frequency and cross moments are added as follows: if the threshold of (5.29) is not satisfied additional frequency moments are added and if the threshold of (5.30) is not satisfied additional cross-moments are added.

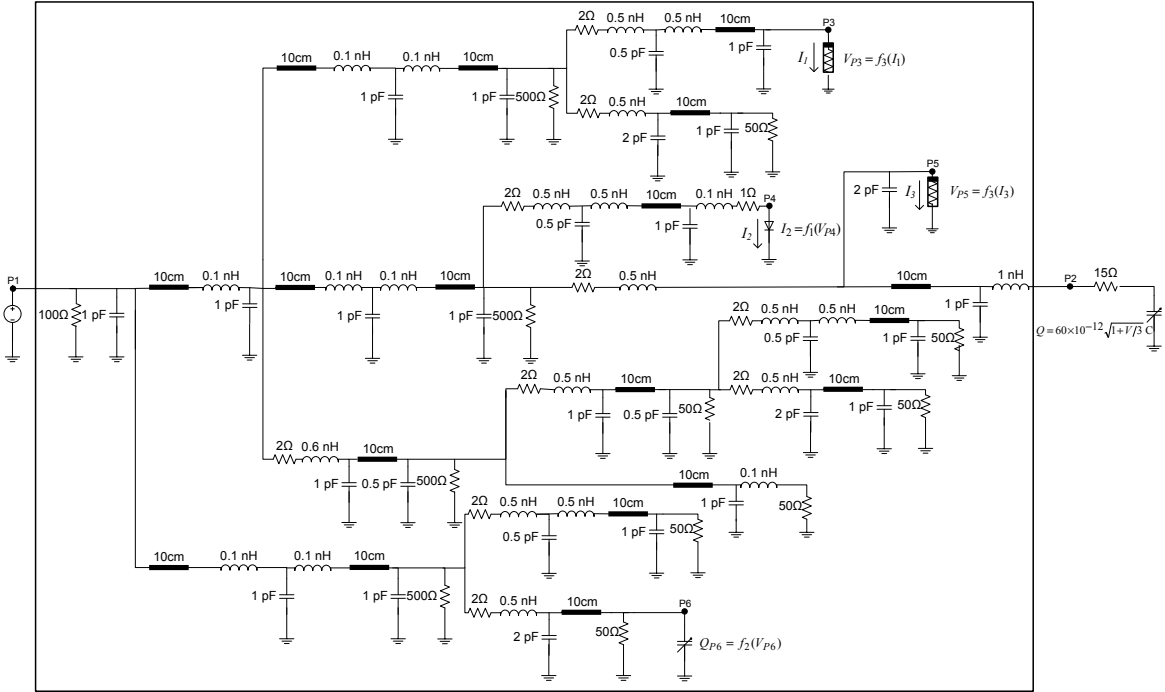


Figure 5.2 Nonlinear Distributed Interconnect Network (Example 5.1).

5.4 Computational Results

Two examples are presented in this section to illustrate the validity and efficiency of the proposed method. The developed algorithm was implemented in MATLAB [87], and the macromodels were realized in HSPICE [72] using the Laplace elements. All computations were performed on an Intel Xeon (3.16 GHz) personal computer with 3.25 GB memory.

5.4.1 Numerical Example 5.1

The first example illustrates an eighteen transmission line subnetwork with three different types of nonlinear elements: two nonlinear voltage sources connected to nodes P3 and P5; a nonlinear current source connected to node P4; and a nonlinear capacitor connected to node P6, as shown in Figure 5.2. The functions of the nonlinear elements are

$$\begin{aligned}
 f_1(v) &= i = 2.682 \times 10^{-9} (e^{21.11v} - 1) A \\
 f_2(v) &= q = 60 \times 10^{-12} \sqrt{1 + v/3} C \\
 f_3(i) &= v = 0.1i(1 + 3.2 \times 10^6 i^6) V
 \end{aligned} \tag{5.32}$$

The per-unit-length parameters of the interconnect lines are $L=10$ nH/m, $C=1.64$ nF/m, $R=5\Omega/m$ and $G=1e-3$ mho/m and the length of each line is 10cm. The interconnect lines were discretized using the conventional lumped model [56] and the MNA equations contained 4386 unknown variables. Using the constraint variable macromodel described in sections 5.3 and 5.5, a two port macromodel is created at nodes P1 and P2 and four constraint variables are used to connect the four nonlinear elements to nodes P3, P4, P5 and P6. Port P1 is connected to a voltage source and port P2 is terminated with a resistance and a nonlinear capacitor (Figure 5.2). The size of the reduced order model is determined following the procedure of section 5.3. To match the frequency response of (5.28) up to 4 GHz, 70 moments with respect to frequency were required for a single

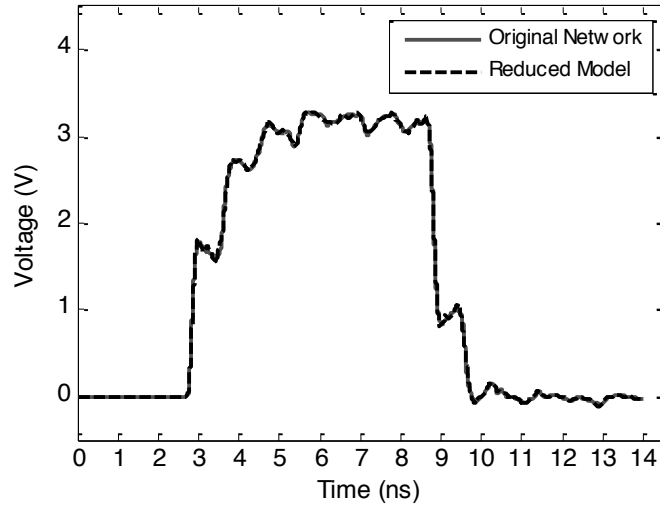


Figure 5.3 The transient response at node P2 for simulation of equation (5.32) (Example 5.1).

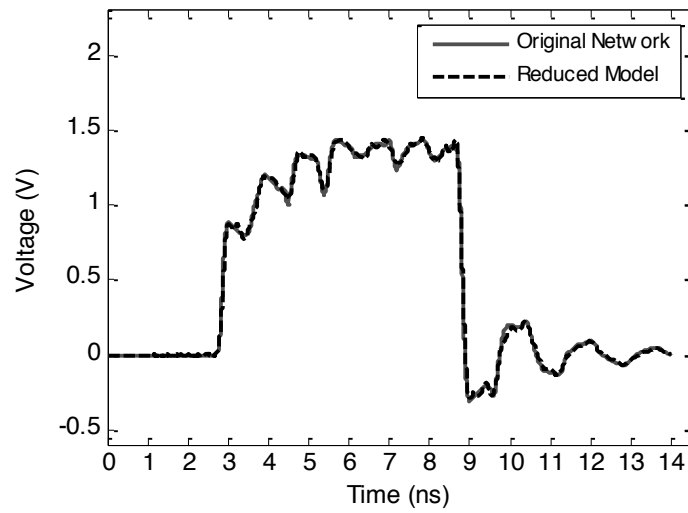


Figure 5.4 The transient response at node P2 for simulation of equation (5.33) (Example 5.1).

Table 5.1 CPU Run Time and Macromodel Size Comparison -Example 5.1.

	Nonlinear Functions of (32)			Nonlinear Functions of (33)		
	Original	Reduced	Savings	Original	Reduced	Savings
Macromodel Size	4386	156	96.44%	4386	156	96.44%
CPU Run Time(s)	85.55	7.33	91.43%	91.56	7.80	91.40%

expansion point at $s_0 = 0$ and $\alpha_{nko} = 0$. To capture the variance of the nonlinear elements required 4 moments for the α_{nk} variables and 4 cross moments to achieve error tolerances of $\varepsilon < 5 \times 10^{-3}$ for (5.29) and $\varepsilon_{nk} < 3 \times 10^{-3}$ for (5.30). The total size of the reduced order model of (5.26), (5.20)-(5.22) contained 156 unknown variables. The eigenvalue pre-processing technique yielded 94% sparse macromodel for (5.26). Figure 5.3 shows the transient response at node P2, corresponding to a unit input pulse with rise/fall time of 0.1ns and a pulse width of 6 ns for the reduced order macromodel and the original system. The reduced system obtained using the proposed approach shows good agreement with the results of the conventional lumped model.

As mentioned in section 5.3, the proposed algorithm provides a mechanism to change the nonlinear functions inside the reduced order system, provided that the variables of the nonlinear functions are the same. To illustrate this point, the nonlinear functions at P3, P4, P5 and P6, defined by (5.32) are changed to

$$\begin{aligned}
 f_1(v) &= i = 1.415 \times 10^{-9} (e^{43.6v} - 1) A \\
 f_2(v) &= q = 30.68 \times 10^{-12} \sqrt{1 + v/2.3} C \\
 f_3(i) &= v = 0.05i(1 + 0.1 \times 10^3 i^2) V
 \end{aligned} \tag{5.33}$$

The transient response using the nonlinear functions of (5.33) corresponding to a unit input pulse with rise/fall time of 0.1ns and a pulse width of 6 ns is shown in Figure 5.4. It is to be noted that the transient response of Figure 5.4 differs from Figure 5.3 due to the change of nonlinear functions inside the reduced order model which is accurately captured using the proposed algorithm. Table 5.1 compares the size and simulation time of the reduced system and the original lumped system. For this example the proposed method is about 12 times faster when compared to the original lumped system.

5.4.2 Numerical Example 5.2

The second example is a 2-port nonlinear subnetwork terminated with nonlinear CMOS inverters as shown in Figure 5.5. The nonlinear subnetwork contains three five-coupled transmission lines and two CMOS inverters. The CMOS inverters employed in this

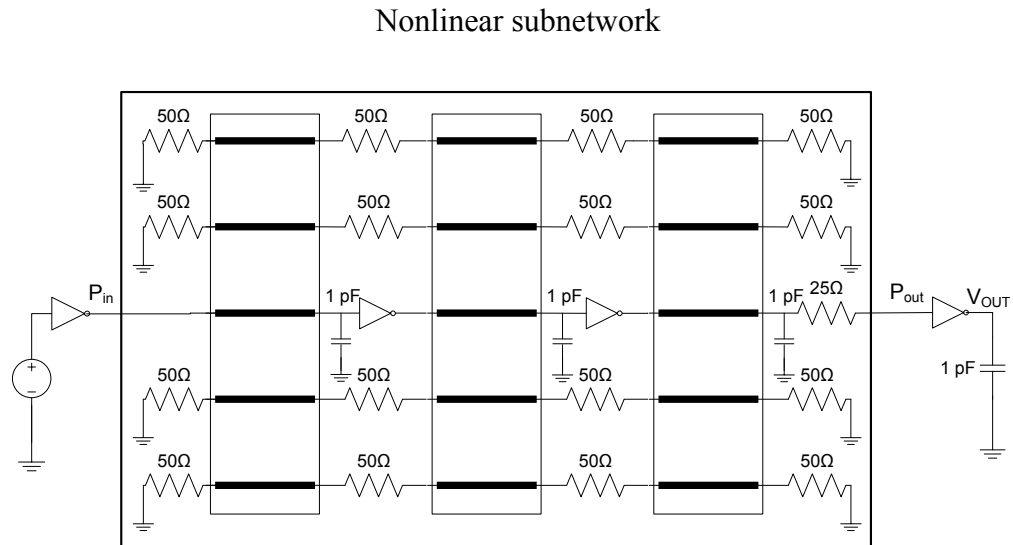


Figure 5.5 A coupled interconnect network with inverter terminations (Example 5.2).

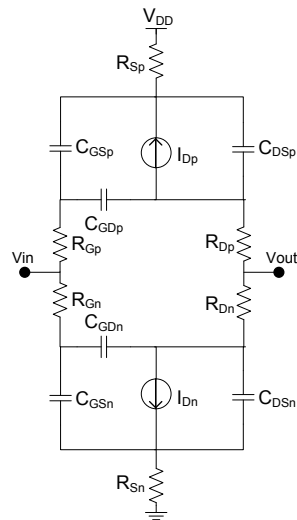


Figure 5.6 Dynamic large-signal model of CMOS inverter (Example 5.2).

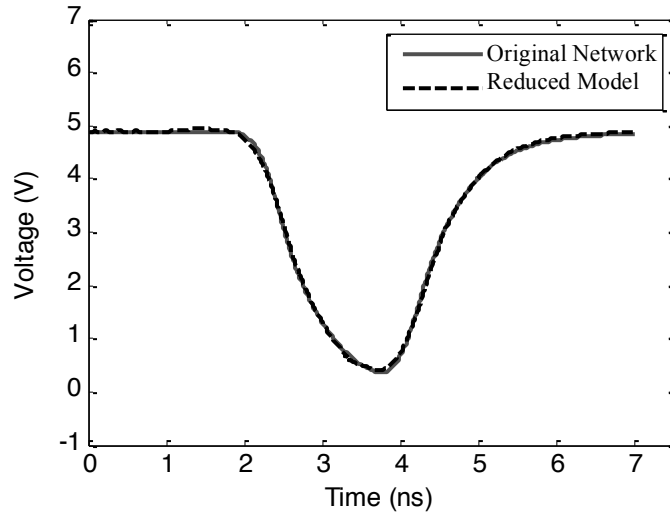
nonlinear example were characterized by MOSFET dynamic large-signal model introduced by [93].

The inverter model, shown in Figure 5.6, consists of two nonlinear current sources and a biasing source which can be considered as constraint variables as described in sections 5.3 and 5.4. The per-unit-length parameters of the transmission line used in this example are

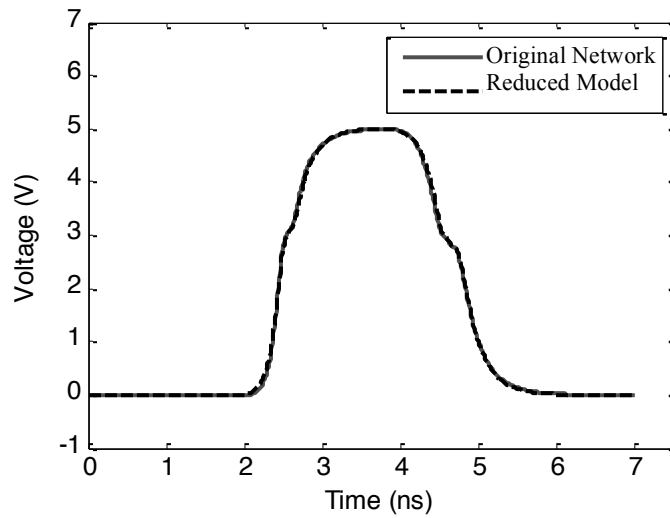
$$\mathbf{R} = \begin{bmatrix} 3.3 & 0 & 0 & 0 & 0 \\ 0 & 3.3 & 0 & 0 & 0 \\ 0 & 0 & 3.3 & 0 & 0 \\ 0 & 0 & 0 & 3.3 & 0 \\ 0 & 0 & 0 & 0 & 3.3 \end{bmatrix} \text{K}\Omega/\text{m}, \quad \mathbf{G} = \mathbf{0}$$

$$\mathbf{C} = \begin{bmatrix} 139.897 & -30.785 & -1.906 & -0.381 & -0.195 \\ -30.785 & 153.674 & -30.514 & -1.850 & -0.382 \\ -1.906 & -30.514 & 153.693 & -30.514 & -1.907 \\ -0.381 & -1.850 & -30.514 & 153.673 & -30.789 \\ -0.195 & -0.382 & -1.907 & -30.789 & 140.136 \end{bmatrix} \text{pF/m} \quad (5.34)$$

$$\mathbf{L} = \begin{bmatrix} 497.842 & 164.707 & 76.965 & 139.897 & 25.539 \\ 164.707 & 490.66 & 162.252 & 76.043 & 41.775 \\ 76.965 & 162.252 & 489.489 & 162.252 & 76.964 \\ 139.897 & 76.043 & 162.252 & 490.660 & 164.707 \\ 25.539 & 41.775 & 76.964 & 164.707 & 497.481 \end{bmatrix} \text{nH/m}$$



(a)



(b)

Figure 5.7 The transient response at nodes (a) P_{out} , and (b) V_{OUT} (Example 5.2).

Table 5.2 CPU Run Time and Macromodel Size Comparison- Example 5.2.

	Original	Reduced	Savings
Macromodel Size	3848	101	97.37%
CPU Run Time(s)	22.50	1.08	95.20%

and the length of each line is 5cm. The interconnect lines were discretized using the conventional lumped model [56] and the MNA equations contained 3848 variables. Using the constraint variable macromodel described in sections 5.3 and 5.4, a two port macromodel is created at nodes P_{in} and P_{out} and five constraint variables are used to connect the two inverters to the reduced order model. The size of the reduced order model required 40 moments with respect to frequency to match the frequency response network of (5.28) up to 4GHz for a single expansion point at $s_0 = 0$ and $\alpha_{nko} = 0$. To capture the variance of the CMOS invertors requires 5 moments for the α_{nk} variables and 5 cross moments to achieve error tolerances of $\varepsilon < 6 \times 10^{-3}$ for (5.29) and $\varepsilon_{nk} < 4 \times 10^{-3}$ for (5.30). The total size of the reduced order model of (5.26), (5.20)-(5.22) contained 101 unknown variables. The eigenvalue pre-processing technique yielded 89% sparse

macromodel for (5.26). Figure 5.7 shows the transient response at nodes P_{out} , and V_{OUT} , corresponding to a unit input pulse with rise/fall time of 0.1ns and a pulse width of 2 ns for the proposed macromodel and original system. Once again, the reduced order system shows good agreement with the results of the conventional lumped model. Table 5.2 shows good agreement with the results of the conventional lumped model. Table 5.2 compares the size and simulation time of the reduced and original systems. For this example, the proposed algorithm is about 20 times faster compared to the conventional lumped model.

Chapter 6

6 Compact Parameterized Model Order Reduction of Weakly Nonlinear System

In this chapter, parameterized model order reduction techniques are extended for weakly nonlinear systems. The proposed algorithm uses a multidimensional subspace method along with variational analysis and singular value decomposition to capture the variances of design parameters and approximates the weakly nonlinear functions as Taylor series. Such an approach is significantly more CPU efficient in optimization and design space exploration problems since a new reduced model is not required each time a design parameter is modified.

The organization of this chapter is as follows: the development of the proposed parametric model order reduction algorithm is described in section 6.1. A methodology for addressing the compactness of parameterized reduced model is presented in

section 6.2 and numerical examples are provided in section 6.3.

6.1 Developing of the Parameterized Reduced Order Model

To derive a parametric reduced order model, the system of (3.12) is expressed as a function of the time and design parameters $\bar{\lambda} = [\lambda_1, \lambda_2, \dots, \lambda_k]$ as

$$\begin{aligned} \mathbf{C}(\bar{\lambda}) \frac{d\mathbf{x}(t, \bar{\lambda})}{dt} + \mathbf{G}(\bar{\lambda})\mathbf{x}(t, \bar{\lambda}) + \mathbf{f}(\mathbf{x}(t, \bar{\lambda}), \bar{\lambda}) &= \mathbf{B}\mathbf{u}(t), \\ \mathbf{i} &= \mathbf{L}^T \mathbf{x}(t, \bar{\lambda}), \end{aligned} \quad (6.1)$$

The system of (6.1) can also be expressed in a form similar to (3.22) by using a polynomial expansion for the nonlinear function

$$\begin{aligned} \mathbf{C}(\bar{\lambda}) \frac{d\mathbf{x}(t, \bar{\lambda})}{dt} + \mathbf{G}_1(\bar{\lambda})\mathbf{x}(t, \bar{\lambda}) + \mathbf{G}_2(\bar{\lambda})\mathbf{x}(t, \bar{\lambda}) \otimes \mathbf{x}(t, \bar{\lambda}) + \\ \mathbf{G}_3(\bar{\lambda})\mathbf{x}(t, \bar{\lambda}) \otimes \mathbf{x}(t, \bar{\lambda}) \otimes \mathbf{x}(t, \bar{\lambda}) + \dots &= \mathbf{B}\mathbf{u}(t) \end{aligned} \quad (6.2)$$

Following a procedure similar to (3.24) the variables of $\mathbf{x}(t, \bar{\lambda})$ is expanded as a power series with respect to a variational parameter a ,

$$\mathbf{x}(t, \bar{\lambda}) = a\mathbf{x}_1(t, \bar{\lambda}) + a^2\mathbf{x}_2(t, \bar{\lambda}) + a^3\mathbf{x}_3(t, \bar{\lambda}) + \dots \quad (6.3)$$

Substituting (6.3) in (6.2) and matching the coefficients of corresponding powers of a the

system can be recursively obtained by solving the same parameterized linear system under different inputs.

$$\begin{aligned} \mathbf{C}(\bar{\lambda}) \frac{d\mathbf{x}_1(t, \bar{\lambda})}{dt} + \mathbf{G}_1(\bar{\lambda}) \mathbf{x}_1(t, \bar{\lambda}) &= \mathbf{B}\mathbf{u}(t), & (a) \\ \mathbf{C}(\bar{\lambda}) \frac{d\mathbf{x}_2(t, \bar{\lambda})}{dt} + \mathbf{G}_1(\bar{\lambda}) \mathbf{x}_2(t, \bar{\lambda}) &= -\mathbf{G}_2(\bar{\lambda}) \mathbf{x}_1(t, \bar{\lambda}) \otimes \mathbf{x}_1(t, \bar{\lambda}) & (b) \end{aligned} \quad (6.4)$$

...

The system of (6.4.a) is treated as a linear state space system and can be expressed in the Laplace domain as

$$\mathbf{Y}(s, \bar{\lambda}) \mathbf{X}_1(s, \bar{\lambda}) = \mathbf{B}\mathbf{u}(s) \quad (6.5)$$

where $\mathbf{Y}(s, \bar{\lambda}) = s\mathbf{C}(\bar{\lambda}) + \mathbf{G}_1(\bar{\lambda})$. For ease of presentation and without loss of generality, the method is described for the case when there is only one design parameter $\bar{\lambda} = [\lambda]$. The vector $\mathbf{X}_1(s, \bar{\lambda})$ is expanded into a multidimensional Taylor series [42], expressed as

$$\mathbf{X}_1(s, \lambda) = \mathbf{M}_0 + \sum_{k=1}^{\infty} s^k \mathbf{M}_{s^k} + \sum_{l=1}^{\infty} \lambda^l \mathbf{M}_{\lambda^l} + \sum_{k=1}^{\infty} \sum_{l=1}^{\infty} s^k \lambda^l \mathbf{M}_{s^k \lambda^l} \quad (6.6)$$

Substituting (6.6) into (6.5) and matching coefficients of corresponding powers of frequency and design parameters yields the following recursive relationship for frequency moments,

$$\begin{aligned} \mathbf{Y}(0, \lambda_0) \mathbf{M}_0 &= \mathbf{B} \\ \mathbf{Y}(0, \lambda_0) \mathbf{M}_i^s &= - \left. \frac{\partial}{\partial s} \mathbf{Y}(s, \lambda_0) \right|_{s=0} \mathbf{M}_{i-1}^s \end{aligned} \quad (6.7)$$

Similarly, matching coefficients of similar powers of λ yields

$$\mathbf{Y}(0, \lambda_0) \mathbf{M}_j^\lambda = \sum_{l=1}^{j-1} \frac{1}{l!} \frac{\partial^l}{\partial \lambda^l} \mathbf{Y}(0, \lambda) \Big|_{\lambda=\lambda_0} \mathbf{M}_{j-l}^\lambda \quad (6.8)$$

The cross moments of $s^i \lambda^j$ are also computed by matching corresponding coefficients of powers of cross terms as

$$\mathbf{Y}(0, \lambda_0) \mathbf{M}_{ij}^{s\lambda} = - \sum_{l=1}^j \frac{1}{l!} \frac{\partial}{\partial s} \frac{\partial^l}{\partial \lambda^l} \mathbf{Y}(s, \lambda) \Big|_{\lambda=\lambda_0, s=0} \mathbf{M}_{i-1, j-l}^{s\lambda} \quad (6.9)$$

Once all the required moments with respect to frequency and parameters are evaluated, the multidimensional subspace \mathbf{Q}_1^p is constructed using multi-order Arnoldi [54] as

$$\mathbf{Q}_1^p = \text{colspan} \left(\begin{bmatrix} \mathbf{M}^s & \mathbf{M}^\lambda & \mathbf{M}^X \end{bmatrix} \right) \quad (6.10)$$

where \mathbf{M}^s contains the series coefficients corresponding to powers of s , \mathbf{M}^λ contains the series coefficients corresponding to powers of λ , and \mathbf{M}^X contains the cross-term coefficients. To derive a reduced model with multiple parameters, the multidimensional

subspace \mathbf{Q}_1^p becomes

$$\mathbf{Q}_1^p = \text{colspan} \left(\left[\begin{array}{ccc} \mathbf{M}^s & \mathbf{M}^{\bar{\lambda}} & \mathbf{M}^{\bar{x}} \end{array} \right] \right) \quad (6.11)$$

where $\mathbf{M}^{\bar{\lambda}} = [\mathbf{M}^{\lambda_1} \quad \mathbf{M}^{\lambda_2} \quad \dots]$ corresponds to the self-moments coefficients of different parameters and $\mathbf{M}^{\bar{x}}$ contains the parameter-frequency and parameter-parameter cross-term moment coefficients. The reduced order model of (6.4.a) is obtained by a change of variables $\mathbf{x}_1(t, \bar{\lambda}) = \mathbf{Q}_1^p \hat{\mathbf{x}}_1(t, \bar{\lambda})$. Using the identity $(\mathbf{Q}_1^p \hat{\mathbf{x}}_1(t, \bar{\lambda})) \otimes (\mathbf{Q}_1^p \hat{\mathbf{x}}_1(t, \bar{\lambda})) = (\mathbf{Q}_1^p \otimes \mathbf{Q}_1^p) (\hat{\mathbf{x}}_1(t, \bar{\lambda}) \otimes \hat{\mathbf{x}}_1(t, \bar{\lambda}))$ and substituting $\mathbf{x}_1(t, \bar{\lambda}) = \mathbf{Q}_1^p \hat{\mathbf{x}}_1(t, \bar{\lambda})$ in (6.4.b) to minimize the number of input variables, yields

$$\mathbf{C}(\bar{\lambda}) \frac{d\mathbf{x}_2(t, \bar{\lambda})}{dt} + \mathbf{G}_1(\bar{\lambda}) \mathbf{x}_2(t, \bar{\lambda}) = \mathbf{B}_2 \mathbf{u}_2(t), \quad (6.12)$$

where $\mathbf{B}_2 = -\mathbf{G}_2(\bar{\lambda}) (\mathbf{Q}_1^p \otimes \mathbf{Q}_1^p)$ and $\mathbf{u}_2(t) = \hat{\mathbf{x}}_1(t, \bar{\lambda}) \otimes \hat{\mathbf{x}}_1(t, \bar{\lambda})$. Now, an orthonormal multidimensional basis \mathbf{Q}_2^p can be calculated following a procedure similar to (6.5)-(6.11). This procedure can be repeated to calculate higher orders of the nonlinear expansion. Once all the moment coefficients for the systems of (6.4) are evaluated, the \mathbf{Q}^p is constructed as

$$\text{colspan}(\mathbf{Q}^p) = \text{colspan}\left(\left[\begin{array}{ccc} \mathbf{Q}_1^p & \mathbf{Q}_2^p & \cdots \end{array}\right]\right) \quad (6.13)$$

Next, substituting $\mathbf{x}(t, \bar{\lambda}) = \mathbf{Q}^p \hat{\mathbf{x}}(t, \bar{\lambda})$ and pre-multiplying by \mathbf{Q}^{p^T} in (6.2) yields the following parameterized reduced order system.

$$\begin{aligned} \hat{\mathbf{C}}(\bar{\lambda}) \frac{d\hat{\mathbf{x}}(t, \bar{\lambda})}{dt} + \hat{\mathbf{G}}_1(\bar{\lambda}) \hat{\mathbf{x}}(t, \bar{\lambda}) + \hat{\mathbf{G}}_2(\bar{\lambda}) \hat{\mathbf{x}}(t, \bar{\lambda}) \otimes \hat{\mathbf{x}}(t, \bar{\lambda}) + \\ \hat{\mathbf{G}}_3(\bar{\lambda}) \hat{\mathbf{x}}(t, \bar{\lambda}) \otimes \hat{\mathbf{x}}(t, \bar{\lambda}) \otimes \hat{\mathbf{x}}(t, \bar{\lambda}) + \cdots = \hat{\mathbf{B}} \mathbf{u}(t), \quad (6.14) \\ \mathbf{i}(t) = \hat{\mathbf{L}}^T \hat{\mathbf{x}}(t, \bar{\lambda}), \end{aligned}$$

where

$$\begin{aligned} \hat{\mathbf{C}}(\bar{\lambda}) = \mathbf{Q}^{p^T} \mathbf{C}(\bar{\lambda}) \mathbf{Q}^p, \quad \hat{\mathbf{G}}_1(\bar{\lambda}) = \mathbf{Q}^{p^T} \mathbf{G}_1(\bar{\lambda}) \mathbf{Q}^p, \\ \hat{\mathbf{G}}_2(\bar{\lambda}) = \mathbf{Q}^{p^T} \mathbf{G}_2(\bar{\lambda}) \mathbf{Q}^p \otimes \mathbf{Q}^p, \quad \cdots, \quad \hat{\mathbf{B}} = \mathbf{Q}^{p^T} \mathbf{B}, \quad \hat{\mathbf{L}} = \mathbf{Q}^{p^T} \mathbf{L} \end{aligned} \quad (6.15)$$

The formulation of (6.14) addresses the issue of obtaining a parametric reduced order model. However as the number of parameters and the variance of parameters increase, more moments are required which increases the size of (6.14). In addition $\hat{\mathbf{G}}_1, \hat{\mathbf{G}}_2, \dots$ in (6.14) are large and dense matrices, where the size of these matrices grows exponentially with the order of polynomial expansion in (6.2) and (6.3). In order to address the above concerns the next section describes an SVD algorithm to improve the efficiency of (6.14).

6.2 Improving the Efficiency of Reduced Order Model using SVD

The moments with respect to frequency, design parameters and cross moments in (6.11) results in a large terminal matrix \mathbf{B}_2 . This increases the computational complexity of the reduced order model of (6.14). In section 6.2.1 it is shown that frequency, design parameter and cross moments of the second order nonlinear system in (6.4.b) only depend on moments of the pervious system (6.4.a) with the same or smaller order. As a result, the higher order moments of (6.11) may not be required to construct \mathbf{B}_2 in (6.12) and are only used to create the subspace of (6.13). This results in much smaller sized terminal matrix \mathbf{B}_2 .

In addition, the vectors of \mathbf{B}_2 may not be independent which causes the redundant frequency domain moments and reduces the efficiency of reduced model order model. To remove the redundant moments, a terminal reduction framework [94]- [95] using SVD is described in section 6.2.2, which leads to a more compact reduced order model in (6.14).

6.2.1 Relationship of Moments in (6.4)

This section shows that the moments with respect to frequency, design parameters and cross moments for the second order nonlinear systems of (6.4.b) depend on the same or

lower order moments of (6.4.a). This proof can be extended to higher order of nonlinear expansion in (6.4).

For ease of presentation and without loss of generality, the MNA equations is derived for a single-input multi-output weakly nonlinear system in (6.1) where the system has parameter dependency only in terminal matrix \mathbf{B} . The nonlinear transfer functions presented in (6.14.b) can be expressed in the two dimensional Laplace domain [84], [96] as

$$[\mathbf{G}_1 + (s_1 + s_2)\mathbf{C}_1]\mathbf{X}_2(s_1, s_2, \lambda) = -\mathbf{G}_2(\mathbf{X}_1(s_1, \lambda) \otimes \mathbf{X}_1(s_2, \lambda)) \quad (6.16)$$

where $\mathbf{X}_1(s, \lambda)$ is defined by (6.6) and

$$\mathbf{X}_2(s_1, s_2, \lambda) = \mathbf{M}'_0 + \sum_{k=1}^{\infty} s_1^k \mathbf{M}'_{s_{1k}} + \sum_{m=1}^{\infty} s_2^m \mathbf{M}'_{s_{2m}} + \sum_{l=1}^{\infty} \lambda^l \mathbf{M}'_{\lambda_l} + \sum_{k=0}^{\infty} \sum_{m=0}^{\infty} \sum_{l=0}^{\infty} s_1^k s_2^m \lambda^l \mathbf{M}'_{s_{\lambda_{kml}}} \quad (6.17)$$

Substituting (6.17) and (6.6) for $s = s_1$ and $s = s_2$ into (6.16) and matching coefficients of corresponding powers of frequencies s_1 , s_2 and parameter λ yields the following recursive relationships for the moments,

$$\mathbf{M}'_0 = \mathbf{G}_1^{-1} \mathbf{G}_2 \mathbf{M}_0 \otimes \mathbf{M}_0 \quad (6.18)$$

$$\mathbf{M}'_{s_{1k}} = \mathbf{F}_1(\mathbf{M}_0, \mathbf{M}_{s_1 \dots s_k}) = \begin{cases} -\mathbf{G}_1^{-1}(\mathbf{G}_2(\mathbf{M}_{s_1} \otimes \mathbf{M}_0) + \mathbf{C}_1 \mathbf{M}'_0) & k=1 \\ -\mathbf{G}_1^{-1}(\mathbf{G}_2(\mathbf{M}_{s_k} \otimes \mathbf{M}_0) + \mathbf{C}_1 \mathbf{M}'_{s_{1k-1}}) & k>1 \end{cases} \quad (6.19)$$

$$\mathbf{M}'_{s_{2m}} = \mathbf{F}_2(\mathbf{M}_0, \mathbf{M}_{s_1 \dots s_m}) = \begin{cases} -\mathbf{G}_1^{-1}(\mathbf{G}_2(\mathbf{M}_0 \otimes \mathbf{M}_{s_1}) + \mathbf{C}_1 \mathbf{M}'_0) & m=1 \\ -\mathbf{G}_1^{-1}(\mathbf{G}_2(\mathbf{M}_0 \otimes \mathbf{M}_{s_m}) + \mathbf{C}_1 \mathbf{M}'_{s_{1m-1}}) & m>1 \end{cases} \quad (6.20)$$

$$\mathbf{M}'_{\lambda_l} = \mathbf{F}_3(\mathbf{M}_{\lambda_1 \dots \lambda_l}) = \begin{cases} -\mathbf{G}_1^{-1} \mathbf{G}_2(\mathbf{M}_{\lambda_1} \otimes \mathbf{M}_0 + \mathbf{M}_0 \otimes \mathbf{M}_{\lambda_1}) & l=1 \\ -\mathbf{G}_1^{-1} \mathbf{G}_2(\mathbf{M}_{\lambda_1} \otimes \mathbf{M}_0 + \mathbf{M}_0 \otimes \mathbf{M}_{\lambda_1} + \sum_{i=1}^l (\mathbf{M}_{\lambda_i} \otimes \mathbf{M}_{\lambda_{l-i}})) & l>1 \end{cases} \quad (6.21)$$

and

$$\mathbf{M}'_{s_{\lambda_{kml}}} = \mathbf{F}_4(\mathbf{M}_0, \mathbf{M}_{s_1 \dots s_k}, \mathbf{M}_{s_{\lambda_{11} \dots s_{\lambda_{\max(k,m),l}}}}) = -\mathbf{G}_1^{-1} \begin{cases} \mathbf{G}_2(\mathbf{M}_0 \otimes \mathbf{M}_{s_{\lambda_{ml}}} + \mathbf{M}_{\lambda_l} \otimes \mathbf{M}_{s_m} + \sum_{n=1}^l \mathbf{M}_{\lambda_n} \otimes \mathbf{M}_{s_{\lambda_{m(l-n)}}}) + \mathbf{C}_1 \mathbf{M}'_{s_{0m-l}} & m, l > 0, k = 0 \\ \mathbf{G}_2(\mathbf{M}_{s_{\lambda_{kl}}} \otimes \mathbf{M}_0 + \mathbf{M}_{s_k} \otimes \mathbf{M}_{\lambda_l} + \sum_{n=1}^l \mathbf{M}_{s_{\lambda_{kn}}} \otimes \mathbf{M}_{\lambda_{(l-n)}}) + \mathbf{C}_1 \mathbf{M}'_{s_{0k-l}} & k, l > 0, m = 0 \\ \mathbf{G}_2 \mathbf{M}_{s_k} \otimes \mathbf{M}_{s_m} + \mathbf{C}_1(\mathbf{M}'_{s_{k-1m0}} + \mathbf{M}'_{s_{km-10}}) & m, k > 0, l = 0 \\ \mathbf{G}_2(\mathbf{M}_{s_k} \otimes \mathbf{M}_{s_{\lambda_{ml}}} + \mathbf{M}_{s_{\lambda_{kl}}} \otimes \mathbf{M}_{s_m} + \sum_{n=1}^l \mathbf{M}_{s_{\lambda_{kn}}} \otimes \mathbf{M}_{s_{\lambda_{m(l-n)}}}) + \mathbf{C}_1(\mathbf{M}'_{s_{k-1ml}} + \mathbf{M}'_{s_{km-1l}}) & m, k, l > 0 \\ \mathbf{0} & \text{otherwise} \end{cases} \quad (6.22)$$

The equations (6.18)-(6.22) show that any moment in the nonlinear system (6.4.b) of frequency order $n=\max(k,m)$ and design parameter order l depends only on frequency moments of order up to n , design parameter moments of orders up to l and cross moments of orders up to nl of the linear kernel (6.4.a). Similar relationship can be derived for higher order nonlinear systems.

This reveals that choosing moments of reduced first order system in (6.4.a) with frequency order of higher than n and parameter order of higher than l does not necessarily increase the efficiency of reduced order model of (6.12). On the other hand, if one would like to have to increase the accuracy of (6.14), the best way is to only make use of the first n and l moments of (6.11) when forming equation (6.12), while the remaining moments are included in the congruent transformation matrix of (6.14).

6.2.2 Terminal Reduction Framework

To remove the redundant moments created by \mathbf{B}_2 , an SVD approach is performed on the zero-order moment \mathbf{M}_0 [94]- [95]. It computes the matrices \mathbf{U} , \mathbf{S} , \mathbf{V} from \mathbf{M}_0 such that:

$$\mathbf{M}_0 = \mathbf{USV}^T \tag{6.23}$$

where \mathbf{U} and \mathbf{V} are orthogonal matrices and \mathbf{S} is a diagonal matrix whose entries are non-

negative elements in falling order. The values on the diagonal of \mathbf{S} provide a measure of the relative importance of the various vectors in the orthonormal subspace defined by the columns of \mathbf{U} . This provides a convenient way to filter out the redundant vectors. Thus, taking only the leading m columns of \mathbf{U} that correspond to large values in \mathbf{S} will give us a compact subspace representing the vectors of \mathbf{M}_0 . The order m is heuristically chosen by the following criteria:

$$\frac{\mathbf{S}_{m,m}}{\mathbf{S}_{1,1}} \leq er \tag{6.24}$$

where $\mathbf{S}_{1,1}$ and $\mathbf{S}_{m,m}$ are the first and the m th elements of the diagonal elements of \mathbf{S} . er is the error bound to choose the dominant vectors. Thus the dominant column-space of \mathbf{M}_0 is constructed as

$$\tilde{\mathbf{M}}_0 = \left[\mathbf{U}_1 \quad \mathbf{U}_2 \quad \cdots \quad \mathbf{U}_m \right] \tag{6.25}$$

where $\mathbf{U}_1 \quad \mathbf{U}_2 \quad \cdots \quad \mathbf{U}_m$ are the first m columns of \mathbf{U} . Now higher order frequency, parameter and cross moments can be calculated by similar recursive equation as (6.7)-(6.98) and by replacing zero-order moment \mathbf{M}_0 by $\tilde{\mathbf{M}}_0$.

$$\mathbf{Y}(0, \lambda_0) \tilde{\mathbf{M}}_i^s = - \frac{\partial}{\partial s} \mathbf{Y}(s, \lambda_0) \Big|_{s=0} \tilde{\mathbf{M}}_{i-1}^s$$

$$\mathbf{Y}(0, \lambda_0) \tilde{\mathbf{M}}_j^\lambda = - \sum_{l=1}^j \frac{1}{l!} \frac{\partial^l}{\partial \lambda^l} \mathbf{Y}(0, \lambda) \Big|_{\lambda=\lambda_0} \tilde{\mathbf{M}}_{j-l}^\lambda \quad (6.26)$$

$$\mathbf{Y}(0, \lambda_0) \tilde{\mathbf{M}}_{ij}^{s\lambda} = - \sum_{l=1}^j \frac{1}{l!} \frac{\partial}{\partial s} \frac{\partial^l}{\partial \lambda^l} \mathbf{Y}(s, \lambda) \Big|_{\lambda=\lambda_0, s=0} \tilde{\mathbf{M}}_{i-1, j-l}^{s\lambda}$$

and $\mathbf{Y}(s, \bar{\lambda}) = s\mathbf{C}(\bar{\lambda}) + \mathbf{G}_1(\bar{\lambda})$. Once all the required moments with respect to frequency and all parameters are evaluated, the multidimensional subspace \mathbf{Q}_2^P is constructed using multi-order Arnoldi [54] as

$$\mathbf{Q}_2^P = \text{colspan} \left(\begin{bmatrix} \tilde{\mathbf{M}}^s & \tilde{\mathbf{M}}^{\bar{\lambda}} & \tilde{\mathbf{M}}^{\bar{x}} \end{bmatrix} \right) \quad (6.27)$$

where $\tilde{\mathbf{M}}^s$ contains the series coefficients corresponding to powers of s . $\tilde{\mathbf{M}}^{\bar{\lambda}}$ contains the series coefficients corresponding to powers of $\bar{\lambda}$, and $\tilde{\mathbf{M}}^{\bar{x}}$ contains the cross-term coefficients. Once all the moment coefficients for the systems of (6.4) are evaluated, the \mathbf{Q}^P is constructed as

$$\text{colspan}(\mathbf{Q}^P) = \text{colspan} \left(\begin{bmatrix} \mathbf{Q}_1^P & \mathbf{Q}_2^P & \cdots \end{bmatrix} \right) \quad (6.28)$$

Next, substituting $\mathbf{x}(t, \bar{\lambda}) = \mathbf{Q}^P \hat{\mathbf{x}}(t, \bar{\lambda})$ and pre-multiplying by \mathbf{Q}^{P^T} in (6.2) yields the parameterized reduced order system as shown in (6.14)-(6.15).

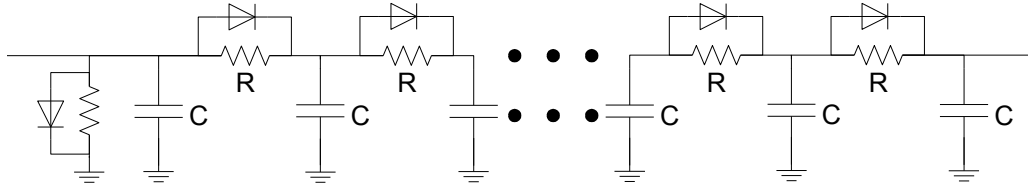


Figure 6.1 A nonlinear transmission line (Example 6.1).

6.3 Computational Results

In this section, two numerical examples are presented to illustrate the validity and efficiency of the proposed method. The proposed algorithm was implemented in MATLAB [87]. All computations were performed on a Pentium 4 (2.80 GHz) PC with 64 GB memory.

6.3.1 Example 6.1: Diode Transmission Line

In this example a nonlinear transmission line as in [34], [97] is considered in Figure 6.1. Transmission line is modeled using 100 sections. The resistance of each section is $R=1\Omega$ and each diode is characterized by

$$I_d = e^{40V} - 1 \tag{6.29}$$

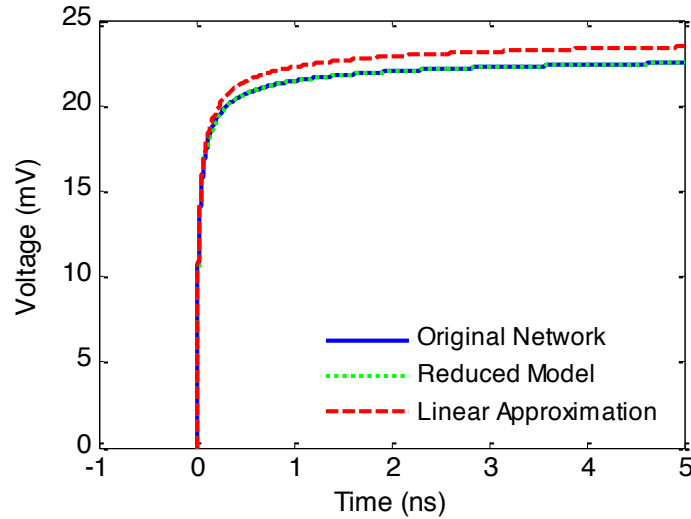


Figure 6.2 Small signal response of nonlinear network (Example 6.1).

where V is the voltage over the diode and I_d is the current of diode as in [97]. The capacitance of the transmission line is treated as a parameter which varies from $C=0.5F$ to $C=2F$. A small signal input $100mA$ step function with rise time of $1ms$ is applied at input of transmission line and the voltage measured at the same node. The size of the original system contained 100 unknown variables and the small signal circuit is characterized using second order Taylor series. The original system is reduced following the procedure of sections 6.1 and 6.2 to obtain a parametric model with respect to the capacitance of the transmission line. To derive reduced order model a single expansion point was selected at frequency $s=0$ and parameter $C=1F$. For this example, 4 frequency

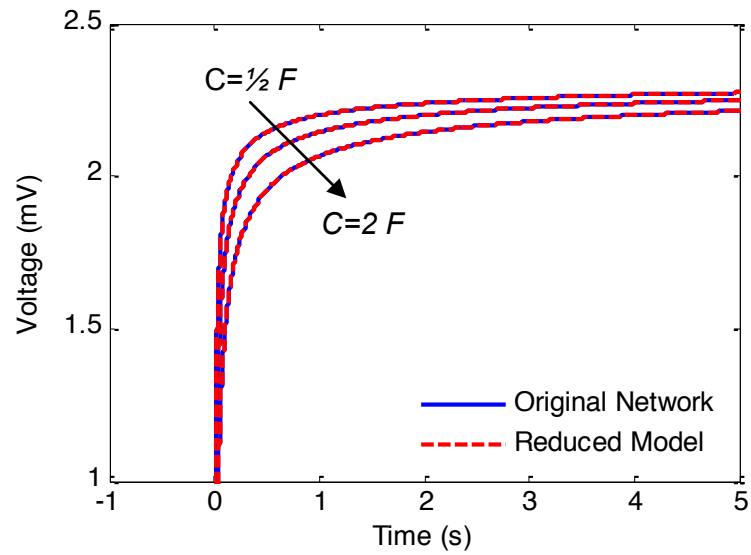


Figure 6.3 Small signal response of nonlinear network parameterized in capacitance (Example 6.1)

Table 6.1 CPU Run Time and Macromodel Size Comparison of Nonlinear Diode Transmission Line-Example 6.1

	Original	Reduced	Savings in Size	Speed-Up Factor
Macromodel Size	100	17	83%	-
CPU Run Time(s)	1134.9	23.7	-	48

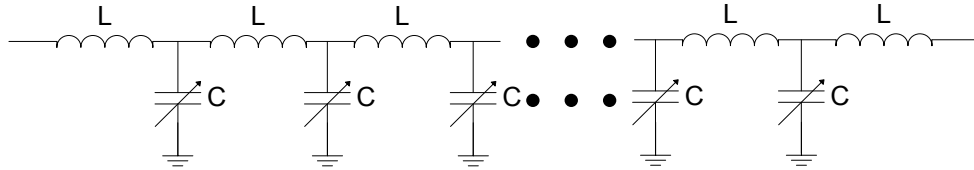


Figure 6.4 A nonlinear pulse narrowing transmission line (Example 6.2).

moments and 1 moments for capacitance are required to match the response of linear system of (6.4.a). To match the response of second order system of (6.4.b) 12 frequency moments are used. The size of the reduced order model consists of 17 variables. The proposed model is compared with original model, and the linear model of (6.4.a) in Figure 6.2. The proposed model is also compared with original model, at different points of parameter range for the capacitance of the transmission line in Figure 6.3. Table 6.1 compares the size and simulation time of the reduced and original systems. A speed up of 48 achieved using the proposed approach when compared to the original

6.3.2 Example 6.2: Pulse Shaping Transmission Line

A nonlinear pulse-narrowing transmission line is considered in Figure 6.4. [48]. Pulse narrowing transmission line is modeled using 333 sections. The characteristic nonlinear

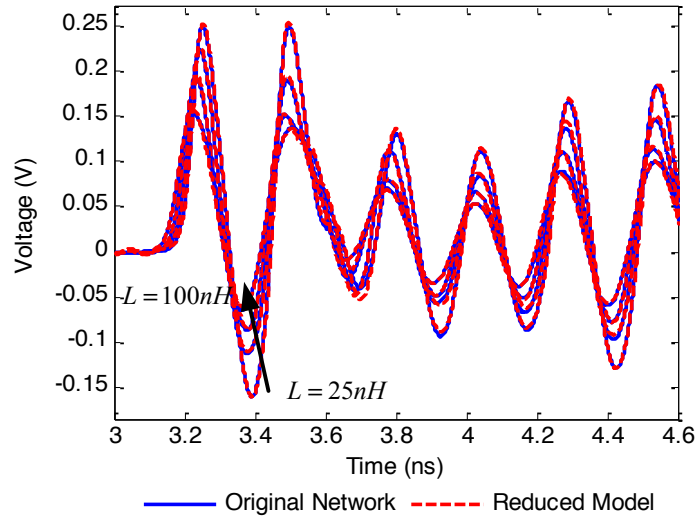


Figure 6.5 Output of nonlinear network parameterized in inductance of pulse narrowing transmission line (Example 6.2).

capacitor is modeled as [98]

$$C(V) = C_0(1 - b_0V) \quad (6.30)$$

where V is the voltage over the capacitor and $C_0 = 1pF$ and $b_0 = 0.01$. The inductance of the pulse-narrowing transmission line is treated as a parameter which varies from $L = 25pH$ to $L = 100pH$.

In this example, a sinusoidal voltage source with amplitude of $2V$ and frequency $4GHz$ is applied at one side of transmission line and voltage measured at the other side of

Table 6.2 CPU Run Time and Macromodel Size Comparison of Pulse Shaping Transmission Line-Example 6.2

	Original	Reduced	Savings in Size	Speed-Up Factor
Macromodel Size	1000	269	73.1%	-
CPU Run Time(s)	14107	1196	-	11.8

the transmission line. The size of the original system contained 1000 unknown variables. The original system is reduced following the procedure of sections 6.1 and 6.2 to obtain a parametric model with respect to the inductance of the pulse-narrowing transmission line. To derive reduced order model a single expansion point was selected at frequency $s=0$ and parameter $L=50pH$. For this example, 110 frequency moments and 26 moments for inductor are required to match the response of linear system of (6.4.a). To match the response of second order system of (6.4.b) 133 moments are used. The size of the reduced order model consists of 269 variables. The proposed model is compared with original model at different points of parameter range for the inductance of the pulse-narrowing transmission line in Figure 6.5. Table 6.2 compares the size and simulation

time of the reduced and original systems. A speed up of 11.8 achieved using the proposed approach when compared to the original simulation time.

Chapter 7

7 Conclusion and Future Research

7.1 Conclusion

In this thesis, three main contributions have been made to address the computational complexities involved in the simulation of high-speed integrated circuits. Firstly, a reduced order model is presented to efficiently solve large PEEC networks that include retardation effects. The proposed algorithm is based on a multi-order Arnoldi algorithm used to implicitly calculate the moments with respect to frequency. This procedure generates reduced order models that preserve the structure of the original system. Furthermore, it is shown that the orthonormal subspace of the proposed multi-order Arnoldi algorithm can be used to construct the same orthonormal subspace obtained using the traditional Arnoldi algorithm. Numerical examples of reduced order models

were shown to be accurate within a frequency range of interest with significant reduction in size and simulation time compared to the original PEEC network.

The second part deals with a computational approach to efficiently link many nonlinear elements to reduced order macromodels. The developed algorithm generates a parametric reduced order macromodel that captures the variances of nonlinear elements using a multidimensional Krylov subspace. In addition, a methodology to construct sparse reduced order models is developed for the proposed algorithm. Numerical examples show significant savings in the size of the macromodel and simulation time when compared to the original system.

The third contribution of the thesis presents an algorithm to reduce the computational complexity of weakly nonlinear systems. The proposed algorithm creates parameterized reduced order models for weakly nonlinear systems by approximating the nonlinear functions as a power series and using multidimensional subspace methods and SVD to capture the variances of design parameters. Numerical examples illustrated that for a weakly nonlinear system the parametric reduced order model was accurate over the desired parameter range of interest with significant reduction in size and simulation time when compared to the original system.

7.2 Suggestions for Future Research

This section provides some suggestions for future research based on the work presented in this thesis.

In chapter 4 an approach is presented to efficiently address the computational complexity of PEEC models with retardation. However, each time a design parameter is changed, the reduced system is no longer valid and the reduction procedure must be repeated to obtain a new reduced order model. In order to address this issue a multidimensional Krylov subspace technique can be developed to include design parameter variations in reduced order models of PEEC networks with retardation. In addition, parameterized MOR techniques can be extended to perform sensitivity analysis.

Development of reduced order model for nonlinear systems is a challenging task. In chapter 5 constraint variables and a multidimensional subspace was used to capture the variance of nonlinear elements. In chapter 6, a multidimensional subspace method along with variational analysis and SVD was used to develop parameterized reduced order models of weakly nonlinear systems. To determine the appropriate size of the models requires verifying the solution of the reduced order model with the original set of equations or comparing the difference between two different size reduced order models. Some interesting error bounds in [88], [92], [99] were developed for

automatically selecting the order of the reduced models. However, these methods require additional memory resources. Additional work is required on how to select the appropriate expansion point and number of moments of reduced order models for nonlinear systems.

References

- [1] M. N. O. Sadiku, *Numerical techniques in electromagnetics*. New York, NY: John Wiley, 2000.
- [2] J. M. Jin, *The finite element method in electromagnetics, 2nd ed.* New York, NY: John Wiley, 2002.
- [3] A. E. Ruehli, "Equivalent circuit models for three dimensional multiconductor systems," *IEEE Trans. Microw. Theory Tech.*, vol. 22, no. 3, pp. 216–221, March 1974.
- [4] A. E. Ruehli and A. C. Cangellaris, "Progress in the methodologies for the electrical modeling of interconnects and electronic packages," *Proceedings of The IEEE*, vol. 89, no. 5, pp. 740–771, May 2001.
- [5] L. W. Nagel, "SPICE2: a computer program to simulate semiconductor circuits," University of California, Berkeley, Berkeley, Technical Report 1975.
- [6] M. Celik, L. Pilegg, and A. Odabasioglu, *IC interconnect analysis*. Norwell, MA: Kluwer Academic Publisher, 2002.
- [7] S. Tan and L. He, *Advanced model order reduction techniques in VLSI design*. Cambridge, UK: Cambridge University Press, 2007.

-
- [8] R. Achar and M. S. Nakhla, "Simulation of high-speed interconnects," *Proceedings of The IEEE*, vol. 89, no. 5, pp. 693-728, May 2001.
- [9] L. Pillage and R. Rohrer, "Asymptotic waveform evaluation for timing analysis," *IEEE Trans. Computer-Aided Design*, vol. 9, pp. 352-366, April 1990.
- [10] D.H. Xie and M. Nakhla, "Delay and crosstalk simulation of high-speed VLSI interconnects with nonlinear terminations," *IEEE Transactions on Computer-Aided Design of Integrated Circuits and Systems*, vol. 12, no. 11, pp. 1798 - 1811 , Nov 1993.
- [11] S. Y. Kim, N. Gopal, and L. T. Pillage, "Time-domain macromodels for VLSI interconnect analysis," *IEEE Trans. Computer-Aided Design*, vol. 13, pp. 1257-1270, Oct 1994.
- [12] M. Celik and A. C. Cangellaris, "Efficient transient simulation of lossy packaging interconnects using moment-matching techniques," *IEEE Transactions on Components, Packaging, and Manufacturing Technology*, vol. 19, pp. 64-73, Feb 1996.
- [13] E. Chiprout and M. Nakhla, "Analysis of interconnect networks using complex frequency hopping (CFH)," *IEEE Trans. Comput.-Aided Des*, vol. 14, no. 2, pp. 186-200, Feb 1995.
- [14] P. Feldmann and R. W. Freund, "Efficient linear circuit analysis by Padé approximation via Lanczos process," *IEEE Transaction on Computer-Aided Design*, vol. 14, pp. 639-649, May 1995.

-
- [15] M. Celik and A. C. Cangellaris, "Simulation of multiconductor transmission lines using Krylov subspace order-reduction techniques," *IEEE Trans. Computer-Aided Design*, vol. 16, pp. 485-496, May 1997.
- [16] Q. Yu, J. M. L. Wang, and E. S. Kuh, "Passive multipoint moment matching model order reduction algorithm on multiport distributed interconnect networks," *IEEE Trans. Circuits Syst. I*, vol. 46, pp. 140-160, Jan 1999.
- [17] L. Silveira, M. Kamon, I. Elfadel, and J. White, "A coordinate-transformed Arnoldi algorithm for generating guaranteed stable reduced-order models of arbitrary RLC circuits," in *Proc. IEEE/ACM Int. Conf. Computer-Aided Design (ICCAD)*, 1996, pp. 288-294.
- [18] I. M. Elfadel and D. D. Ling, "A block rational Arnoldi algorithm for multiport passive model order reduction for multiport RLC networks," in *Proc. IEEE/ACM ICCAD*, 1997, pp. 66-71.
- [19] A. Odabasioglu, M. Celik, and L. Pileggi, "Prima: Passive reduced-order interconnect macromodeling algorithm," *IEEE Transactions on Computer-Aided Design of Integrated Circuits and Systems*, vol. 17, no. 8, pp. 645-654, 1998.
- [20] R. Achar, P. K. Gunupudi, M. S. Nakhla, and E. Chiprout, "Passive interconnect reduction algorithm for distributed/measured networks," *IEEE Trans. Circuits Systems*, vol. II, no. 47, pp. 287-301, April 2000.
- [21] M. Ma and R. Khazaka, "Model order reduction with parametric port formulation," *IEEE Transactions on Advanced Packaging*, vol. 30, no. 4, pp. 763 - 775, Nov 2007.

-
- [22] J. R. Phillips, L. Daniel, and L. M. Silveira, "Guaranteed passive balancing transformations for model order reduction," *IEEE Trans. Comput.-Aided Design Integr. Circuits Syst.*, vol. 22, pp. 1027-1041, Aug 2003.
- [23] J.V.R. Ravindra and M.B. Srinivas, "Generating reduced order models for high speed VLSI interconnects using balancing-free square root method," in *IEEE Workshop on Signal Propagation on Interconnects*, 2008, p. May.
- [24] W.T. Smith and S.K. Das, "Application of asymptotic waveform evaluation for EMC analysis of electrical interconnects," in *IEEE International Sym. on Electromagnetic Compatibility*, Atlanta,GA, 1995, pp. 429-434.
- [25] R. D. Slone, W. T. Smith, and Z. Bai, "Using partial element equivalent circuit full wave analysis and Pade via Lanczos to numerically simulate EMC problems," in *Proc. IEEE Int. Symp. Electromagnetic Compat.*, Austin, TX, 1997, pp. 608–613.
- [26] A E. Ruehli, H. Heeb, J. E. Bracken, and R. A. Rohrer, "Three dimensional circuit oriented electromagnetic modeling for VLSI interconnects," in *Packaging, Interconnects, Optoelectronics for Design of Parallel Computers Workshop*, Schaumburg, IL, 1992, pp. 218 - 221.
- [27] E. Chiprout, H. Heeb, M. S. Nakhla, and A. E. Ruehli, "Simulating 3-D retarded interconnect models using complex frequency hopping (CFH)," in *Proc. IEEE Int. Conf. Computer-Aided Design*, Santa Clara, CA, 1993, pp. 66–72.
- [28] N.A. Marques, M. Kamon, L.M. Silveira, and J.K White, "Generating compact, guaranteed passive reduced-order models of 3-D RLC interconnects," *IEEE Trans.*

-
- Advanced Packaging*, vol. 27, no. 4, pp. 569-580, Nov 2004.
- [29] H. Wu and A. C. Cangellaris, "Model-order reduction of finite-element approximations of passive electromagnetic devices including lumped electrical-circuit models," *IEEE Trans. Microwave Theory Tech.*, vol. 52, no. 9, pp. 2305–2313, Sept 2004.
- [30] F. Ferranti, G. Antonini, T. Dhaene, and L. Knockaert, "Guaranteed passive parameterized model order reduction of the Partial Element Equivalent Circuit (PEEC) method," *IEEE Trans. Electromagnetic Compatibility*, vol. 52, no. 4, pp. 974-984, Nov 2010.
- [31] J. R. Phillips, E. Chiprout, and D. Ling, "Efficient full-wave electromagnetic analysis via model-order reduction of fast integral transforms," in *in Proc. Design Automation Conf.*, Las Vegas, NV, 1996, pp. 377–382.
- [32] J. Cullum, A. Ruehli, and T. Zhang, "A method for reduced-order modeling and simulation of large interconnect circuits and its application to PEEC models with retardation," *IEEE Trans. Circuits and Systems*, vol. 47, no. 4, pp. 261-273, April 2000.
- [33] M. Ma and R. Khazaka, "Sparse macromodeling for parametric nonlinear networks," *IEEE Transactions on Microwave Theory and Techniques*, vol. 54, no. 12, pp. 4305-4315, Nov 2006.
- [34] J. R. Phillips, "Projection frameworks for model reduction of weakly nonlinear systems," in *37th ACM/IEEE Design Automation Conf*, 2000, pp. 184-189.

-
- [35] J. Chen and S-M. Kang, "An algorithm for automatic model-order reduction of nonlinear MEMS devices," in *IEEE Symp. on Circuits and Systems*, vol. 2, 2000, pp. 445-448.
- [36] Y. Chen and J. White, "A quadratic method for nonlinear model order reduction," in *International Conf. on Modeling and Simulation of Microsystems*, 2000, pp. 477-480.
- [37] P. Li and L. T. Pileggi, "Compact reduced-order modeling of weakly nonlinear analog and RF circuits," *IEEE Trans. Comp.-Aided Design*, vol. 24, pp. 184-203, Feb 2005.
- [38] M. Rewienski and J. White., "A trajectory piecewise-linear approach to model order reduction and fast simulation of nonlinear circuits and micromachined devices," *IEEE Trans. Comp.-Aided Design*, vol. 22, pp. 155-170, Feb 2003.
- [39] M. Rewienski, *A trajectory piecewise-linear approach to model order reduction of nonlinear dynamical systems.*: PhD thesis, Massachusetts Institute of Technology, 2003.
- [40] D. Vasilyev, M. Rewienski, and J. White, "A TBR-based trajectory piecewise-linear algorithm for generating accurate low-order models for nonlinear analog circuits and mems," in *40th ACM/IEEE Design Automation Conf*, 2003, pp. 490-495.
- [41] D. Ning and J. Roychowdhury, "General-Purpose Nonlinear Model-Order Reduction Using Piecewise-Polynomial Representations," *IEEE Trans. Comp.-Aided Design*, vol. 27, no. 2, pp. 249-264, Feb 2008.

-
- [42] P. Gunupudi and M. Nakhla, "Multi-dimensional model reduction of VLSI interconnects," in *Custom Integrated Circuits Conf.*, 2000, pp. 499–502.
- [43] L. Daniel, C. S. Ong, S. C. Low, K. H. Lee, and J. K. White, "A multiparameter moment matching model reduction approach for generating geometrically parameterized interconnect performance models," *IEEE Trans. Comp.-Aided Design*, vol. 23, no. 5, pp. 678–93, May 2004.
- [44] J.R. Phillips, "Variational interconnect analysis via PMTBR," in *IEEE/ACM Conf. on Comp. Aided-Design*, 2004, pp. 872-879.
- [45] P. Heydari and M. Pedram, "Model reduction of variable-geometry interconnects using variational spectrally-weighted balanced truncation," in *IEEE/ACM Conf. on Comp. Aided-Design*, 2001, pp. 586-591.
- [46] K. C. Sou, A. Megretski, and L. Daniel, "A Quasi-Convex Optimization Approach to Parameterized Model Order Reduction," *IEEE Trans. Comp.-Aided Design*, vol. 27, no. 3, pp. 456-469, March 2008.
- [47] Y. Shi and L. He, "EMPIRE: An efficient and compact multiple-parameterized model-order reduction method for physical optimization," *IEEE Trans. VLSI*, vol. 18, pp. 108-118, Jan 2010.
- [48] B. Bond and L. Daniel, "A piecewise-linear moment-matching approach to parameterized model-order reduction for highly nonlinear systems," *IEEE Trans. Comp.-Aided Design*, vol. 26, no. 12, pp. 2116-2129, Dec 2007.

-
- [49] Y. Su et al., "SAPOR: Second-order Arnoldi method for passive order reduction of RCS circuits," in *IEEE Proc. Int. Conf. Comput.-Aided Design*, San Jose, CA, 2004, pp. 74–79.
- [50] Z. Bai and Y. Su, "Dimension reduction of second-order large-scale dynamical systems via a second-order Arnoldi method," *SIAM J. Sci. Comput.*, vol. 26, no. 5, pp. 1692–1709, 2005.
- [51] Z. Bai and Y. Su, "SOAR: A second-order Arnoldi method for the solution of the quadratic eigenvalue problem," *SIAM J. Matrix Anal.*, vol. 26, no. 3, pp. 640–659, 2005.
- [52] H. Wu and A. Cangellaris, "Krylov model order reduction of finite element models of electromagnetic structures with frequency-dependent material properties," in *IEEE MTT-S Int. Microwave Symp. Digest*, 2006, pp. 52-55.
- [53] B. Salimbahrami, R. Eid, and B. Lohmann, "Model reduction by second order Krylov subspaces: Extensions, stability and proportional damping," in *IEEE Int. Symp. Intelligent*, 2006, pp. 2997–3002.
- [54] M. Ahmadloo and A. Dounavis, "Parameterized model order reduction of electromagnetic systems using multiorde arnoldi," *IEEE Trans. Advanced Packaging*, vol. 33, no. 4, pp. 1012-1020, Nov 2010.
- [55] R. D. Slone, R. Lee, and J.-F. Lee, "Broadband model order reduction of polynomial matrix equations using single-point well-conditioned asymptotic waveform evaluation: Derivations and theory," *Int. J. Numer. Meth. Eng.*, vol. 58, pp. 2325–

- 2342, 2003.
- [56] C. R. Paul, *Analysis of multiconductor transmission lines*. New York, NY: John Wiley and Sons, 1994.
- [57] A. Deutsch, "Electrical characteristics of interconnections for high-performance systems," *Proceedings of the IEEE*, vol. 86, pp. 315-355, Feb. 1998.
- [58] T. R. Arabi, A. T. Murphy, T. K. Sarkar, R. F. Harrington, and A. R. Djordjevic, "On the modeling of conductor and substrate losses in multiconductor, multi-dielectric transmission lines systems," *IEEE Trans. Microwave Theory Tech*, vol. 39, pp. 1090-1097, July 1991.
- [59] F. H. Branin, "Transient analysis of lossless transmission lines," *Proceedings of the IEEE*, vol. 55, pp. 2012-2013, 1967.
- [60] A. J. Chang and C.S. Gruodis, "Coupled lossy transmission line characterization and simulation," *IBM Journal of Research and Development*, vol. 25, pp. 25-41, Jan 1981.
- [61] F. Y. Chang, "The generalized method of characteristics for wave-form relaxation analysis of coupled transmission lines," *IEEE Trans. Microwave Theory Tech.*, vol. 37, pp. 2028-2038, Dec 1989.
- [62] S. Lin and E. S. Kuh, "Transient simulation of lossy interconnects based on the recursive convolution formulation," *IEEE Trans. Circuits Systems*, vol. 39, no. 1, pp. 879-892, Nov. 1992.

-
- [63] S. Grivet-Talocia and F. G. Canavero, "TOPLine: a delay-pole-residue method for the simulation of lossy and dispersive interconnects," *Proc. IEEE Electrical Performance of Electronics Packaging*, pp. 359-363, Oct 2002.
- [64] O. A. Palusinski and A. Lee, "Analysis of transients in nonuniform and uniform multiconductor transmission lines," *IEEE Trans. Microwave Theory Tech.*, vol. 37, pp. 127-138, Jan 1989.
- [65] M. Celik, A. C. Cangellaris, and A. Yaghmour, "An all-purpose transmission-line model for interconnect simulation in SPICE," *IEEE Trans. Microwave Theory Tech.*, vol. 45, pp. 1857-1867, Oct 1997.
- [66] M. Raugi, "Wavelet transform solution of MTL transients," *IEEE Trans. Magnetics*, vol. 35, pp. 1554-1557, may 1999.
- [67] S. Barmada and M. Raugi, "Transient numerical solutions of nonuniform MTL equations with nonlinear loads with wavelet expansion in time or space-domain," *IEEE Trans. Circuits Systems I*, vol. 47, pp. 1178-1190, Aug 2000.
- [68] A. Dounavis, R. Achar, and M. Nakhla, "A general class of passive macromodels for lossy multiconductor transmission lines," *IEEE Transactions on Microwave Theory and Techniques*, vol. 49, no. 10, pp. 1686 - 1696, Oct 2001.
- [69] E. Gad and M. Nakhla, "Efficient simulation of nonuniform transmission lines using integrated congruence transform," *IEEE Transactions on VLSI*, vol. 12, no. 12, pp. 1307 - 1320, Dec 2004.

-
- [70] T. Dhane and D. Zutter, "Selection of lumped element models for coupled lossy transmission lines," *IEEE Trans. Computer-Aided Design*, vol. 11, pp. 957-067, July 1992.
- [71] H. W. Johnson and M. Graham, *High-speed digital design*. Englewood Cliffs, NJ: Prentice-Hall, 1993.
- [72] Synopsys Inc, "HSPICE U-2003.09-RA," Mountain View, CA, 2003.
- [73] M. S. Nakhla, "Analysis of pulse propagation on high-speed VLSI chips," *IEEE Journal of Solid-State Circuits*, vol. 25, pp. 490-494, April 1990.
- [74] S. Grivet-Talocia, Hao-Ming Huang, A.E. Ruehli, F. Canavero, and I.M. Elfadel, "Transient analysis of lossy transmission lines: an efficient approach based on the method of Characteristics," *IEEE Transactions on Advanced Packaging*, vol. 27, no. 1, pp. 45 - 56, Feb 2004.
- [75] A. Dounavis and V.A. Pothiwala, "Passive closed-form transmission line macromodel using method of characteristics," *IEEE Transactions on Advanced Packaging*, vol. 31, no. 1, pp. 190 - 202, Feb 2008.
- [76] A. Dounavis, V.A. Pothiwala, A. Beygi, and , "Passive macromodeling of lossy multiconductor transmission lines based on the method of characteristics," *IEEE Transactions on Advanced Packaging*, vol. 32, no. 1, pp. 184 - 198, Feb 2009.
- [77] D. K. Cheng, *Field and Wave Electromagnetics, 2nd ed.* Reading, MA: Addison-Wesley, 1989.

-
- [78] A. E. Ruehli, "Inductance calculations in a complex integrated circuit environment," *IBM J. Res. Develop.*, vol. 16, no. 5, pp. 470–481, Sept 1972.
- [79] A. E. Ruehli and P. A. Brennan, "Efficient capacitance calculations for three-dimensional multiconductor systems," *IEEE Trans. Microwave Theory Tech.*, vol. 21, pp. 76–82, Feb 1973.
- [80] J. W. Demmel, *Applied numerical linear algebra*. Philadelphia, PA: SIAM, 1997.
- [81] D. L. Boley, "Krylov space methods on state-space control models," *IEEE Trans. Circuits Syst. Signal Processing*, vol. 13, no. 6, pp. 733–758, 1994.
- [82] W. Tseng, C. Chen, E. Gad, M. Nakhla, and R. Achar, "Passive order reduction for RLC circuits with delay elements," *IEEE Trans. Advanced Packaging*, vol. 30, no. 4, pp. 830-840, 2007.
- [83] C. Ho, A. Ruehli, and P. Brennan, "The modified nodal approach to network analysis," *IEEE Trans. Circuits Syst.*, vol. 22, pp. 504-509, Jun 1975.
- [84] M. Schetzen, *The volterra and wiener theories of nonlinear systems*. New York, NY: Wiley, 1980.
- [85] J. R. Phillips, "Projection-based approaches for model reduction of weakly nonlinear, time-varying systems," *IEEE Trans. Comput.-Aided Design Integr. Circuits Syst.*, vol. 22, no. 2, pp. 171–187, Feb 2003.
- [86] IBM Systems & Technology Group, "PowerPEEC," RTP, NC, USA, 2007.

-
- [87] MathWorks, "MATLAB and Simulink R2007b," Natick, MA, USA, 2007.
- [88] Z. Bai, R. D. Slone, W. T. Smith, and Q. Ye, "Error bound for reduced system model by Padé approximation via the Lanczos process," *IEEE Trans. Computer-Aided Design*, vol. 18, pp. 133 - 141, Feb 1999.
- [89] E. J. Grimme, *Krylov projection methods for model reduction. Ph.D. dissertation.* Urbana-Champaign, IL: Univ. Illinois.
- [90] E. Rasekh and A. Dounavis, "A multidimensional krylov reduction technique with constraint variables to model nonlinear distributed networks," *IEEE Transactions of Advanced Packaging*, vol. 33, no. 3, pp. 738 - 746, Aug 2010.
- [91] J. Vlach and K. Singhal, *Computer Methods for Circuit Analysis and Design.* New York, NY: Van Nostrand Reinhold, 1983.
- [92] A. Odabasioglu, M. Celik, and L. T. Pileggi, "Practical considerations for passive reduction of RLC circuits," in *Proc. Int. Conf. Computer Aided-Design*, San Jose, CA, 1999, pp. 214-219.
- [93] B. Toner and V.F. Fusco, "Waveform based MOSFET dynamic large-signal parameter estimation," *IEE Proc. Microwaves, Antennas and Prop*, vol. 150, no. 6, pp. 451-458, Dec 2003.
- [94] P. Feldmann and F. Liu, "Sparse and efficient reduced order modeling of linear subcircuits with large number of terminals," in *Proc. Int. Conf. on Computer Aided Design (ICCAD)*, 2004, pp. 88-92.

-
- [95] P. Liu, S.X.-D Tan, B. McGaughy, L. Wu, and L. He, "TermMerg: an efficient terminal-reduction method for interconnect circuits ," *IEEE Tran. on Computer-Aided Design of Integrated Circuits and Systems*, vol. 26, no. 8, pp. 1382-1392, Aug. 2007.
- [96] S. A. Maas, *Nonlinear microwave and RF circuits*. Norwood, MA: Artech House, 2003.
- [97] Y. Chen, *Model order reduction for nonlinear systems.*: M.S. Thesis, Massachusetts Institute of Technology, 1999.
- [98] E. Afshari and A. Hajimiri, "Nonlinear transmission lines for pulse shaping in silicon," *IEEE Jour. Solid-State Circuits*, vol. 40, no. 3, pp. 744-752, March 2005.
- [99] C. Prud'homme et al., "Reliable real-time solution of parameterized partial differential equations: Reduced-basis output bounds methods," *Journal of Fluids Eng.*, vol. 124, no. 1, pp. 70-80, 2002.

Curriculum Vitae

Name: Ehsan Rasekh

Post-secondary Education and Degrees: Shiraz University
Shiraz, Fars, Iran
1999-2003 B.S.

Shahid Beheshti University
Evin, Tehran, Iran
2003-2006 M.S.

The University of Western Ontario
London, Ontario, Canada
2007-2011 Ph.D.

Honours and Awards: Award for Outstanding Presentation in Graduate Symposium,
June 2011.
Western ECE Department Travel Grant, May 2011.
Graduate Thesis Research Award, January 2011.
Western Graduate Scholarship, September 2007-August 2011.

Related Work Experience Teaching Assistant
The University of Western Ontario
2007-2011

Research Assistant
The University of Western Ontario
2007-2011

Publications:

Rasekh, E; Dounavis, A; "A Multidimensional Krylov Reduction Technique With Constraint Variables to Model Nonlinear Distributed Networks", IEEE Transactions on Advanced Packaging, vol.33, no.3, pp.738-746, 2010.

Rasekh, E.; Eshghi, M., "An Efficient Hybrid Solution for Pronouncing Farsi Text," Springer International Journal of Speech Technology, vol 10, pp. 153-161 2007.

Rasekh, E; Dounavis, A; "Parameterized Model Order Reduction of Weakly Nonlinear Systems" Design Automation Conference (DAC), 2011 48th ACM/IEEE, San Diego, CA, 5-9 June 2011 (Removed from preceding because of US visa issues).

Rasekh, E; Dounavis, A; "An Order Reduction Technique for Nonlinear 3D Interconnects Using Constraint Variables" Conference on Electrical and Computer Engineering, 2011 24th IEEE Canadian, Niagara Falls, Canada, 8-11 May 2011.

Rasekh, E; Rasekh, I.; Eshghi, M., "PWL Approximation of Hyperbolic Tangent and the First Derivative for VLSI Implementation" Conference on Electrical and Computer Engineering, 2010 23th IEEE Canadian, Alberta, Canada , 2-5 May 2010.

Rasekh, I; Rasekh, E.; Eshghi, M., "An Approach to Recognize and Pronounce Words with Alternative Pronunciations in Farsi" Conference on Electrical and Computer Engineering, 2010 243th IEEE Canadian, Alberta, Canada , 2-5 May 2010..

Rasekh, E.; Eshghi, M., "An Efficient Network for Farsi Text to Speech Conversion Using Vowel State, " TENCON 2006. 2006 IEEE Region 10 Conference, pp.1-4, Nov. 2006.

Rasekh, E.; Eshghi, M., "A Syllable-Phoneme Solution for Efficient Farsi Text-to-Speech Systems, " TENCON 2006. 2006 IEEE Region 10 Conference, pp.1-5, Nov. 2006.